(12) INTERNATIONAL APPLICATION PUBLISHED UNDER THE PATENT COOPERATION TREATY (PCT)

(19) World Intellectual Property Organization
International Bureau

(43) International Publication Date
15 May 2025 (15.05.2025)

WIPO | PCT

(10) International Publication Number
WO 2025/101606 A1

(51) International Patent Classification:
A61B 7/04 (2006.01) *A61B 5/08* (2006.01)
A61B 7/00 (2006.01) *A61B 5/11* (2006.01)
A61B 5/00 (2006.01)

(21) International Application Number:
PCT/US2024/054723

(22) International Filing Date:
06 November 2024 (06.11.2024)

(25) Filing Language: English

(26) Publication Language: English

(30) Priority Data:
63/547,447 06 November 2023 (06.11.2023) US

(71) Applicants: **NORTHWESTERN UNIVERSITY** [US/US]; 633 Clark Street, Evanston, Illinois 60208 (US). **ANN AND ROBERT H. LURIE CHILDREN'S HOSPITAL OF CHICAGO** [US/US]; 225 E. CHICAGO AVENUE, NO. 205, CHICAGO, Illinois 60611 (US). **THE ROYAL INSTITUTION FOR THE ADVANCEMENT OF LEARNING/MCGILL UNIVERSITY** [CA/CA]; 845 Sherbrooke Street West, James Administration Building, Montreal, Québec H3A 0G4 (CA). **SIBEL HEALTH INC.** [US/US]; 2017 N. Mendell Street, Suite 2SE, Chicago, Illinois 60614 (US).

(72) Inventors: **ROGERS, John A.**; 1236 Greenwood Avenue, Wilmette, Illinois 60091 (US). **BANKS, Anthony R.**; 633 Clark Street, Evanston, Illinois 60208 (US). **YOO, Jaeyoung**; 633 Clark Street, Evanston, Illinois 60208 (US). **BHARAT, Ankit**; 633 Clark Street, Evanston, Illinois 60208 (US). **WEESE-MAYER, Debra E.**; 225 E. CHICAGO AVENUE, NO. 205, CHICAGO, Illinois 60611 (US). **SHALISH, Wissam**; 845 Sherbrooke Street West, James Administration Building, Montreal, Québec H3A 0G4 (CA). **OH, Seyong**; 633 Clark Street, Evanston, Illinois 60208 (US). **LEE, Jong Yoon**; 2017 N. Mendell Street, Suite 2SE, Chicago, Illinois 60614 (US).

(74) Agent: **XIA, Tim Tingkang**; P.O. Box 55874, Boston, Massachusetts 02205 (US).

(81) Designated States *(unless otherwise indicated, for every kind of national protection available)*: AE, AG, AL, AM, AO, AT, AU, AZ, BA, BB, BG, BH, BN, BR, BW, BY, BZ, CA, CH, CL, CN, CO, CR, CU, CV, CZ, DE, DJ, DK, DM, DO, DZ, EC, EE, EG, ES, FI, GB, GD, GE, GH, GM, GT, HN, HR, HU, ID, IL, IN, IQ, IR, IS, IT, JM, JO, JP, KE, KG, KH, KN, KP, KR, KW, KZ, LA, LC, LK, LR, LS, LU, LY, MA, MD, MG, MK, MN, MU, MW, MX, MY, MZ, NA,

(54) Title: WIRELESS BROADBAND ACOUSTO-MECHANICAL SENSORS AS BODY AREA NETWORKS FOR CONTINUOUS PHYSIOLOGICAL MONITORING

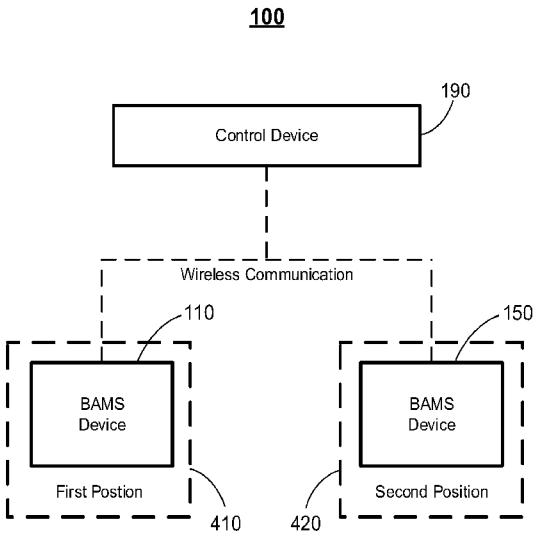

FIG. 1A

(57) Abstract: This invention relates to broadband acousto-mechanical sensing (BAMS) systems and methods for monitoring physiological signals of a living subject, and applications of the same. Specifically, the system includes one or more wireless, skin-interfaced BAMS devices disposed on the living subject to form a body area network. The BAMS devices are time-synchronized and wirelessly communicate with each other, and each BAMS device includes an accelerometer, such as an inertial measurement unit (IMU), to capture acceleration data from the living subject and an acoustic mechanical device configured to capture body sounds from the living subject. A control device being time-synchronized and wirelessly communicate with the BAMS devices is used to manage and process the acceleration data and the body sounds from the one or more BAMS devices in order to generate information of body movements and body sounds of the living subject.

WO 2025/101606 A1

[Continued on next page]

NG, NI, NO, NZ, OM, PA, PE, PG, PH, PL, PT, QA, RO, RS, RU, RW, SA, SC, SD, SE, SG, SK, SL, ST, SV, SY, TH, TJ, TM, TN, TR, TT, TZ, UA, UG, US, UZ, VC, VN, WS, ZA, ZM, ZW.

(84) **Designated States** *(unless otherwise indicated, for every kind of regional protection available)*: ARIPO (BW, CV, GH, GM, KE, LR, LS, MW, MZ, NA, RW, SC, SD, SL, ST, SZ, TZ, UG, ZM, ZW), Eurasian (AM, AZ, BY, KG, KZ, RU, TJ, TM), European (AL, AT, BE, BG, CH, CY, CZ, DE, DK, EE, ES, FI, FR, GB, GR, HR, HU, IE, IS, IT, LT, LU, LV, MC, ME, MK, MT, NL, NO, PL, PT, RO, RS, SE, SI, SK, SM, TR), OAPI (BF, BJ, CF, CG, CI, CM, GA, GN, GQ, GW, KM, ML, MR, NE, SN, TD, TG).

Published:

— *with international search report (Art. 21(3))*

WIRELESS BROADBAND ACOUSTO-MECHANICAL SENSORS AS BODY AREA NETWORKS FOR CONTINUOUS PHYSIOLOGICAL MONITORING

CROSS-REFERENCE TO RELATED APPLICATION

This PCT application claims priority to and the benefit of U.S. Provisional Patent Application Serial No. 63/547,447, which was filed November 6, 2023. The content of the above-identified application is incorporated herein by reference in its entirety.

FIELD OF THE INVENTION

The present invention relates generally to healthcare and vital sign monitoring, and more particularly to wireless broadband acousto-mechanical sensing (BAMS) system and methods using BAMS sensor devices as body area networks for continuous physiological monitoring of a living subject, and applications of the same.

BACKGROUND OF THE INVENTION

The background description provided herein is for the purpose of generally presenting the context of the invention. The subject matter discussed in the background of the invention section should not be assumed to be prior art merely as a result of its mention in the background of the invention section. Similarly, a problem mentioned in the background of the invention section or associated with the subject matter of the background of the invention section should not be assumed to have been previously recognized in the prior art. The subject matter in the background of the invention section merely represents different approaches, which in and of themselves may also be inventions. Work of the presently named inventors, to the extent it is described in the background of the invention section, as well as aspects of the description that may not otherwise qualify as prior art at the time of filing, are neither expressly nor impliedly admitted as prior art against the invention.

In 2020, cardiovascular and respiratory diseases were responsible for over 796,000 deaths in the United States, making them the first and third leading causes of death in adults, according to the Centers for Disease Control and Prevention (CDC). In children and neonates, cardiorespiratory and gastro-intestinal problems are major causes of death during the first 5 years of life. The use of continuous monitoring systems can help guide clinical decisions and improve outcomes. Current hospital systems continue, however, to rely on a variety of sensors, wires and

cables connected to bedside monitors. Fortunately, advances in bioengineering are leading to broad classes of wireless, skin-interfaced sensors to address these limitations, with easy installation and use in the acquisition of multiple classes of signals simultaneously.

Assessments of cardiac, respiratory, and gastro-intestinal sounds represent important parts of routine care, as changes or absences of body sounds can represent signs of disease, disease progress, or disease resolution. Digital stethoscopes, including some recently reported in wearable designs, can provide complementary information on cardiac activity, airway obstruction, adventitious lung sounds, and intestinal motility. These technologies cannot, however, be used effectively for continuous monitoring of those sounds during routine activities due to limitations that include some combination of the following: (1) rigid and bulky engineering designs, (2) inability to support time-synchronized operation across multiple locations of the body, (3) susceptibility to confounding effects of ambient sounds, and (4) sensitivity to noise generated by movements and physical contact. As a result, the clinical use of body sounds for health monitoring occurs typically through episodic measurements, with few examples of applications outside of the hospital.

Therefore, a heretofore unaddressed need exists in the art to address the aforementioned deficiencies and inadequacies.

SUMMARY OF THE INVENTION

In one aspect, the invention relates to a broadband acousto-mechanical sensing (BAMS) system for monitoring physiological signals of a living subject. In one embodiment, the BAMS system includes: one or more wireless, skin-interfaced BAMS devices disposed on the living subject, being time-synchronized and wirelessly communicate with each other, wherein each BAMS device comprises an accelerometer configured to capture acceleration data from the living subject and an acoustic mechanical device configured to capture body sounds from the living subject, and the accelerometer and the acoustic mechanical device in each BAMS device are time-synchronized; and a control device being time-synchronized and wirelessly communicate with the one or more BAMS devices, configured to manage and process the acceleration data and the body sounds from the one or more BAMS devices and to generate information of body movements and body sounds of the living subject based on the acceleration data and the body sounds obtained by the one or more BAMS devices.

Another aspect of the invention relates to a method of monitoring physiological signals of

a living subject with a broadband acousto-mechanical sensing (BAMS) system. In one embodiment, the method includes: managing and processing, by a control device being time-synchronized and wirelessly communicate with one or more, skin-interfaced BAMS devices, acceleration data and body sounds from the one or more BAMS devices, wherein the one or more BAMS device are disposed on the living subject, the one or more BAMS devices are time-synchronized and wirelessly communicate with each other, each BAMS device comprises an accelerometer configured to capture the acceleration data from the living subject and an acoustic mechanical device configured to capture the body sounds from the living subject, and the accelerometer and the acoustic mechanical device in each BAMS device are time-synchronized; and generating, by the control device, information of body movements and body sounds of the living subject based on the acceleration data and the body sounds obtained by the one or more BAMS devices.

In one embodiment, the body movements include chest wall movements and abdominal wall excursions, and the body sounds include respiratory sounds, lung sounds, gastro-intestinal sounds, bowel sounds, and cardiac sounds.

In one embodiment, each BAMS device includes: a flexible printed circuit board (fPCB); an inertial measurement unit (IMU) disposed on the fPCB, wherein the IMU functions as the accelerometer configured to capture 3-axis acceleration data from the living subject; and two microphones, respectively disposed on a body-facing side and an ambient-facing side of the FPCB, configured to capture the body sounds from the living subject ambient sounds from the environment.

In one embodiment, each BAMS device further comprises a top elastomer layer and a bottom elastomer layer sandwiching the fPCB, wherein the bottom elastomer layer forms the body-facing surface attached to the living subject, and the top elastomer layer forms the ambient-facing surface.

In one embodiment, each BAMS device further comprises a Bluetooth Low Energy (BLE) system on a chip (SoC) disposed on the fPCB, configured to wirelessly communicate with the control device.

In one embodiment, each BAMS device further comprises an embedded power supply disposed on the fPCB or a wireless charging power supply.

In one embodiment, each BAMS device is configured to generate the body sound by applying an adaptive filtering algorithm to perform sound separation to the body sounds and the

ambient sounds in order to minimize contribution of the ambient sounds to the body sounds.

In one embodiment, the control device comprises a graphical user interface (GUI) configured to real-time display quantitative information of the body movements and the body sounds of the living subject.

In one embodiment, the one or more BAMS devices are disposed at one or more of the following locations of the living subject: a right upper chest area; a right lower chest area; a right axilla area; a right upper back area; a right mid back area; a right lower back area; a left upper chest area; a left lower chest area; a left axilla area; a left upper back area; a left mid back area; a left lower back area; and a suprasternal notch area.

In another aspect of the present invention, a BAMS device for capturing physiological signals of a living subject is provided. In one embodiment, the BAMS device includes: a flexible printed circuit board (fPCB); an inertial measurement unit (IMU) disposed on the fPCB, wherein the IMU functions as the accelerometer configured to capture 3-axis acceleration data from the living subject; and two microphones, respectively disposed on a body-facing side and an ambient-facing side of the FPCB, configured to capture the body sounds from the living subject ambient sounds from the environment.

In one embodiment, the BAMS device further comprises a top elastomer layer and a bottom elastomer layer sandwiching the fPCB, wherein the bottom elastomer layer forms the body-facing surface attached to the living subject, and the top elastomer layer forms the ambient-facing surface.

In one embodiment, the BAMS device further comprises a Bluetooth Low Energy (BLE) system on a chip (SoC) disposed on the fPCB, configured to wirelessly communicate with the control device.

In one embodiment, the BAMS device further comprises an embedded power supply disposed on the fPCB or a wireless charging power supply.

In one embodiment, the BAMS device is configured to generate the body sound by applying an adaptive filtering algorithm to perform sound separation to the body sounds and the ambient sounds in order to minimize contribution of the ambient sounds to the body sounds.

The BAMS system and the BAMS device may be utilized in a variety of applications. In one embodiment, a method of determining regional lung function of a living subject using the BAMS system as described is provided. In one embodiment, a method of monitoring bilateral lung function of a living subject using the BAMS system as described is provided. In one

embodiment, a method of monitoring athletic performance of a living subject for conditioning using the BAMS system as described is provided.

In a further aspect, a non-transitory tangible computer-readable medium is provided for storing instructions which, when executed by one or more processors, cause the method as described to be performed.

Yet another aspect of the invention relates to a method of detecting hypopnea and central apnea of a living subject with a BAMS system. In one embodiment, the method includes: managing and processing, by a control device being time-synchronized and wirelessly communicate with one or more, skin-interfaced BAMS devices, acceleration data and body sounds from the one or more BAMS devices, wherein the one or more BAMS device are disposed on the living subject, the one or more BAMS devices are time-synchronized and wirelessly communicate with each other, each BAMS device comprises an accelerometer configured to capture the acceleration data from the living subject and an acoustic mechanical device configured to capture the body sounds from the living subject, and the accelerometer and the acoustic mechanical device in each BAMS device are time-synchronized; generating, by the control device, information of body movements and body sounds of the living subject based on the acceleration data and the body sounds obtained by the one or more BAMS devices; detecting, by the control device, whether the information of the body movements and the body sounds of the living subject show a partial reduction or an absence thereof; and in response to detecting the information of the body movements and the body sounds of the living subject showing the partial reduction or the absence thereof, determining, by the control device, the living subject to have a hypopnea or a central apnea, wherein the partial reduction of the body movements and the body sounds of the living subject indicates the hypopnea, and the absence of the body movements and the body sounds of the living subject indicates the central apnea.

Yet a further aspect of the invention relates to a BAMS system for detecting hypopnea and central apnea of a living subject. In one embodiment, the BAMS system includes: one or more wireless, skin-interfaced BAMS devices disposed on the living subject, being time-synchronized and wirelessly communicate with each other, wherein each BAMS device comprises an accelerometer configured to capture acceleration data from the living subject and an acoustic mechanical device configured to capture body sounds from the living subject, and the accelerometer and the acoustic mechanical device in each BAMS device are time-synchronized; and a control device being time-synchronized and wirelessly communicate with the one or more

BAMS devices, configured to manage and process the acceleration data and the body sounds from the one or more BAMS devices and to generate information of body movements and body sounds of the living subject based on the acceleration data and the body sounds obtained by the one or more BAMS devices, detect whether the information of the body movements and the body sounds of the living subject show a partial reduction or an absence thereof, and determine, in response to detecting the information of the body movements and the body sounds of the living subject showing the partial reduction or the absence thereof, the living subject to have a hypopnea or a central apnea, wherein the partial reduction of the body movements and the body sounds of the living subject indicates the hypopnea, and the absence of the body movements and the body sounds of the living subject indicates the central apnea.

In certain embodiments, each BAMS device is configured to generate the body sound by applying an adaptive filtering algorithm to perform sound separation to the body sounds and the ambient sounds in order to minimize contribution of the ambient sounds to the body sounds.

In certain embodiments, each BAMS device further comprises a Bluetooth Low Energy (BLE) system on a chip (SoC), configured to wirelessly communicate with the control device.

In certain embodiments, the body movements include chest wall movements and abdominal wall excursions, and the body sounds include respiratory sounds and lung sounds.

In certain embodiments, the control device comprises a graphical user interface (GUI) configured to real-time display quantitative information of the body movements and the body sounds of the living subject.

These and other aspects of the present invention will become apparent from the following description of the preferred embodiment taken in conjunction with the following drawings, although variations and modifications therein may be affected without departing from the spirit and scope of the novel concepts of the invention.

BRIEF DESCRIPTION OF THE DRAWINGS

The accompanying drawings illustrate one or more embodiments of the invention and together with the written description, serve to explain the principles of the invention. Wherever possible, the same reference numbers are used throughout the drawings to refer to the same or like elements of an embodiment.

FIG. 1A schematically shows a functional block diagram of a BAMS system according to certain embodiments of the present invention.

FIG. 1B schematically shows a control device of FIG. 1A according to certain embodiments of the present invention.

FIG. 2A shows wireless networks of skin-interfaced miniaturized sensors of body sounds and motions for continuous physiological monitoring and diagnostics, where (A) shows a schematic illustration of a system for tracking (i) cardiorespiratory activity, (ii) gastro-intestinal sounds, and (iii) multi-location respiratory sounds; (B) shows a photograph of the BAMS device on a neonatal model and associated real-time GUI; (C) shows a schematic exploded-view illustration of a BAMS device; and (D) shows a block diagram of the physiological monitoring scheme that combines an IMU with body-facing and ambient-facing microphones.

FIG. 2B shows a diagram illustrating data for comparison of clinical results obtained with a BAMS device (chest wall movements, respiratory sounds, and cardiac sounds) and with systems for recording electrocardiograms, and exhaled CO_2 tracing from a 19-month-old patient in the pediatric intensity care unit (PICU).

FIG. 3 shows thermal stability tests of the microphone and IMU, where (A) shows a photograph of the thermal test set-up, (B) and (C) show histogram plots of (B) accelerations and (C) sound intensities captured at two different temperatures, (D) shows acceleration, microphone, and temperature data measured as a function of temperature from 32°C to 40°C, and (E) and (F) show magnified views of acceleration, microphone, and sound intensity data at (E) 32°C and (F) 40°C.

FIG. 4 shows a real-time wireless network of skin-integrated sensors of body sounds and movements for continuous physiological monitoring and visual feedback.

FIG. 5 shows a table of performance comparison of digital stethoscopes.

FIG. 6 shows data on power consumption and wireless charging, where (A) shows current consumption and (B) shows 1-second average current during standby and during operation of the device, (C) shows battery residual voltage as a function of operating time starting with a fully charged battery, and (D) shows battery voltage during wireless charging.

FIG. 7A shows characterization of individual BAMS systems and wireless networks for cardiorespiratory monitoring, where (A) shows a schematic illustration of sound separation using a pair of microphone setup; (B) shows cardiorespiratory sound captured in an ambient environment with white noise and with crying sounds at 90 dB (i) time series data from the body-facing and ambient-facing microphones, and spectrogram representation of the former, (ii) corresponding results after two-step adaptive filtering; (C) shows a schematic illustration of body

locations for cardiorespiratory monitoring; (D) shows spectrogram of sounds collected on the (i) suprasternal notch (SN), (ii) upper chest, and (iii) lower chest; and (E) shows normalized data for chest wall movements extracted from the IMU of the device on the SN and the sound intensity associated with respiration (respiratory sound, > 150 Hz) at each location.

FIG. 7B shows characterization of individual BAMS systems and wireless networks for cardiorespiratory monitoring, where (1) shows normalized ECG data and sound intensity associated with cardiac activity (cardiac sound, < 150 Hz) at each location; (2) shows comparison of heart rate interval range between ECG and cardiac sound from the microphone; and (3) shows cardiac sound intensity during resting and exercising.

FIG. 8 shows a flow chart of two-step adaptive acoustic filtering for separate measurements of body and ambient sounds.

FIG. 9 shows characterization of noise cancellation using the BAMS system, where (A) and (B) shows experimental setup using a lung sound trainer, sound meter, with (A) a BAMS system and (B) a commercial digital stethoscope (3M™ Littmann® CORE, Eko) with active noise cancellation; (C) shows breath sound and heart sound intensity recorded in an ambient of 90 dB white noise across frequency from 20 to 400 Hz; and (D) and (E) shows signal-to-noise ratio (SNR) of breath sound and heart sound for the BAMS system and the commercial digital stethoscope, measured in different ambient conditions, including (D) levels of white noise and (E) types of sounds with a noise level of 75 dB.

FIG. 10 shows comparison of cardiac activity captured by microphone and IMU in white noise, where (A) shows spectrogram of body sound without and with noise cancellation, as well as IMU data, in an ambient white noise across frequencies from 20 to 400 Hz; (B) and (C) shows magnified signals at 40 dB and 80 dB noise levels; and (D) shows the signal-to-noise ratio (SNR) of cardiac activity for the microphone and IMU, measured in different ambient noise conditions.

FIG. 11 shows calibration of BAMS system sound, where (A) shows time series data from the microphone and corresponding spectrogram representation captured at various level of white noise sound across frequency from 20 to 400 Hz; (B) shows correlation between decibel readings from the sound meter and the intensity measured by the BAMS system; and (C) shows comparison of sound levels between the sound meter and the calibrated BAMS system.

FIG. 12 shows continuous long-term cardiorespiratory monitoring during sleep and vigorous activity.

FIG. 13 shows respiratory sound monitoring in quiet and noisy environments and while

rubbing clothing against the device, patting the body and directly tapping the device.

FIG. 14A shows cardiopulmonary monitoring and cardio-respiratory coupling analysis during daily activities, where (A) shows data corresponding to skin temperature, physical activity, and body sounds captured during daily activities; and (B) and (C) shows spectrogram images and intensity of breath and heart sounds as a function of time for recordings collected indoors and outdoors.

FIG. 14B shows cardiopulmonary monitoring and cardio-respiratory coupling analysis during daily activities, where (1) shows respiratory rate, heart rate, heart sound intensity, heart rate variability, and cardio-respiratory coupling extracted from data collected indoors and outdoors; (2) shows correlation between heart rate and respiratory rate; and (3) shows cardio-respiratory coupling values as a function of physical activity levels.

FIG. 15 shows monitoring of swallowing signals using the BAMS system on the (A) suprasternal notch, (B) upper chest and (C) middle chest, where (i) shows a schematic illustration of the device mounting location for each placement, (ii) shows chest movement and swallowing signal using lowpass filtered IMU and highpass filtered IMU, and (iii) shows spectrogram and intensity of body sound for each placement.

FIG. 16 shows estimation of cardiac activity during and after exercise from measurements on the lower chest, where (A) shows data corresponding to physical activity, heart rate intervals, heart sound intensity, root mean square of continuous difference (RMSSD) between heartbeats captured by FDA-approved ECG monitoring system and from the microphone and IMU data of a BAMS device during and after exercise; (B) and (C) shows the ECG signal, spectrogram images, and intensity of heart sounds during (B) resting and (C) exercising; and (D) shows Bland-Altman plots comparing measurements for heart rate.

FIG. 17 shows Bland-Altman plots comparing measurements for root mean square of continuous difference (RMSSD).

FIG. 18 shows analysis of cardiac sound intensities, where (A) shows continuous blood pressure monitoring data and cardiac sound intensities during resting, breath holding, and cold pressor tests; and (B) shows correlation between cardiac sound intensity and blood pressure.

FIG. 19 shows heart sound monitoring during vocalization (A) without noise cancellation and (B) with noise cancellation.

FIG. 20 shows continuous, wireless monitoring of respiratory sounds and other physiological parameters from neonates in a neonatal intensive care unit (NICU), where (A)

shows a photograph of the BAMS device on a neonate (born at 30 weeks' gestation, 33 weeks' post-menstrual age, and weighing 1.56kg); (B) shows representative respiration waveforms associated with a pneumotachograph device and with a BAMS system (chest movements and acoustic spectrograms) from a neonate; (C) shows ambient noise level, body rotation angle, heart rate, respiratory rate, breathing intensity, and breathing intervals determined from data collected using a BAMS system and FDA-approved clinical monitors from a neonate; (D) shows correlation of normalized intensity of pneumotachograph data and respiratory sounds; (E) shows breathing intervals; and (F) shows respiratory sound intensity recorded from ten different neonates for 500 seconds; the box plot shows the range between the 25th and 75th percentiles, and the midline indicates the median of each data set.

FIG. 21 shows a photograph of the BAMS device on a neonate (born at 30 weeks' gestation, 33 weeks' post-menstrual age, and weighing 1.56kg) with wire-based nasal temperature sensor, RIP band and ECG system.

FIG. 22 shows Bland–Altman plots of measurements of respiratory rate using the BAMS system and pneumotach module in continuous, wireless monitoring of respiratory sounds from neonates in a neonatal intensive care unit (NICU).

FIG. 23 shows a table of comparison of Pearson correlation values between airflow rate and breath sound intensity from previous research.

FIG. 24 shows monitoring of neonatal cardiac activity using the BAMS system, where (A) shows ECG signal, spectrogram image, and heart sound intensity, and (B) shows Bland-Altman plots comparing heart rate determined using the BAMS system with ECG measurements (5 neonates, 136,013 data points).

FIG. 25 shows spectrogram images and time series results comparing respiratory behaviors obtained from breath sounds measured with the microphone in a BAMS system, temperature measured with a nasal thermistor, chest wall movement measured with the IMU in a BAMS system, and the summation of respiratory inductance plethysmograms measured with chest and abdomen RIP bands.

FIG. 26 shows Bland-Altman plots comparing respiratory rate determined using the BAMS system with nasal temperature flow measurements (5 neonates, 42,738 data points).

FIG. 27 shows monitoring of internal air flow using time-synchronized sensors. Schematic illustration and images showing the mounting locations of the devices, including (i) Device-A: Suprasternal notch, and (ii) Device-B: Right upper chest).

FIG. 28 shows gastrointestinal activity monitoring using a microphone and EMG sensor, where (A) shows spectrogram of bowel sounds, (B) shows bowel sound intensity recorded by the microphone, and (C) shows EMG signal during gastrointestinal activity.

FIG. 29 shows continuous, wireless monitoring of gastro-intestinal sounds (bowel sounds) from neonates in a neonatal intensive care unit (NICU), where (A) shows a photograph of a pair of BAMS devices on an infant (46 weeks' post-menstrual age); (B) and (C) show spectrograms and sound intensities (> 150Hz) for data collected (B) before feeding and (C) after feeding using a BAMS system placed on the upper right abdomen of a neonate; (D) shows bowel sound peak counts, normalized bowel sound intensity at the upper right and lower left abdomen, and difference in normalized bowel sound intensities between the upper right and lower left abdomen; (E)-(G) show comparison of (E) bowel sound peak counts per minutes and (F) bowel sound intensity before and after feeding, and (G) difference in normalized bowel sound intensities between upper right and lower left abdomen at 15 min after feeding and 15-30 min after feeding, where the box plot shows the range between the 25th and 75th percentiles, and the midline indicates the median of each data set.

FIG. 30 shows a flowchart of data processing steps for detecting bowel sounds.

FIG. 31 shows time synchronization of a wireless network of BAMS systems, where (A) shows a block diagram of the scheme for time synchronization; (B) shows a photograph of the test setup using 13 BAMS devices and a vibration generator; (C) shows sound data recorded by the 13 BAMS devices; (D) shows cross-correlation results and time differences between BAMS devices; (E) shows average time differences between BAMS devices; and the error bars correspond to the standard deviation of time differences between devices.

FIG. 32A shows wireless networks of BAMS systems and results for simultaneous spatio-temporal mapping lung sounds and chest wall movements, where (A) and (B) shows (i) CT image and sound distribution of (ii) anterior and (iii) posterior thorax of (A) healthy subject (patient A) and (B) chronic lung disease patient (patient B).

FIG. 32B shows additional results for simultaneous spatio-temporal mapping lung sounds and chest wall movements, where (1) and (2) shows distribution of (i) chest movement, (ii) sound intensity, (iii) dominant sound frequency of (1) a healthy subject and (2) a lung disease patient during exhalation.

FIG. 33 shows a schematic illustration of the locations of devices in a wireless network for lung sound monitoring.

FIG. 34 shows CT images showing coronal and axial sections of a healthy subject, Patient A.

FIG. 35 shows CT images showing coronal and axial sections of a patient with chronic lung disease (Patient B), exhibiting a left upper lobe consolidation, volume loss, and bronchiectasis, consistent with radiation pneumonitis, as well as right peripheral pleuroparenchymal fibrosis.

FIG. 36 shows crackle respiratory sounds detected in the posterior chest of Patient B, where (A) shows a schematic illustration of the locations of a wireless network of device for lung sound monitoring; and (B) shows representative data that illustrate crackle sounds.

FIG. 37 shows analysis of the distribution of lung sounds across healthy subjects and patients with chronic lung disease, where (A) and (B) show correlation of (A) lung sound intensity and air flow rate and (B) lung sound energy and air volume from BAMS systems located on the suprasternal notch, upper and lower posterior chest for 10 healthy subjects; (C) shows dominant frequency of lung sounds on the suprasternal notch, upper chest and lower chest location for 10 healthy subjects during exhalation; (D) shows distribution of the ratio of the upper right and upper left anterior chest lung sound intensity and sound intensity at the suprasternal notch during exhalation for healthy subjects, lung disease patients with both lungs intact, and lung disease patients with either left upper lung resection or right upper lung resection; (E) shows distribution of the right upper posterior dominant expiratory frequency and sound intensity at the suprasternal notch during exhalation in patients with lung disease in the right upper lung, and subjects without lung disease; (F) shows the box plot about ratio of the upper right and upper left anterior chest lung sound intensity for healthy subjects, lung disease patients with both lungs intact, and lung disease patients with either left upper lung resection or right upper lung resection; and (G) shows the box plot about right upper posterior dominant expiratory frequency in patients with lung disease in the right upper lung, and subjects without lung disease; box plots show the range between the 25th and 75th percentiles, and the midline indicates the median for each type of subject.

FIG. 38 shows spectrogram image and the intensity of lung sounds during inhalation and exhalation, where inhale/exhale intensity corresponds to peak sound intensity, and the inhale/exhale sound energy is determined by integrating sound intensity during inhalation and exhalation, as a surrogate for airflow volume.

FIG. 39 shows comparison of left upper and right upper lung sound intensity ratios across

a collection of device mounting locations, where (A) shows a schematic illustration of device locations; and (B) shows the ratios of left upper and right upper anterior chest lung sound intensities, where the error bars correspond to the standard deviation of ratio of intensities.

FIG. 40 shows analysis of the distribution of lung sound intensity across healthy subjects and adult patients with chronic lung disease, where distribution of the ratio of right and left anterior lung sound intensity and sound intensity at the suprasternal notch during exhalation for healthy subjects and lung disease patients with either left lung or right lung resection at (A) the upper chest and (C) the lower chest; and box plots depicting the ratio of right and left anterior lung sound at (B) the upper chest and (D) the lower chest.

FIG. 41A shows analysis of the distribution of lung sound frequency across healthy subjects and patients with chronic lung disease, where distribution of the right posterior dominant expiratory frequency and sound intensity at the suprasternal notch during exhalation in patients with lung disease and subjects without lung disease at the upper chest, and the box plot depicting the dominant expiratory frequency at the upper chest.

FIG. 41B shows analysis of the distribution of lung sound frequency across healthy subjects and patients with chronic lung disease, where distribution of the right posterior dominant expiratory frequency and sound intensity at the suprasternal notch during exhalation in patients with lung disease and subjects without lung disease at the middle chest, and the box plot depicting the dominant expiratory frequency at the middle chest.

FIG. 41C shows analysis of the distribution of lung sound frequency across healthy subjects and patients with chronic lung disease, where distribution of the right posterior dominant expiratory frequency and sound intensity at the suprasternal notch during exhalation in patients with lung disease and subjects without lung disease at the lower chest; and the box plot depicting the dominant expiratory frequency at the lower chest.

FIG. 42 shows scenarios for long-term data storage using streaming data and local flash memory.

FIG. 43 shows an RF system for wireless charging a device while worn on a baby, where (A) shows a schematic illustration and (B) shows a photograph of the wireless charging system integrated into the base of an incubator; (C) shows an infrared (IR) image, and (D) shows temperature of the device during an 8-hour charging period.

FIG. 44 shows time synchronization on the anterior and posterior body surfaces, where (A) shows a schematic illustration of the layout for evaluating errors in time synchronization, (B)

shows microphone data from 13 sensors corresponding to the 60 bpm sound from a metronome, (C) shows a magnified view of sound peak signals, and (D) shows time difference between BAMS sensors and the master sensor during a 2-hour 30-minute recording period.

FIG. 45 shows effects of ambient noise on measurements of respiratory sounds, where (A) shows microphone data and spectrogram image of respiratory sounds with and without 70 dB white noise, (B) shows frequency distribution of respiratory sounds determined by FFT of recorded data, (C) shows a spectrogram image and respiratory sound intensity with bandpass filtering from 150 Hz to 300 Hz, and (D) shows a spectrogram image and respiratory sound intensity with sound separation.

FIG. 46 shows cardiorespiratory sound information, where (A) shows a photograph of the cardiorespiratory sound monitoring set-up using a child heart and lung sounds trainer (Simulaids, Nasco Education), (B) and (D) show spectrogram images of (B) respiratory sounds and (D) cardiac sounds, and (C) and (E) show frequency distribution of (C) respiratory sounds and (E) cardiac sounds determined by FFT of the measured signals.

FIG. 47 shows respiratory rate detection algorithm, where (A) shows a revised respiratory rate detection flowchart; and (B) shows inhale (Marker: x) and exhale (Marker: o) marks and signals of pneumotach, chest movement (IMU), respiratory sound intensity (microphone), and spectrogram of respiratory sound at low and high respiratory signals.

FIG. 48 shows signal associated with activity level, acceleration (x, y, z axis), bandpass filtered acceleration along the z axis from the IMU, and spectrogram plot of data from the microphone during resting, walking, and squatting.

FIG. 49 shows optical images of securely mounted devices adhered to convex and concave regions of an infant model.

FIG. 50 shows the cardiac sound intensity on the Child Heart and Lung Sounds Trainer (Simulaids, Nasco Education) as a function of distance between the body and the microphone.

FIG. 51 shows intestinal motility and gastrointestinal sound in infants in the PICU in response to patient-controlled Analgesia, where (A) and (B) show spectrogram and sound intensity of GI sound (A) before and (B) after patient-controlled analgesia; and (C) shows GI sound peak counts per minute and normalized bowel sound intensity.

FIG. 52 shows an example of periodic breathing detected using a wireless acoustic sensor.

FIG. 53 shows an example of hypopnea and central apnea detected using the wireless

acoustic sensor.

DETAILED DESCRIPTION OF THE INVENTION

The invention will now be described more fully hereinafter with reference to the accompanying drawings, in which exemplary embodiments of the invention are shown. This invention may, however, be embodied in many different forms and should not be construed as limited to the embodiments set forth herein. Rather, these embodiments are provided so that this specification will be thorough and complete, and will fully convey the scope of the invention to those skilled in the art. Like reference numerals refer to like elements throughout.

The terms used in this specification generally have their ordinary meanings in the art, within the context of the invention, and in the specific context where each term is used. Certain terms that are used to describe the invention are discussed below, or elsewhere in the specification, to provide additional guidance to the practitioner regarding the description of the invention. For convenience, certain terms may be highlighted, for example using italics and/or quotation marks. The use of highlighting has no influence on the scope and meaning of a term; the scope and meaning of a term are the same, in the same context, whether or not it is highlighted. It will be appreciated that same thing can be said in more than one way. Consequently, alternative language and synonyms may be used for any one or more of the terms discussed herein, nor is any special significance to be placed upon whether or not a term is elaborated or discussed herein. Synonyms for certain terms are provided. A recital of one or more synonyms does not exclude the use of other synonyms. The use of examples anywhere in this specification including examples of any terms discussed herein is illustrative only, and in no way limits the scope and meaning of the invention or of any exemplified term. Likewise, the invention is not limited to various embodiments given in this specification.

It will be understood that, as used in the description herein and throughout the claims that follow, the meaning of "a", "an", and "the" includes plural reference unless the context clearly dictates otherwise. Also, it will be understood that when an element is referred to as being "on" another element, it can be directly on the other element or intervening elements may be present therebetween. In contrast, when an element is referred to as being "directly on" another element, there are no intervening elements present. As used herein, the term "and/or" includes any and all combinations of one or more of the associated listed items.

It will be understood that, although the terms first, second, third, etc. may be used herein

to describe various elements, components, regions, layers and/or sections, these elements, components, regions, layers and/or sections should not be limited by these terms. These terms are only used to distinguish one element, component, region, layer or section from another element, component, region, layer or section. Thus, a first element, component, region, layer or section discussed below could be termed a second element, component, region, layer or section without departing from the teachings of the invention.

Furthermore, relative terms, such as "lower" or "bottom" and "upper" or "top," may be used herein to describe one element's relationship to another element as illustrated in the figures. It will be understood that relative terms are intended to encompass different orientations of the device in addition to the orientation depicted in the figures. For example, if the device in one of the figures. is turned over, elements described as being on the "lower" side of other elements would then be oriented on "upper" sides of the other elements. The exemplary term "lower", can, therefore, encompasses both an orientation of "lower" and "upper," depending on the particular orientation of the figure. Similarly, if the device in one of the figures is turned over, elements described as "below" or "beneath" other elements would then be oriented "above" the other elements. The exemplary terms "below" or "beneath" can, therefore, encompass both an orientation of above and below.

It will be further understood that the terms "comprises" and/or "comprising," or "includes" and/or "including" or "has" and/or "having", or "carry" and/or "carrying," or "contain" and/or "containing," or "involve" and/or "involving, and the like are to be open-ended, i.e., to mean including but not limited to. When used in this specification, they specify the presence of stated features, regions, integers, steps, operations, elements, and/or components, but do not preclude the presence or addition of one or more other features, regions, integers, steps, operations, elements, components, and/or groups thereof.

Unless otherwise defined, all terms (including technical and scientific terms) used herein have the same meaning as commonly understood by one of ordinary skill in the art to which this invention belongs. It will be further understood that terms, such as those defined in commonly used dictionaries, should be interpreted as having a meaning that is consistent with their meaning in the context of the relevant art and this specification, and will not be interpreted in an idealized or overly formal sense unless expressly so defined herein.

As used in this specification, "around", "about", "approximately" or "substantially" shall generally mean within 20 percent, preferably within 10 percent, and more preferably within 5

percent of a given value or range. Numerical quantities given herein are approximate, meaning that the term "around", "about", "approximately" or "substantially" can be inferred if not expressly stated.

As used in this specification, the phrase "at least one of A, B, and C" should be construed to mean a logical (A or B or C), using a non-exclusive logical OR. As used herein, the term "and/or" includes any and all combinations of one or more of the associated listed items.

The description below is merely illustrative in nature and is in no way intended to limit the invention, its application, or uses. The broad teachings of the invention can be implemented in a variety of forms. Therefore, while this invention includes particular examples, the true scope of the invention should not be so limited since other modifications will become apparent upon a study of the drawings, the specification, and the following claims. For purposes of clarity, the same reference numbers will be used in the drawings to identify similar elements. It should be understood that one or more steps within a method may be executed in a different order (or concurrently) without altering the principles of the invention.

As discussed above, the human body generates various forms of subtle, broadband mechano-acoustic signals that contain valuable information on cardiorespiratory and gastro-intestinal health, as important biomarkers for continuous physiological monitoring. Existing device options, ranging from digital stethoscopes to inertial measurement units, offer useful capabilities but with disadvantages that restrict measurement locations, prevent continuous, longitudinal tracking, limit use to controlled environments, and support only single-point measurements. These constraints are significant for many applications, such as those in monitoring airway obstruction, adventitious lung sounds, and intestinal motility.

In view of the above-mentioned deficiencies, certain aspects of the present invention introduce a wireless, skin-interfaced sensor technology that combines skin-integrated microphones and accelerometers to capture broadband signals that provide information on processes ranging from slow body movements, to digestive activity, to respiratory sounds, to cardiac cycles, all with clinical grade accuracy and independent of artifacts from ambient sounds. In certain embodiments, the broadband signals may span high frequency body sounds (up to frequencies of ~1 kHz) to slow body movements (near 0 Hz), with capabilities for time-synchronized measurements at several body locations simultaneously. These novel wireless, skin-interfaced broadband acousto-mechanical sensing (BAMS) systems have several key features that facilitate the practical application in both the hospital and home environments. First,

the devices include capabilities for separate, simultaneous recordings of sounds from internal body processes and the external environment, as sound is captured using an integrated pair of opposing microphones and interpreted with associated signal-processing algorithms. Second, the small sizes, the lightweight construction, the soft mechanical properties, and the gentle adhesive interfaces allow for measurements from nearly any location of the body, and across broad ranges of patients, from premature infants to elderly patients. This collection of features is currently unavailable in existing research devices such as those that rely exclusively on accelerometers without the ability for sensitive high frequency measurements, or those that leverage advanced digital stethoscopes without the dual-microphone architecture, the skin-compatible form, and the capacity for multimodal continuous operation. The system can also perform spatio-temporal mapping the dynamics of gastro-intestinal processes and airflow into/out of the lungs. Studies demonstrate utility in various aspects of patient care, from premature infants in neonatal intensive care units to adult patients in thoracic surgery clinics.

Real-time monitoring with this BAMS system enables quantitative, continuous tracking of essential body sounds, ranging from multiple aspects of cardiorespiratory function, gastro-intestinal activity, swallowing and respiration, and spatially mapped dynamic properties of air flow into and out of the lungs. Here the inventors report the successful deployment of these BAMS systems in monitoring and providing clinical data for premature babies in neonatal intensive care units (15 subjects) and adult patients (55 subjects) in thoracic surgery clinic. The results suggest broad potential applications of this technology in many aspects of patient care. The following describes the detailed engineering aspects of these technology platforms, quantifies their various measurement capabilities and, where possible, compares the results to state-of-the-art clinically approved technologies.

In view of this, one aspect of the invention relates to a broadband acousto-mechanical sensing (BAMS) system for monitoring physiological signals of a living subject. In one embodiment, the BAMS system includes: one or more wireless, skin-interfaced BAMS devices disposed on the living subject, being time-synchronized and wirelessly communicate with each other, wherein each BAMS device comprises an accelerometer configured to capture acceleration data from the living subject and a pair of microphones configured to capture body sounds from the living subject, and the accelerometer and the acoustic mechanical device in each BAMS device are time-synchronized; and a control device being time-synchronized and wirelessly communicate with the one or more BAMS devices, configured to manage and process

the acceleration data and the body sounds from the one or more BAMS devices and to generate information of body movements and body sounds of the living subject based on the acceleration data and the body sounds obtained by the one or more BAMS devices.

FIG. 1A schematically shows a functional block diagram of a BAMS system according to certain embodiments of the present invention. It should be noted that the BAMS system as shown in FIG. 1A is an exemplary system, and is not intended to limit the apparatus for monitoring physiological parameters of a living subject. In one embodiment, the living subject is a human subject or a non-human subject.

As shown in FIG. 1A, the exemplary system 100 includes a plurality of BAMS devices 110 and 150, namely a first BAMS device 110 and a second BAMS device 150, and a control device 190 adapted in wireless communication with the BAMS devices 110 and 150. The BAMS devices 110 and 150 are wireless, skin-interfaced devices which are time-synchronized and communicate with the control device 190 wirelessly and bidirectionally, and are respectively attached to different positions of the living subject to capture acceleration data and body sounds from the living subject. In one embodiment, each of the BAMS devices 110 and 150 may include an accelerometer configured to capture acceleration data from the living subject and a pair of microphones configured to capture body sounds from the living subject. The accelerometer and the acoustic mechanical device in each BAMS device 110 and 150 are time-synchronized. Specifically, the first BAMS device 110 is disposed at a first position 410 of the living subject, and the second BAMS device 150 is disposed at a second position 420 of the living subject. The control device 190 may be implemented by, for example, a microcontroller unit (MCU) that is being time-synchronized and communicate with the first and second BAMS devices 110 and 150 wirelessly, and is used to manage and process the acceleration data and the body sounds from the first and second BAMS devices 110 and 150 and to generate information of body movements and body sounds of the living subject based on the acceleration data and the body sounds obtained by the first and second BAMS devices 110 and 150.

In one embodiment, the body movements include chest wall movements and abdominal wall excursions, and the body sounds include respiratory sound, lung sounds, gastro-intestinal sounds, bowel sound, and cardiac sounds.

In one embodiment, each of the BAMS devices 110 and 150 may include: a flexible printed circuit board (fPCB); an inertial measurement unit (IMU) disposed on the fPCB, wherein the IMU functions as the accelerometer configured to capture 3-axis acceleration data from the

living subject; and two microphones, respectively disposed on a body-facing side and an ambient-facing side of the FPCB, configured to capture the body sounds from the living subject ambient sounds from the environment.

In one embodiment, each of the BAMS devices 110 and 150 may further include a top elastomer layer and a bottom elastomer layer sandwiching the fPCB, wherein the bottom elastomer layer forms the body-facing surface attached to the living subject, and the top elastomer layer forms the ambient-facing surface.

In one embodiment, each of the BAMS devices 110 and 150 may further include a Bluetooth Low Energy (BLE) system on a chip (SoC) disposed on the fPCB, configured to wirelessly communicate with the control device.

In one embodiment, each of the BAMS devices 110 and 150 may further include an embedded power supply disposed on the fPCB or a wireless charging power supply.

In one embodiment, each of the BAMS devices 110 and 150 may further include is configured to generate the body sound by applying an adaptive filtering algorithm to perform sound separation to the body sounds and the ambient sounds in order to minimize contribution of the ambient sounds to the body sounds.

In one embodiment, the control device comprises a graphical user interface (GUI) configured to real-time display quantitative information of the body movements and the body sounds of the living subject.

It should be noted that, although FIG. 1A shows the BAMS system 100 having two BAMS devices 110 and 150, it is possible that the BAMS system 100 may have only one BAMS device or more than two BAMS devices. In other words, the BAMS system 100 may have one or more BAMS devices.

FIG. 1B schematically shows a control device of FIG. 1A according to certain embodiments of the present invention. As shown in FIG. 1B, the control device 190 is in the form of a computing device, which includes a processor 192, a memory 194, and a storage device 196, and a bus 198 interconnecting the processor 192, the memory 194 and the storage device 196. In one embodiment, the control device 190 may be in the form of a general computer, such as a desktop computer, a laptop computer, a tablet or a mobile device, or a specialized computer or other types of computing devices. In certain embodiments, the control device 190 may include necessary hardware and/or software components (not shown) to perform its corresponding tasks. Examples of these hardware and/or software components may include,

but not limited to, other required memory modules, network ports, interfaces, buses, Input/Output (I/O) modules and peripheral devices, and details thereof are not elaborated herein.

The processor 192 controls operation of the control device 190, which may be used to execute any computer executable code or instructions. In certain embodiments, the processor 192 may be a central processing unit (CPU), and the computer executable code or instructions being executed by the processor 192 may include an operating system (OS) and other applications, codes or instructions stored in the control device 190. In certain embodiments, the control device 190 may run on multiple processors, which may include any suitable number of processors.

The memory 194 may be a volatile memory module, such as the random-access memory (RAM), for storing the data and information during the operation of the control device 190. In certain embodiments, the memory 194 may be in the form of a volatile memory array. In certain embodiments, the control device 190 may run on more than one memory 194.

The storage device 196 is a non-volatile storage media or device for storing the computer executable code or instructions, such as the OS and the software applications for the control device 190. Examples of the storage device 196 may include hard drives, flash memory, memory cards, USB drives, or other types of non-volatile storage devices such as floppy disks, optical drives, or any other types of data storage devices. In certain embodiments, the control device 190 may have more than one storage device 196, and the software applications of the control device 190 may be stored in the more than one storage device 196 separately.

As shown in FIG. 1B, the computer executable code or instructions stored in the storage device 196 may include computer executable instructions 199 for managing and processing the BAMS devices 110 and 150 as shown in FIG. 1A. Specifically, the computer executable instructions 199, when executed at the processor 110, manage and process acceleration data and body sounds obtained from the BAMS devices 110 and 150, and generate corresponding information of body movements and body sounds of the living subject based on the acceleration data and the body sounds obtained by the BAMS devices 110 and 150. In certain embodiments, the computer executable instructions 199, when executed at the processor 110, may further provide a graphical user interface (GUI), such that the GUI may real-time display quantitative information of the body movements and the body sounds of the living subject.

Another aspect of the invention relates to a method of monitoring physiological signals of a living subject with a broadband acousto-mechanical sensing (BAMS) system. In one

embodiment, the method includes: disposing one or more wireless, skin-interfaced BAMS devices on the living subject, wherein the one or more BAMS devices are time-synchronized and wirelessly communicate with each other, and wherein each BAMS device comprises an accelerometer configured to capture acceleration data from the living subject and a pair of microphones configured to capture body sounds from the living subject, and the accelerometer and the acoustic mechanical device in each BAMS device are time-synchronized; and providing a control device being time-synchronized and wirelessly communicate with the one or more BAMS devices, to manage and process the acceleration data and the body sounds from the one or more BAMS devices and to generate information of body movements and body sounds of the living subject based on the acceleration data and the body sounds obtained by the one or more BAMS devices.

In another aspect of the present invention, a BAMS device for capturing physiological signals of a living subject is provided. In one embodiment, the BAMS device includes: a flexible printed circuit board (fPCB); an inertial measurement unit (IMU) disposed on the fPCB, wherein the IMU functions as the accelerometer configured to capture 3-axis acceleration data from the living subject; and two microphones, respectively disposed on a body-facing side and an ambient-facing side of the FPCB, configured to capture the body sounds from the living subject ambient sounds from the environment. The accelerometer and the microphones are time-synchronized.

In certain embodiments, the BAMS system and the method of monitoring physiological signals of the living subject as described above may be applied for detecting specific physiological signals. For example, yet another aspect of the invention relates to a method of detecting hypopnea and central apnea of a living subject with a BAMS system. In one embodiment, the method includes: managing and processing, by a control device being time-synchronized and wirelessly communicate with one or more, skin-interfaced BAMS devices, acceleration data and body sounds from the one or more BAMS devices, wherein the one or more BAMS device are disposed on the living subject, the one or more BAMS devices are time-synchronized and wirelessly communicate with each other, each BAMS device comprises an accelerometer configured to capture the acceleration data from the living subject and an acoustic mechanical device configured to capture the body sounds from the living subject, and the accelerometer and the acoustic mechanical device in each BAMS device are time-synchronized; generating, by the control device, information of body movements and body sounds of the living

subject based on the acceleration data and the body sounds obtained by the one or more BAMS devices; detecting, by the control device, whether the information of the body movements and the body sounds of the living subject show a partial reduction or an absence thereof; and in response to detecting the information of the body movements and the body sounds of the living subject showing the partial reduction or the absence thereof, determining, by the control device, the living subject to have a hypopnea or a central apnea, wherein the partial reduction of the body movements and the body sounds of the living subject indicates the hypopnea, and the absence of the body movements and the body sounds of the living subject indicates the central apnea.

Yet a further aspect of the invention relates to a BAMS system for detecting hypopnea and central apnea of a living subject. In one embodiment, the BAMS system includes: one or more wireless, skin-interfaced BAMS devices disposed on the living subject, being time-synchronized and wirelessly communicate with each other, wherein each BAMS device comprises an accelerometer configured to capture acceleration data from the living subject and an acoustic mechanical device configured to capture body sounds from the living subject, and the accelerometer and the acoustic mechanical device in each BAMS device are time-synchronized; and a control device being time-synchronized and wirelessly communicate with the one or more BAMS devices, configured to manage and process the acceleration data and the body sounds from the one or more BAMS devices and to generate information of body movements and body sounds of the living subject based on the acceleration data and the body sounds obtained by the one or more BAMS devices, detect whether the information of the body movements and the body sounds of the living subject show a partial reduction or an absence thereof, and determine, in response to detecting the information of the body movements and the body sounds of the living subject showing the partial reduction or the absence thereof, the living subject to have a hypopnea or a central apnea, wherein the partial reduction of the body movements and the body sounds of the living subject indicates the hypopnea, and the absence of the body movements and the body sounds of the living subject indicates the central apnea.

In certain embodiments, each BAMS device is configured to generate the body sound by applying an adaptive filtering algorithm to perform sound separation to the body sounds and the ambient sounds in order to minimize contribution of the ambient sounds to the body sounds.

In certain embodiments, each BAMS device further comprises a BLE SoC, configured to wirelessly communicate with the control device.

In certain embodiments, the body movements include chest wall movements and abdominal wall excursions, and the body sounds include respiratory sounds and lung sounds.

In certain embodiments, the control device comprises a GUI configured to real-time display quantitative information of the body movements and the body sounds of the living subject.

These and other aspects of the invention are further described below. Without intent to limit the scope of the invention, exemplary instruments, apparatus, methods and their related results according to the embodiments of the invention are given below. Note that titles or subtitles may be used in the examples for convenience of a reader, which in no way should limit the scope of the invention. Moreover, certain theories are proposed and disclosed herein; however, in no way they, whether they are right or wrong, should limit the scope of the invention so long as the invention is practiced according to the invention without regard for any particular theory or scheme of action.

EXAMPLES

Designs of the broadband acousto-mechanic sensing network system

As discussed above, the BAMS system as discussed above has one or more BAMS devices. FIG. 2A(A) illustrates three clinically relevant applications of the BAMS network system, where recordings capture sounds and physical motions across a frequency range from 1 kHz to near 0 Hz. Gently adhering a single BAMS device at the suprasternal notch allows for simultaneous measurements of cardiac and respiratory sounds, providing continuous monitoring of cardiorespiratory activity, as shown in FIG. 2A(A)(i). Time-synchronized devices placed on the abdomen enable spatio-temporal monitoring of gastro-intestinal sounds, for tracking the progress of digestion, as shown in FIG. 2A(A)(ii). An advanced implementation involves 13 wirelessly time-synchronized devices placed at targeted sites across the anterior and posterior chest for regional monitoring of pulmonary health, rehabilitation, and disease progression, as shown in FIG. 2A(A)(iii). The applicability of this technology spans across nearly any type of patient and age, from premature babies in neonatal intensive care units (NICUs) to patients with chronic lung diseases in the outpatient clinic or in the intensive care unit and patients following lung resection, as demonstrated in the following sections. The picture in FIG. 2A(B) shows a BAMS device on a neonate model, positioned for cardiorespiratory monitoring. A real-time graphical user interface (GUI) displays quantitative information on body movements and a

spectrogram of body sounds at 100 ms intervals, thereby capturing parameters such as body orientations, physical activities, along with sound intensities and frequencies associated with both the body and the ambient sounds. Data communication exploits standard Bluetooth Low Energy (BLE) protocols.

FIG. 2A(C) depicts an exploded view illustration of a BAMS device, which includes an inertial measurement unit (IMU, LSM6DSL, STMicroelectronics), a pair of microphones (ICS-40180, TDK), one body-facing (toward the body) and the other ambient-facing (toward the surroundings), a BLE system on a chip (SoC, ISP-1807, Insight SIP), a 2GB flash memory (MT29F2G, Micron), and a wireless charging antenna mounted, all on a flexible printed circuit board (FPCB). The BAMS system achieves broadband operation by combining an IMU and a pair of microphones with an analog-to-digital converter with high sampling rate, thereby enabling detection of signals across a wide frequency range from measurements of body orientation (fraction of a Hz, ~0.01 Hz) to body sounds (~500 Hz). The 3-axis acceleration data captured by the IMU related to body orientation (~0 Hz), body motion (~1 Hz) and physical activity (~20 Hz) without interference from ambient sounds. The IMU lacks, however, the sensitivity required to measure subtle body sounds such as those associated with respiratory and cardiac activity, and bowel movements. In contrast, the microphone system exhibits high sensitivity in the frequency range of 20 Hz to 20 kHz, making it efficient for capturing even weak body sounds, up to frequencies limited by the analog-to-digital converter in the BLE SoC (~20 kHz samples/second). High fidelity measurements of body sounds represent an advanced capability of the technology reported here, following from the integration of a pair of opposing microphones. These body-facing and ambient-facing microphones allow selective measurements of body and ambient sounds, using algorithms described subsequently. The spectral and temporal characteristics of body sounds without confounding effects of ambient sounds provide insights into subtle activities associated with respiration, digestion, sub-audible vocalizations and cardiac cycles, as the basis of diverse, clinically actionable information for patient care, as shown in FIG. 2A(D). Separate measurements of ambient sounds provide essential circumstantial information that can be important in clinical decision-making. Furthermore, the IMU and microphone sensors exhibit stable performance with deviations of 0.1% and 0.4%, respectively, within the typical body temperature range of 32 °C to 40 °C. This stability enables reliable and consistent use in various clinical cases, as shown in FIG. 3. Real-time data analytics on the time-series data related to body sounds enable detection of risk events ranging from tachycardia and bradycardia to

severe wheezing/coughing, apneic events and digestive abnormalities. An LED encapsulated within the device structure can be activated based on threshold settings to serve as an alarm to caregivers, in addition to warnings and phone calls that can be initiated through the user interface, as shown in FIG. 4.

FIG. 2B shows the results of cardiorespiratory monitoring using an FDA-approved ECG device and a monitoring system for exhaled CO_2, together with the output of a single BAMS device located at the suprasternal notch of a 19-month-old infant. High pass ($f_{cut\text{-}high}$ = 150 Hz) and low pass ($f_{cut\text{-}low}$ = 150 Hz) filtering applied to the microphone data isolates the sounds of respiratory and cardiac activity, respectively. Passing the acceleration data through a bandpass filter ($f_{bandpass}$ = 0.1 - 1 Hz) yields signals related to movements of the chest. The results exhibit strong correlations between chest movements, respiratory sound intensities, and exhaled CO_2 levels, signifying respirations. Also, the S1 and S2 features associated with the cardiac sounds align with the R and T peaks of the ECG data, as expected. FIG. 5 presents a table of comparison of data collected using the BAMS device, with a recently reported wearable stethoscope and with a commercial stethoscope (3M™ Littmann® CORE, Eko). The BAMS system is much smaller (240 times smaller in volume), and lighter (21 times lower in weight) than the commercial stethoscope (3M™ Littmann® CORE, Eko), thereby allowing for continuous hands-free monitoring. The soft and flexible mechanical properties of the BAMS system, the ability for separate measurements of body and ambient sounds, and the capacity for time-synchronized operation across a wireless network of devices represent additional distinguishing features. Additionally, the low power consumption of BAMS system (which is 0.036mA at 3.7V in the stand-by mode, and 2.8 mA at 3.7 V in the active mode) allows for extended periods of continuous monitoring, lasting up to 29 hours. Furthermore, the BAMS system features a wireless charging scheme that enables a fully depleted battery to be charged to its full state in approximately 4 hours, as shown in FIG. 6.

Adaptive algorithms for sound separation.

As mentioned above, the body-facing and ambient-facing microphones capture sound information from two directions to enable differential detection of sounds from the body and the surroundings, as shown in FIG. 7A(A). A two-step adaptive filtering algorithm applied to the data recorded by these two microphones minimizes the contribution of ambient sounds to body sounds as shown in FIG. 8, and vice versa. The application of adaptive filtering algorithm is

unique in the context of body-worn microphones, specifically for continuous physiological monitoring. Additionally, the methods serve dual purposes of separately measuring body and ambient sounds, providing important contextual information to aid in the interpretation of the physiological signals. As an example, without this scheme, environments with crying sounds at 90 dB render detection of cardiopulmonary sounds impossible, as shown in FIG. 7A(B)(i). Sound separation resolves this difficulty, as illustrated in spectrogram representations of data in FIG. 7A(B)(ii) for cardiopulmonary sounds and in audio reconstructions of data. Without separation, the presence of 90 dB white noise, comparable to the sounds of a crying baby or subway noise, decreases the SNR of respiratory sound and cardiac sound by more than 60% and nearly 50%, respectively, as shown in FIG. 9. Separation reduces this decrease to only 2% and 4% for respiratory sound and cardiac sound, respectively. This level of performance surpasses the 12% and 15% reduction associated with the most widely used commercial digital stethoscope (3M™ Littmann® CORE, Eko) which relies on a thick diaphragm and conventional active scheme for noise cancellation. In an environment with 90 dB of white noise, the sound-separated cardiac features extracted from the dual microphone setup and the seismocardiogram data captured by the IMU exhibit SNR values of 20 dB and 12 dB, respectively, for the case of a device mounted on the suprasternal notch. Both results indicate negligible confounding effects of ambient sound, as shown in FIG. 10. Applying the same separation algorithm to data from the ambient-facing microphone using data from the body-facing microphone yields sounds in the environment, with complementary value in understanding the context of patient care, as shown in FIG. 11. This system can also be used in various daily life scenarios, where comprehensive monitoring of not only standard parameters such as heart rate and respiratory rate are possible, but also autonomic measures including heart rate variability (HRV), cardiorespiratory coupling (CRC), and swallowing, all with simultaneous measurements of body orientation and physical activity enabled by the IMU, as shown in FIG. 14A, FIG. 14B and FIG. 15. Moreover, the system demonstrates exceptional performance across various activities, encompassing sleep to exercise, providing high-quality data on physical activity levels, respiratory rate, respiratory sounds (frequency and intensity), heart rate, and cardiac sound intensity over extended periods of time, as shown in FIG. 12. The data collected during sleep also reveal patterns of snoring. Even during intense physical activity, the recordings allow for stable monitoring of respiratory and cardiac sounds. While it is acknowledged that the algorithms have challenges in removing artifacts resulting from physical contact with the devices, the system's overall versatility and

reliability make it a promising tool for continuous and comprehensive health monitoring in diverse real-life situations, as shown in FIG. 13.

Monitoring cardiorespiratory sounds with time-synchronized networks of devices

Multiple devices can be operated simultaneously, as the basis for spatially mapping body sounds from different anatomical locations. For example, high-frequency tracheal and low-frequency vesicular sounds can be captured by recording from the suprasternal notch and the chest area, respectively, as shown in FIG. 7A(D). Reduced speeds of airflow and increased movements of the chest wall at the lower chest lead to decreases in the intensity of the respiratory sounds, defined as the cumulative power spectral density above 150 Hz after a short-time Fourier transform (STFT), as shown in FIG. 7A(E). The intensities of the S1 cardiac sounds are higher than those of S2 on the lower chest, at locations close to the tricuspid and mitral valves of the heart. Conversely, the intensities of S2 sounds generated by the pulmonic and aortic valves are higher than those of S1 on the upper chest and suprasternal notch, as shown in FIG. 7B(1).

The S1 sound appears clearly in data from the lower chest, even during and after exercise, despite short R-R intervals (363 ms, heart rate of 165 beats per min). These intervals and the heart rates determined from the microphone data match those extracted from ECG recordings, with an average error of 0.2 ms and 0.02 beats per min (bpm), thereby establishing the capacity for reliable measurements of HRV, as shown in FIG. 7B(2) and FIG. 16. These results are within regulatory guidelines set by the US FDA (errors less than ±10% or ±5 bpm for HR). The Bland-Altman (BA) plot quantitatively compares the root mean square of continuous difference (RMSSD) between cardiac cycles for HRV. The average difference and standard deviation between RMSSD values extracted from BAMS and ECG waveforms are 0.2 ms and 0.5 ms, respectively, as shown in FIG. 17. Furthermore, the intensity of cardiac sounds, as depicted in FIG. 7B(3), showed an increase during exercise. These sounds have the potential to correlate with blood pressure, as they occur when a moving column of blood comes to a sudden stop or decelerates significantly. Comparing the results from a blood pressure monitor (Finapres® NOVA) with cardiac sound intensity revealed a high correlation trend (FIG. 18) with a Pearson's correlation coefficient of 0.83. The low-frequency nature of cardiac sounds (<150 Hz) provides clean separation from those associated with vocalization, enabling accurate cardiac activity monitoring in daily life scenarios such as exercising, walking, and speaking, after sound

separation, as shown in FIG. 19.

Real-time, continuous measurements of ambient and respiratory sounds in the neonatal intensive-care unit

Premature infants in the NICU are at risk of cardiorespiratory instability due to immature respiratory control centers and respiratory airflow obstruction, which typically manifest as central or obstructive apneas with fluctuations in heart rate and/or oxygen saturation. Noise in the environment can further adversely affect these physiological responses, and excessive auditory stimulation can lead to additional risks of hearing loss and abnormal sensory responses. As a result, continuous monitoring of both cardiopulmonary activity and noise characteristics local to the infant are equally important. Traditional methods for detecting airway obstruction, such as pneumotachography, capnography, nasal pressure or temperature measurements are non-ideal for continuous use due to their bulky wired designs, their sensitivity to artifacts associated with movements and basic operations in clinical care (feeding, diaper changes, and bathing), and their incompatibility with nasal interfaces commonly used to provide non-invasive respiratory support in these infants. Additionally, levels of noise in the NICU room are seldom characterized or monitored. The technology introduced here addresses these shortcomings in a manner that is compatible with standard care practices.

FIG. 20(A) highlights an example of the results of monitoring respiration from premature infants in an academic NICU. FIG. 20(B) shows results from a pneumotach module, with simultaneous chest movements and sound data from a BAMS device on the suprasternal notch. Clear cardiac and respiratory signals appear in the spectrogram below and above 150 Hz, respectively. The pneumotach module detects adequate and reduced airflows, consistent with sound intensities observed in the spectrogram. Segments of absent airflow appear in both body sound and pneumotach measurements. Importantly, these periods of airflow obstruction are not consistently accompanied by absent movements of the chest. Several physiological reasons can explain these discrepancies. First, measurements of chest movements using accelerometry can be susceptible to noise caused by body motion. As a result, the amplitude of the chest movement signal does not necessarily equate with an equivalent and proportional change in lung volume during inspiration and expiration. Second, neonates (and especially preterm infants) are at risk of chest wall distortion due to their highly compliant chest wall. As a result, a rise in the chest movement signal indicates the presence of a respiratory effort but may not correlate with the

degree of airflow during that breath. Third, during brief periods of airflow limitation due to upper airway obstruction, infants continue to make respiratory efforts. For all those reasons, the magnitude of airflow and chest movement signals may not always correspond.

FIG. 20(C) summarizes representative BAMS data from an in-NICU neonate, including ambient noise, body orientation, heart rate, and respiratory rate, in comparison with the readings obtained from FPA-approved clinical monitors, as shown in FIG. 21. The breathing interval and sound intensity determined with the BAMS device correlate with pauses in breathing and breathing airflow rate. FIG. 22 compares respiratory rates determined using pneumotach and body sounds for 10 in-NICU neonates. The average difference and standard deviation of the respiratory rates are 0.44 bpm and 2.13 bpm, respectively. This result lies within the range of FDA-cleared bedside monitoring systems (±3 bpm). The data for normalized airflow rates and respiratory sound intensities of 10 in-NICU newborns show a Pearson's correlation value of 0.87, as shown in FIG. 20(D). Our findings reveal a high level of correlation values compared to those reported in previous studies (the table as shown in FIG. 23). Additionally, FIG. 20(E) and (F) display the distribution of breathing intervals and respiratory sound intensity of 10 neonates over 500 seconds, showcasing the expected inter- and intra-variability in respiratory rates and airflow. The data demonstrate instances with more prolonged periods of airflow obstruction, providing valuable insights into respiratory patterns and abnormalities. FIG. 20Furthermore, the BAMS device reliably monitors respiratory sounds, heart rate, and other physiological parameters over a more prolonged period of 3 hours in a cohort of 5 in-NICU neonates. The difference in heart rate determined using cardiac sounds and ECG waveforms is 0.015 bpm, with a standard deviation of 0.85 bpm, as shown in FIG. 24. Respiratory sounds align well with chest movements and with data from respiratory inductance plethysmography (RIP) and nasal temperature, as shown in FIG. 25. The difference in respiratory rate determined by respiratory sounds and nasal temperature data is 0.06 bpm, with a standard deviation of 1.92 bpm, as shown in FIG. 26. Moreover, the system's capabilities can be extended by mounting two devices with time synchronization—one at the suprasternal notch and the other at the right upper chest—to investigate the movement of air through the trachea and the percentage of air transmitted to the lungs, as shown in FIG. 27. Specifically, in FIG. 27, signals from the microphone in time series and spectrogram representations, along with extracted cardiac sound intensity, breath sound intensity, and breath sound intensity ratio between right upper chest and suprasternal notch. This extension adds valuable insights into the respiratory process, enhancing our understanding of

breathing dynamics. In sum, our BAMS continuous breathing monitoring system simultaneously tracks auditory stimuli, breathing intensity, breathing interval, heart rate, and physical activity, allowing caregivers to better characterize and respond to periods of cardiorespiratory instability in premature infants.

Spatio-temporal tracking of bowel sounds in the neonatal intensive-care unit and in the pediatric intensive care unit

Sounds that result from the movement of food, gas and fluids during intestinal peristalsis provide valuable information on gastro-intestinal (GI) health, of particular importance to the care of newborns in the NICU and the PICU. Tracking these bowel sounds can aid in diagnosis of intestinal motility disorders. In our research, we have observed a correlation between bowel sounds recorded by BAMS devices and electromyography (EMG) signals from an adult's abdomen, as shown in FIG. 28. The intestinal motility and associated muscular contractions in the intestines lead to simultaneous bowel sounds and corresponding EMG signals. Furthermore, the unique capabilities of time-synchronized networks of BAMS devices allow for long-term continuous monitoring of GI sounds, which holds significant promise for studying and understanding the dynamics of intestinal peristalsis over extended periods.

FIG. 29(A) displays such a system attached to the right upper and left lower abdomen of an infant. FIGS. 19(B) and 19(C) present spectrograms and sound intensities recorded from the right upper abdomen before and after feeding, respectively. The data processing flow presented in FIG. 30 identifies peaks in the sound intensity that exceed a certain threshold when accelerations associated with motion are less than 0.1 g, to eliminate artifacts that can arise from physical contact with the device. The trends in normalized intensity and bowel sound peak counts captured from the right and left abdomen appear in FIG. 29(D). The difference in normalized intensities yields spatio-temporal information related to intestinal motility. The number of peaks in bowel sounds for 3 infants increase from an average of 5/min to 21/min before and after feeding, respectively, as shown in FIG. 29(E). The average intensity in the right upper abdomen is 27.5 dB before feeding and 36.9 dB after, as shown in FIG. 29(F). Post feeds, peaks distribute mainly in the right upper quadrant of the abdomen for the first 15 minutes and then largely migrate to the left lower quadrant of the abdomen for the next 15 minutes, as shown in FIG. 29(G). These results align with expectation based on measurements of adult bowel sounds using standard wire-based systems. Additionally, in the investigation of intestinal

motility changes in PICU infants after surgery with patient-controlled analgesia (PCA), a PCA dose of 34 mcg (2 mcg/kg/dose × 16.8 kg) was administered based on patient requests as shown in FIG. 51. We monitored the distribution of GI sounds in the right lower abdomen for around 4 hours. Following PCA delivery, GI sound peaks decreased from an average of 8 to 3 per minute. These results suggest the potential utility of our monitoring system in tracking post-surgery intestinal motility.

High resolution, spatio-temporal mapping of lung sounds from patients in thoracic surgery clinic

Strategies for wireless, time-synchronized operation of BAMS devices such as the one described in the previous section enable measurements with an average timing difference of 0.2 ms and a standard deviation of 6 ms, as shown in FIG. 31. This feature can be exploited to capture the distribution of lung sounds and body motions at many anatomical locations simultaneously so that the same breath may be analyzed across a range of lung regions. By utilizing positional information from sensors attached to the chest and back, a time-synchronized signal is used to create spatio-temporal maps of lung sound intensity, frequency, and chest displacement. This process involves linear interpolation to accurately represent the distribution of lung sounds and body motions over time and space. The results obtained from these spatio-temporal map can enhance diagnosis and monitoring of various lung pathologies. The following pilot study utilized 13 BAMS devices mounted on the anterior and posterior chests of 20 healthy subjects and 35 patients with chronic lung disease, as depicted in FIG. 33. FIG. 32A(A) and FIG. 34 display CT images of the lungs of a healthy subject (Patient A) alongside spectrograms of sounds over 150 Hz captured by the BAMS devices during inhalation and exhalation. FIG. 32A(B) and FIG. 35 display corresponding results for a patient with chronic lung disease (radiation pneumonitis and fibrosis), who additionally had their right upper lung lobe, and part of their left upper lung lobe and right lower lung lobe resected (Patient B). Data from healthy subject, Patient A, exhibit similar distributions of chest wall movement, maximum sound intensities, and sound frequencies for the left and right sides of the body, as shown in FIG. 32B(1). The decrease in the frequencies and intensities of sounds from the lower chest result from physiologic reduced rates of airflow and increased thickness of the chest wall.

Similar measurements performed on patients with chronic lung diseases and patients who have undergone surgical lung resections reflect their condition. For the Patient B featured in FIG.

32A(B) and FIG. 35, Patient B with a history of resection surgery in the right upper and lower lobes and the left upper lobe showed decreased pulmonary function in the removed lobes, resulting in reduced airflow rates and lower sound intensity in the corresponding mapping, as shown in FIG. 32B(2)(ii). Additionally, Patient B's condition, with right peripheral pleuroparenchymal fibrosis, exhibited high-frequency lung sounds and crackle sounds in the right lung, as seen in FIG. 32B(2)(iii) and FIG. 36. These findings serve as valuable indicators for monitoring the progression of lung disease.

FIG. 37 presents a comparative analysis of data obtained from healthy subjects and patients with chronic lung diseases. This analysis highlights the significance of airflow rate, airflow volume, and sound frequency for the diagnosis of obstructive and restrictive lung diseases. The results rely on data from BAMS devices mounted on the suprasternal notch and the upper and lower posterior regions of the chest, along with separate measurements of nasal airflow rate and flow volume using a peak flow meter. During exhalation, the airflow rate corresponds to the maximum sound intensity of the cumulative power spectral density at 150 Hz and higher. An additional parameter, the sound energy, can be calculated by integrating the sound intensity over time, for comparison to the nasal airflow volume, as shown in FIG. 38. FIG. 37(A) shows a correlation between sound intensity measured at different locations (suprasternal notch, upper posterior and lower posterior thorax) and nasal airflow rate for 10 healthy subjects. The Pearson's correlation values between sound intensity and nasal airflow rate are 0.73, 0.79, and 0.75 at the suprasternal notch, upper and lower posterior positions, respectively. Similarly, correlation values between sound energy and nasal airflow volume are 0.71, 0.76, and 0.75 at these corresponding locations, respectively, as shown in FIG. 37(B). FIG. 37(C) illustrates the dominant frequency distribution of lung sounds in healthy subjects at each location. This information is relevant in monitoring obstruction and airway conditions in patients with heterogeneous lung disease states. Specifically, as a marker of both airflow and volume, these parameters can assist with tracking of disease progression or response to treatment in these chronic lung disease patients. The estimation of airflow rate and air volume based on data from the BAMS devices can additionally facilitate monitoring of the Tiffeneau-Pinelli index, with the potential for routine, daily monitoring of lung disease and diagnosis of obstructive and restrictive pulmonary diseases.

FIG. 37(D) and (F) show the sound intensity measured at the suprasternal notch and the ratio of intensities from the left and right upper anterior chest for healthy subjects, chronic lung

disease patients with no lung resections, and patients with right upper lobe or left upper lobe resections. Healthy subjects exhibit higher sound intensity at the suprasternal notch than chronic lung disease patients, with an average intensity of 54 dB. In contrast, chronic lung disease patients without lung resections, those with left upper lung resections, and right upper lung resections have average intensities of 38 dB, 30 dB, and 36 dB, respectively. Moreover, the average sound intensity ratios (left upper lung sound intensity / right upper lung sound intensity) are 0.98, 1.01, 0.78, and 1.5, respectively, consistent with a reduction in sound intensities at locations of resected lung tissues. The variations in this ratio exceed those attributable to uncertainties in attachment position, as depicted in FIG. 39. FIG. 37(E) and (G) compare the dominant expiratory frequency of the right upper posterior lung between healthy patients and those with chronic lung disease. The latter group exhibits an average frequency of 256 Hz. The healthy subjects show frequencies of 219 Hz, distinguishing them from the patients with lung disease (P-value < 0.05). The onset of lung disease increases airway restrictions, thereby increasing the dominant sound frequency. Furthermore, sound intensity and frequency analyses conducted at diverse locations of the upper, middle, and lower lobes of the lungs reveal notable differences between healthy subjects and patients with lung conditions, as presented in FIGS. 40, 41A, 41B and 41C. Specifically, in each of FIGS. 40, 41A, 41B and 41C, the box plots show the range between the 25th and 75th percentiles, with the median indicated by the midline for each subject type. These findings contribute to a deeper understanding of lung pathologies and assist in the diagnosis and management of respiratory disorders.

Discussion

The present study introduces a technology designed for simultaneous measurements of body movements and sounds as a reliable source of physiological signals, with applicability in the hospital and at home. Demonstration examples span from premature neonates with respiratory and digestive disorders in the NICU to adult patients with lung disease in pulmonology clinics and patients in thoracic surgery clinic. Various characterization studies and performance benchmarking measurements confirmed the accuracy of the system, and the uniqueness of its operational capabilities. The dual-microphone (body- and ambient-facing) design, the sound separation algorithms, the broadband capabilities, the time-synchronized operation of networks of devices, and the small, skin-compatible form factors, have created a broad range of unique possibilities in patient monitoring that deserve evaluation.

In the NICU, assessment of respiratory, cardiac, and gastro-intestinal sounds is an integral part of every aspect of nursing and medical care provided to all patients regardless of gestational age at birth. The incorporation of BAMS devices into clinical practice offers the possibility for continuous monitoring of these body sounds, allowing decreased patient handling, reduced exposure to external vectors of infection (including the stethoscope), and timely feedback in cases of physiological alterations. When placed at the suprasternal notch, the BAMS device can detect both airflow (using the dual-microphone setup) and chest movements (using the IMU component), which in combination allow for the identification and classification of all apnea subtypes (central, obstructive, and mixed apneas). Indeed, apneas are ubiquitous in preterm infants and are a leading cause of in-hospital morbidities and prolonged NICU hospitalization, yet cannot be accurately distinguished in terms of subtype (central, obstructive, mixed) using current monitoring standards. As such, enhanced apnea detection and classification in this population may lead to more targeted and personalized management approaches, improved patient outcomes, and reduced length of hospitalization and costs. In addition, the BAMS system may aid in quantifying the degree of airflow obstruction in at-risk term neonates, such as infants with severe hypotonia (ex: Trisomy 18, Prader-Willi Syndrome) and congenital upper airway obstruction (ex: Pierre-Robin Sequence). When placed simultaneously at the right and left anterior chest in mechanically ventilated neonates, resulting data can provide real-time feedback whenever the air entry is diminished on one side relative to the other; this may promptly alert the clinician of a possible pathology such as atelectasis, consolidation, or a pneumothorax, thereby leading to early diagnosis and treatment. When placed at different quadrants of the abdomen, reduced bowel sounds may act as an early warning sign for impending gastro-intestinal complication such as bowel dysmotility, obstruction or necrotizing enterocolitis, or sensitivity to opiates. In contrast, increasing bowel sounds may serve as objective markers of improved peristalsis and bowel health after a gastro-intestinal surgery, thereby aiding in the decision to resume or progress feeds.

Sleep is essential to health and well-being at all ages, but especially in infancy and childhood when complex maturational processes are evolving over several years. Sleep-disordered breathing is reported in 11% of children, but access to pediatric sleep laboratories is limited especially for traditionally underserved patients. Delays in evaluation in pediatric sleep laboratories may place these vulnerable children at risk for morbidity and potentially mortality. Once in a pediatric sleep laboratory, the child must undergo continuous physiologic recording

with a multitude of wired electrodes on the head, chest, and extremities in an unfamiliar bed, likely disrupting natural sleep patterns. Once validated across varied body habitus and clinical conditions, these devices introduced here offer the opportunity to wirelessly and non-invasively collect physiologic data in-laboratory for children from infancy to adulthood. The logical next advance is to introduce this technology in the home, allowing for characterization of each child's personal signature for cardiorespiratory regulation in health and then with ill-health, and to identify which child will benefit from more comprehensive and attended in-laboratory testing.

The other area of opportunity explored here involves advanced assessment of lung health. Performing a thorough auscultation evaluation of the lungs with a stethoscope requires considerable expertise and requires, typically, 10 minutes in a manual process. With the time constraints placed on physicians, this may lead to inaccurate, rushed examinations yielding delays in appropriate diagnostic work-ups and treatments. Furthermore, a recent meta-analysis by Arts et al, indicates that lung auscultation has poor sensitivity for different pulmonary pathologies and breath sounds. A network of time-synchronized BAMS devices overcomes these limitations, with a broad range of clinical applications, especially in the management of critically ill patients as well as pulmonary and thoracic surgery patients. Standard pulmonary function tests do not provide regional lung function assessments, as they provide just a single numeric value meant to represent both lungs as an aggregate. These tests operate under the assumption that all regions of the lung contribute equally to function, which is not the case, particularly in chronic lung disease. The technology reported here can be utilized alone or in conjunction with pulmonary function tests, and in both the inpatient and outpatient setting, where it can provide real time insight into regional lung function and disease status. These capabilities are of particular interest to thoracic surgeons when performing pre-operative planning as it provides information on how much an area of lung that they are planning to resect may contribute to overall respiratory function. This knowledge can allow thoracic surgeons to better advise on patients' management and more appropriately risk stratify patients at high risk for post-operative complications. Furthermore, the portable nature of the BAMS system allows for easy use in various settings, including home environments. As a result, it facilitates post-operative management of lung resection through daily monitoring, enabling tracking of regional lung recovery and the development of any detrimental complications, ultimately enhancing the quality of medical management. Additionally, if the time scale is extended to many hours /days, this would allow for the gathering of more clinical information to assess if any underlying pathology

has temporal or circadian symptoms (*i.e.*, worse in morning, at night, when exercising or sleeping) or environmental perturbations (*i.e.*, orthostatic or other postural changes). Interest extends to providers who treat chronic lung diseases, such as chronic obstructive pulmonary disease, interstitial lung disease and pneumonia, as these devices can allow them to monitor patient's regional lung function to assess the efficacy of current medical management.

Uses extend to ventilatory management in the intensive care units for adults. Children, and neonates. Managing ventilated patients is an art augmented by science, with many guidelines/practices that are controversial and variable, as clearly evident during the COVID-19 pandemic. The BAMS devices may assist providers in determining ventilator settings, by giving them real-time feedback on regional lung ventilation to ensure adequate respiratory support. Given the lack of portable diagnostic tools, providing real-time regional lung function assessment at the bedside is critically important since patients currently must be transferred off the intensive care unit to obtain other diagnostic tests, which can put the patient in danger.

Additional possibilities, examined by not systematically explored in the results presented here, include (1) monitoring of swallowing events and respiratory cycles for patients with dysphagia, (2) tracking of patterns of speech for patients with dementia and (3) measuring a collection of parameters, including HRV, related to cardiorespiratory function for patients with diabetes, high blood pressure, cardiac arrhythmias, asthma, anxiety, and depression. These and other possibilities in recordings of unusual biophysical markers represent areas of current work.

Methods

Fabrication of BAMS devices

Each device included five components: a pair of microphones, an IMU, Flash memory, a Bluetooth SoC, and hardware for power and wireless charging. Locating the first two components on separate islands with serpentine traces as interconnects enhanced the mechanical deformability of the system. The ambient-facing and body-facing microphones (ICS-40180, TDK) each connected to an amplifier circuit with a 64-fold gain and a bandpass filter from 10 Hz to 2 kHz. The amplified signal was converted into a 14-bit ADC value at a sampling rate of 1 kHz. The IMU (LSM6DSL, STMicroelectronics) delivered three-axis acceleration data at a sampling rate of 104 Hz to the Bluetooth SoC (ISP-1807, Insight SIP) via serial peripheral interface communication protocols. The microphone data at 1 kHz and the IMU data at 104 Hz passed into 2 GB Flash memory (MT29F2G, Micron) with time stamps defined using an internal

clock at 16 MHz. By utilizing a 2GB Flash memory, the inventors are able to store data in the local memory for up to 16 hours. For continuous monitoring over periods longer than 16 hours, we can transfer the data in real-time to an iPad/iPhone placed nearby. Local memory can then be used for data storage during other times, as shown in FIG. 42. The wireless charging and power components included a charging coil with a resonance frequency of 13.56 MHz, a voltage rectifier, a voltage regulator, a battery charger IC, and a 3.7 V lithium-polymer battery (110 mAh). Customized firmware was uploaded to the Bluetooth SoC using Segger Embedded Studio. A silicone elastomer (Silbione-4420) defined an encapsulating structure, with overall dimensions of 40 × 20 mm^2, a thickness of 8 mm, and a weight of 6 g.

Wireless Charging System

The BAMS system incorporates a wireless charging scheme that operates at a standard radio frequency band of 13.56 MHz, which is approved by the Federal Communications Commission (FCC) for use in industrial, scientific, and medical devices. This frequency band is chosen for its minimal absorption in living tissues, ensuring the safety and well-being of the user during charging. During routine use, the BAMS device is removed from the body for charging, ensuring a convenient and hassle-free charging experience. However, in certain demanding situations where continuous monitoring is crucial, such as with infants, the device can be considered for charging while still being worn by the baby. To assess the safety and efficacy of in-situ charging, we conducted tests using an infant model and monitored the temperature during an 8-hour charging period using an IR camera (FLIR ONE pro, FLIR Inc.). The results showed that the temperature difference between the device and the ambient environment was consistently maintained within 0.5 °C throughout the charging process, as shown in FIG. 43. This temperature stability demonstrates the safe and controlled charging performance of the BAMS device, ensuring that it remains well within the acceptable temperature range for use with infants.

Characterization of the body-facing and ambient-facing microphones

Experiments with white noise (frequencies from 20 Hz to 400 Hz) and a commercial sound meter in a sound-proof RF room served as the basis for characterizing the performance of the microphones. A linear fitting process calibrated the decibels of white noise to the sound intensity measured as integration of the power spectral density from 20 Hz to 400 Hz associated with short-time Fourier transforms of the microphone data, as shown in FIG. 11.

Tests of sound separation algorithms using two-step adaptive filtering involved a BAMS device and a commercial digital stethoscope (3M™Littmann® CORE, Eko) with active noise cancellation mounted on a lung sound trainer to produce constant breath and lung sounds. Measurements examined the effects of the decibel level of various types of noise sources. In the presence of 90 dB white noise (frequencies from 20 Hz to 400 Hz), the signal-to-noise ratio (SNR) of respiratory and cardiac sounds captured using the commercial digital stethoscope decreased by 12% and 15%, respectively. Without sound separation in the BAMS device, the SNR decreased by 62% and 48%, respectively (FIG. 9). However, with separation, the reduction in SNR was only 2% and 4% for the BAMS device.

Time-synchronized network system

The scheme for time synchronization between multiple devices exploited a master device to broadcast its 16 MHz local clock information through RF signals at 100 ms intervals to slave devices with different RF addresses. Updates to the local clock information of the slave devices used the clock information received from the master. This clock information also passed to the mobile device, for storage in memory with the coordinated universal time.

Characterization of the accuracy of this scheme involved monitoring the peak delay between 13 devices exposed to sound swept from 500 Hz to 1 kHz sourced from a vibration generator at a speed of 5 Hz/s. Cross-correlation of time series sound data defined the time delays between each device. The results showed an average timing difference of 0.2 ms and a standard deviation of 6 ms, as shown in FIG. 31. During on-body testing, a master device was placed next to the monitoring iPad to transmit accurate time information. We attached 13 BAMS devices to the chest and back of the body, and they received time information from the master through RF communication. To assess time synchronization errors, sound from an external metronome was used to calculate the time differences of sound peaks recorded by each sensor. The results, as shown in FIG. 44, revealed an average time difference of 0.4 ms and a maximum time difference of 6 ms over a duration of 2 hours and 30 minutes. With Bluetooth 5 standards used in recent iPhone and iPad models, it is possible to connect and control more than 30 Bluetooth devices simultaneously. This capability allowed us to control time-synchronized devices simultaneously through a graphical user interface (GUI). To minimize communication load on the control iPad, which connects all 13 sensors, we stored the data in local flash memory instead of streaming the data in real-time.

Sound separation

Data collected from the body-facing and ambient-facing microphones included contributions from body sounds and ambient sounds. Sound separation used a two-step adaptive filtering method, as depicted in FIG. 8. In the first adaptive filtering, the ambient sound noise signal is extracted by subtracting the body-facing microphone's sound signal from the ambient-facing microphone's sound signal. In the second adaptive filtering, the body sound signal is obtained by subtracting the ambient sound noise signal, extracted by the first adaptive filtering, from the sound signal of the body-facing microphone. These processes use the recursive least squares (RLS) adaptive filter provided in MATLAB at each adaptive filtering step. The RLS filtering parameters involve a filter length of 10 taps and a forgetting factor of 0.98.

To verify the effectiveness of sound separation, a validation experiment was conducted using respiratory sound measurements. Initially, respiratory sounds were recorded for 24 seconds without any ambient noise on the lung sound trainer (Simulaids, Nasco Education), as shown in FIG. 45(A). Subsequently, respiratory sound measurements were continued, this time with the addition of 70 dB white noise. When examining the frequency distribution of respiratory sounds without ambient noise, a relatively even distribution was observed above 150 Hz, as shown in FIG. 45(B). However, when ambient sound noise above 150 Hz was present, it significantly distorted the respiratory sound signals. Even after applying bandpass filtering within the range of 150 Hz to 300 Hz, where respiratory sounds are relatively strong, the respiratory sound signals remained unclear due to the presence of ambient noise, as shown in FIG. 45(C). The respiratory sound intensity between 150 Hz and 300 Hz exhibited a signal-to-noise ratio (SNR) of 27 dB without ambient noise, but it decreased to 17 dB in the presence of 70 dB ambient noise. However, the sound separation techniques employed in the BAMS device effectively separated the respiratory sound signals from the ambient noise, as shown in FIG. 45(D). Clear respiratory sound signals were observed on the spectrogram even in the presence of ambient noise after applying the sound separation process. The SNR of the sound intensity was maintained at 26 dB.

Cardiorespiratory sound analysis

The data were processed using a two-step adaptive filtering method and subjected to low-pass and high-pass filtering (third order, with an attenuation rate of -58 dB/decade) with a cutoff frequency of 150 Hz. This filtering process effectively distinguished between respiratory and

cardiac sounds based on their frequency characteristics. The analysis revealed that 76% of the total signal for respiratory sounds exists above 150 Hz, while 81% of the total signal for cardiac sounds exists below 150 Hz, as shown in FIG. 46. Short-time Fourier transform (STFT) yielded power spectral density information for each frequency of the filtered signal, with a window size of 0.03 seconds and overlap length of 0.027 seconds. The respiratory sound intensity values followed from integrating the power spectral density across frequencies higher than 150 Hz. Similar data for cardiac sounds followed from integrating the power spectral density associated across frequencies between 20 Hz and 150 Hz. The respiratory and cardiac sound intensity data were then used to identify peaks in respiratory and cardiac cycles. For calculating the respiratory rate, intensity peaks corresponding to inhalation and exhalation events were identified on the respiratory sound intensity graph. Chest movement data was used to distinguish between inhalation and exhalation during the detection of each sound intensity peak. The respiratory rate was then calculated by selecting the maximum value between the count of inhalation sound peaks and exhalation sound peaks over a 60-second period. This approach prevents the underestimation of the respiratory rate caused by the overlap of inhalation and exhalation sounds in the high respiratory rate, as shown in FIG. 47.

For body orientation analysis, the 3-axis acceleration signal obtained from the IMU was filtered using a Butterworth low-pass filter (third order) with a cut-off frequency of 0.1 Hz. The body orientation was calculated from the filtered signals via simple trigonometry. Additionally, the chest movement signal was obtained by applying a bandpass filter (third order) with a frequency range between 0.1 Hz and 1 Hz. The chest movement signal correlated well with the detected respiratory sounds from the microphone, even under low-frequency movements such as resting (near 0 Hz movement), walking (0.8 Hz movement), and squatting (0.2 Hz movement), as shown in FIG. 48. Physical activity levels were monitored using the root mean square of the acceleration values along the x, y, and z axes, processed with a Butterworth bandpass filter (third order) between 1-10 Hz.

Bowel sound analysis.

The data were processed using a two-step adaptive filtering method with a bandpass filtered between 150 Hz and 400 Hz to eliminate heart sound. A short-time Fourier transform (STFT) of the filtered signal, with a window size of 0.03 seconds and overlap length of 0.027 seconds, yielded the power spectral density. Integration of these data over frequencies higher

than 150 Hz yielded bowel sound intensity data. Sound peaks with widths of less than 100 ms and intensities greater than 20 dB were then identified. To eliminate signals that can result from movements or physical contacts with the device, only features during periods of physical activity (accelerations from the IMU) with magnitudes less than 0.1 g were included in the identification of bowel sound peaks.

Device mounting

A medical-grade adhesive (2477P, 3M Medical Materials & Technologies, NM,USA) is used as interface between BAMS and skin body that is widely recognized and approved for use in the context of bandages (ISO 10993-5) and for the fragile skin of preterm infants. This adhesive allowed for reliable and secure fixation of the device to the infants in this study, with a median gestational age of 28 weeks (min 25 to max 31 weeks) and a median postmenstrual age of 35 weeks (min 33 to max 36 weeks), with no adverse skin reactions during placement or after removal of the sensors. Furthermore, we previously reported on a slightly larger wireless wearable device using the same adhesive in a cohort of 50 neonates with gestational ages 23 to 40 weeks and postnatal ages 1 week to 4 years, with no instances of skin breakdown or dermatitis (as graded by a certified dermatologist). Furthermore, these Silicone-based adhesives also conform rapidly and easily to uneven surfaces, which makes them practical in infants with limited space options for placement of the sensor, as shown in FIG. 49. The microphone collects data from the skin through the bottom layer, PI film, and adhesive. We used a thickness of 0.3mm for the bottom layer, 50um for the PI film, and 0.5mm for the adhesive to achieve high sensitivity in capturing acoustic signals to place the sensor close to the body, as shown in FIG. 50.

Clinical tests

The study protocol was approved by the Northwestern Medicine Institutional Review Board (STU00218021) and the McGill University Health Center Research Ethics Board (IRB00010120). Informed consent was obtained from all participants or their guardians. Trained research staff placed BAMS devices on the participants in a location that did not interfere with clinical monitoring equipment. Monitoring in the neonatal intensive care unit included ECG, nasal temperature, chest and abdomen movements using respiratory inductance plethysmography (RIP), and a pneumotachograph device. Research staff recorded additional information such as

clinical data, infant movement, and fussing during data collection. For the lung sound patient study, the research staff attached 13 devices to the anterior and posterior chest as follows.

- Right upper chest (2nd intercoastal space, mid-clavicular line)
- Right lower chest (4th intercoastal space, mid-clavicular line)
- Right axilla (6th intercoastal space, mid-axillary line)
- Right upper back (2nd intercoastal space, between the medial scapular edge and spine)
- Right mid back (5th intercoastal space, between the medial scapular edge and spine)
- Right lower back (8th intercoastal space, just inferior to the tip of the scapula)
- Left. Upper chest (2nd intercoastal space, mid-clavicular line)
- Left lower chest (4th intercoastal space, mid-clavicular line)
- Left axilla (6th intercoastal space, mid-axillary line)
- Left upper back (2nd intercoastal space, between the medial scapular edge and spine)
- Left mid back (5th intercoastal space, between the medial scapular edge and spine)
- Left lower back (8th intercoastal space, just inferior to the tip of the scapula)
- Suprasternal notch

After attaching the devices, participants took five deep breaths, inhaling and exhaling fully. Patient information was obtained retrospectively from the medical records, including demographic data, smoking status, medical history, spirometry data, vital signs, and results from diagnostic tests, including computed tomography images.

Data statistics

Statistical analysis was performed with a one-way multivariate analysis of variance (MANOVA) in MATLAB, with an assumption that data points for each group are normally distributed. The analysis of neonatal heart rate involved the use of 136,013 body sound datapoints and FDA-approved ECG monitor data collected from 5 neonates. Respiratory data analysis utilized a cumulative 43,750 body sound datapoints, 43,738 nasal temperature recordings, and 1,012 pneumotach datapoints collected from 15 neonates. Bowel sound analysis was performed on data collected from 3 neonates, consisting of 251 bowel sound peaks data. Lung sound analysis was conducted on 10,660 lung sound datapoints collected from 20 healthy subjects and 35 lung patients, using 13 BAMS devices.

FIG. 52 shows an example of periodic breathing detected using a wireless acoustic sensor. The data as shown in FIG. 52 was obtained from a sample recording of a preterm infant in the pilot project. Specifically, the following signals are presented in FIG. 52, from top to bottom: (1) airflow signal derived from the microphone component of the wireless acoustic sensor; (2) abdominal excursions derived from respiratory inductance plethysmography; (3) chest wall movements derived from the inertial measurement unit component of the wireless acoustic sensor; and (4) oxygen saturation signal. The recording shows an example of periodic breathing, as there are three normal breathing cycles separated by two brief central apneas (absence of airflow and chest or abdominal wall excursions). This respiratory event led to an oxygen desaturation.

FIG. 53 shows an example of hypopnea and central apnea detected using the wireless acoustic sensor. The data as shown in FIG. 53 was obtained from a sample recording of a preterm infant in the pilot project. Specifically, the following signals are presented in FIG. 53, from top to bottom: (1) airflow signal derived from a nasal thermistor; (2) airflow signal derived from the microphone component of the wireless acoustic sensor; (3) abdominal excursions derived from respiratory inductance plethysmography; (4) chest wall movements derived from the inertial measurement unit component of the wireless acoustic sensor; and (5) oxygen saturation signal. The recording shows an example of a hypopnea, characterized by a partial reduction in the amplitude of the airflow signal and chest and abdominal wall excursions (red dotted rectangle). This is followed by a brief period of regular breathing and then a brief central apnea, characterized by absence of airflow and chest or abdominal wall excursions (green dotted rectangle).

The foregoing description of the exemplary embodiments of the invention has been presented only for the purposes of illustration and description and is not intended to be exhaustive or to limit the invention to the precise forms disclosed. Many modifications and variations are possible in light of the above teaching.

The embodiments were chosen and described in order to explain the principles of the invention and their practical application so as to enable others skilled in the art to utilize the invention and various embodiments and with various modifications as are suited to the particular use contemplated. Alternative embodiments will become apparent to those skilled in the art to which the invention pertains without departing from its spirit and scope. Accordingly, the scope of the invention is defined by the appended claims rather than the foregoing description and the

exemplary embodiments described therein.

Some references, which may include patents, patent applications, and various publications, are cited and discussed in the description of this invention. The citation and/or discussion of such references is provided merely to clarify the description of the invention and is not an admission that any such reference is "prior art" to the invention described herein. All references cited and discussed in this specification are incorporated herein by reference in their entireties and to the same extent as if each reference was individually incorporated by reference.

REFERENCE LIST:

1. Virani, S.S., *et al.* Heart Disease and Stroke Statistics-2020 Update: A Report From the American Heart Association. *Circulation* **141**, e139-e596 (2020).
2. Rajaratnam, J.K., *et al.* Neonatal, postneonatal, childhood, and under-5 mortality for 187 countries, 1970-2010: a systematic analysis of progress towards Millennium Development Goal 4. *Lancet* **375**, 1988-2008 (2010).
3. Choi, Y.S., *et al.* A transient, closed-loop network of wireless, body-integrated devices for autonomous electrotherapy. *Science* **376**, 1006-1012 (2022).
4. Jeong, H., *et al.* Differential cardiopulmonary monitoring system for artifact-canceled physiological tracking of athletes, workers, and COVID-19 patients. *Science advances* **7**, eabg3092 (2021).
5. Kaszala, K. & Ellenbogen, K.A. Device sensing: sensors and algorithms for pacemakers and implantable cardioverter defibrillators. *Circulation* **122**, 1328-1340 (2010).
6. Liu, C., *et al.* Wireless, Skin-Interfaced Devices for Pediatric Critical Care: Application to Continuous, Noninvasive Blood Pressure Monitoring. *Adv Healthc Mater* **10**, e2100383 (2021).
7. Chung, H.U., *et al.* Binodal, wireless epidermal electronic systems with in-sensor analytics for neonatal intensive care. *Science* **363**, eaau0780 (2019).
8. Chung, H.U., *et al.* Skin-interfaced biosensors for advanced wireless physiological monitoring in neonatal and pediatric intensive-care units. *Nature medicine* **26**, 418-429 (2020).
9. Wang, M., *et al.* A wearable electrochemical biosensor for the monitoring of metabolites and nutrients. *Nature Biomedical Engineering*, 1-11 (2022).
10. Boriosi, J.P., Zhao, Q., Preston, A. & Hollman, G.A. The utility of the pretracheal stethoscope in detecting ventilatory abnormalities during propofol sedation in children. *Pediatric Anesthesia* **29**, 604-610 (2019).
11. Du, X., Allwood, G., Webberley, K.M., Osseiran, A. & Marshall, B.J. Bowel sounds identification and migrating motor complex detection with low-cost piezoelectric acoustic sensing device. *Sensors* **18**, 4240 (2018).
12. Jahin, S., Moniruzzaman, M., Alvee, F.M., Haque, I.U. & Kalpoma, K.A. A Modern Approach to AI Assistant for Heart Disease Detection by Heart Sound through created e-Stethoscope. in *2022 25th International Conference on Computer and Information Technology (ICCIT)* 669-674 (IEEE, 2022).

13. Kölle, K., Aftab, M.F., Andersson, L.E., Fougner, A.L. & Stavdahl, Ø. Data driven filtering of bowel sounds using multivariate empirical mode decomposition. *BioMedical Engineering OnLine* **18**, 1-20 (2019).
14. Lee, S.H., *et al.* Fully portable continuous real-time auscultation with a soft wearable stethoscope designed for automated disease diagnosis. *Science Advances* **8**, eabo5867 (2022).
15. Pasterkamp, H. The highs and lows of wheezing: a review of the most popular adventitious lung sound. *Pediatric pulmonology* **53**, 243-254 (2018).
16. Sharma, P., Imtiaz, S.A. & Rodriguez-Villegas, E. Acoustic sensing as a novel wearable approach for cardiac monitoring at the wrist. *Scientific reports* **9**, 20079 (2019).
17. Zhou, L., *et al.* Acoustic analysis of neonatal breath sounds using digital stethoscope technology. *Pediatric Pulmonology* **55**, 624-630 (2020).
18. Jeong, H., *et al.* Closed-loop network of skin-interfaced wireless devices for quantifying vocal fatigue and providing user feedback. *Proceedings of the National Academy of Sciences* **120**, e2219394120 (2023).
19. Kang, Y.J., *et al.* Soft skin-interfaced mechano-acoustic sensors for real-time monitoring and patient feedback on respiratory and swallowing biomechanics. *NPJ digital medicine* **5**, 147 (2022).
20. Lee, K., *et al.* Mechano-acoustic sensing of physiological processes and body motions via a soft wireless device placed at the suprasternal notch. *Nature biomedical engineering* **4**, 148-158 (2020).
21. Chowdhury, M.E., *et al.* Real-time smart-digital stethoscope system for heart diseases monitoring. *Sensors* **19**, 2781 (2019).
22. Islam, M.A., Bandyopadhyaya, I., Bhattacharyya, P. & Saha, G. Multichannel lung sound analysis for asthma detection. *Computer methods and programs in biomedicine* **159**, 111-123 (2018).
23. Rao, A., Ruiz, J., Bao, C. & Roy, S. Tabla: A proof-of-concept auscultatory percussion device for low-cost pneumonia detection. *Sensors* **18**, 2689 (2018).
24. Shimoda, T., *et al.* Lung sound analysis helps localize airway inflammation in patients with bronchial asthma. *Journal of Asthma and Allergy*, 99-108 (2017).
25. Wang, F., *et al.* A flexible skin-mounted wireless acoustic device for bowel sounds monitoring and evaluation. *Science China Information Sciences* **62**, 1-11 (2019).
26. Vanden Berghe, J. & Wouters, J. An adaptive noise canceller for hearing aids using two nearby microphones. *The Journal of the Acoustical Society of America* **103**, 3621-3626 (1998).
27. Bland, J.M. & Altman, D. Statistical methods for assessing agreement between two methods of clinical measurement. *The lancet* **327**, 307-310 (1986).
28. Dipietro, J.A., Caughy, M.O.b., Cusson, R. & Fox, N.A. Cardiorespiratory functioning of preterm infants: Stability and risk associations for measures of heart rate variability and oxygen saturation. *Developmental Psychobiology: The Journal of the International Society for Developmental Psychobiology* **27**, 137-152 (1994).
29. Hasenstab, K.A., Nawaz, S., Lang, I.M., Shaker, R. & Jadcherla, S.R. Pharyngoesophageal and cardiorespiratory interactions: potential implications for premature infants at risk of clinically significant cardiorespiratory events. *American Journal of Physiology-Gastrointestinal and Liver Physiology* **316**, G304-G312 (2019).

30. Ludington-Hoe, S., Anderson, G.C., Swinth, J., Thompson, C. & Hadeed, A. Randomized controlled trial of kangaroo care: cardiorespiratory and thermal effects on healthy preterm infants. *Neonatal Network* **23**, 39-48 (2004).
31. Wachman, E.M. & Lahav, A. The effects of noise on preterm infants in the NICU. *Archives of Disease in Childhood-Fetal and Neonatal Edition* **96**, F305-F309 (2011).
32. Inderjeeth, A.-J., Webberley, K.M., Muir, J. & Marshall, B.J. The potential of computerised analysis of bowel sounds for diagnosis of gastrointestinal conditions: A systematic review. *Systematic reviews* **7**, 1-18 (2018).
33. Tomomasa, T., *et al.* Gastrointestinal sounds and migrating motor complex in fasted humans. *The American journal of gastroenterology* **94**, 374-381 (1999).
34. Chien, C.-H., Huang, H.-T., Wang, C.-Y. & Chong, F.-C. Two-dimensional static and dynamic display system of bowel sound magnitude map for evaluation of intestinal motility. *Biomedical Engineering: Applications, Basis and Communications* **21**, 333-342 (2009).
35. Li, B., Wang, J.-R. & Ma, Y.-L. Bowel sounds and monitoring gastrointestinal motility in critically ill patients. *Clinical Nurse Specialist* **26**, 29-34 (2012).
36. Nowak, J.K., Nowak, R., Radzikowski, K., Grulkowski, I. & Walkowiak, J. Automated bowel sound analysis: an overview. *Sensors* **21**, 5294 (2021).
37. O'flaherty, N. & Fenelon, L. The stethoscope and healthcare-associated infection: a snake in the grass or innocent bystander? *Journal of Hospital Infection* **91**, 1-7 (2015).
38. Wright, I., Orr, H. & Porter, C. Stethoscope contamination in the neonatal intensive care unit. *Journal of Hospital Infection* **29**, 65-68 (1995).
39. Youngster, I., Berkovitch, M., Heyman, E., Lazarovitch, Z. & Goldman, M. The stethoscope as a vector of infectious diseases in the paediatric division. *Acta Paediatrica* **97**, 1253-1255 (2008).
40. Guilleminault, C. & Pelayo, R. Sleep-disordered breathing in children. *Annals of medicine* **30**, 350-356 (1998).
41. Pasterkamp, H., Kraman, S.S. & Wodicka, G.R. Respiratory sounds: advances beyond the stethoscope. *American journal of respiratory and critical care medicine* **156**, 974-987 (1997).
42. Wilkins, R.L. Is the stethoscope on the verge of becoming obsolete? , Vol. 49 1488-1489 (Respiratory Care, 2004).
43. Arts, L., Lim, E.H.T., van de Ven, P.M., Heunks, L. & Tuinman, P.R. The diagnostic accuracy of lung auscultation in adult patients with acute pulmonary pathologies: a meta-analysis. *Scientific Reports* **10**, 7347 (2020).

CLAIMS

What is claimed is:

1. A broadband acousto-mechanical sensing (BAMS) system for monitoring physiological signals of a living subject, comprising:

one or more wireless, skin-interfaced BAMS devices disposed on the living subject, being time-synchronized and wirelessly communicate with each other, wherein each BAMS device comprises an accelerometer configured to capture acceleration data from the living subject and an acoustic mechanical device configured to capture body sounds from the living subject, and the accelerometer and the acoustic mechanical device in each BAMS device are time-synchronized; and

a control device being time-synchronized and wirelessly communicate with the one or more BAMS devices, configured to manage and process the acceleration data and the body sounds from the one or more BAMS devices and to generate information of body movements and body sounds of the living subject based on the acceleration data and the body sounds obtained by the one or more BAMS devices.

2. The BAMS system of claim 1, wherein the body movements include chest wall movements and abdominal wall excursions, and the body sounds include respiratory sound, lung sounds, gastro-intestinal sounds, bowel sound, and cardiac sounds.

3. The BAMS system of claim 1, wherein each BAMS device comprises:

a flexible printed circuit board (fPCB);

an inertial measurement unit (IMU) disposed on the fPCB, wherein the IMU functions as the accelerometer configured to capture 3-axis acceleration data from the living subject; and

two microphones functioning as the acoustic mechanical device, respectively disposed on a body-facing side and an ambient-facing side of the fPCB, configured to capture the body sounds from the living subject ambient sounds from the environment.

4. The BAMS system of claim 3, wherein each BAMS device further comprises a top

elastomer layer and a bottom elastomer layer sandwiching the fPCB, wherein the bottom elastomer layer forms the body-facing surface attached to the living subject, and the top elastomer layer forms the ambient-facing surface.

5. The BAMS system of claim 3, wherein each BAMS device further comprises a Bluetooth Low Energy (BLE) system on a chip (SoC) disposed on the fPCB, configured to wirelessly communicate with the control device.

6. The BAMS system of claim 3, wherein each BAMS device further comprises an embedded power supply disposed on the fPCB or a wireless charging power supply.

7. The BAMS system of claim 3, wherein each BAMS device is configured to generate the body sound by applying an adaptive filtering algorithm to perform sound separation to the body sounds and the ambient sounds in order to minimize contribution of the ambient sounds to the body sounds.

8. The BAMS system of claim 1, wherein the control device comprises a graphical user interface (GUI) configured to real-time display quantitative information of the body movements and the body sounds of the living subject.

9. The BAMS system of claim 1, wherein the one or more BAMS devices are disposed at one or more of the following locations of the living subject:

a right upper chest area;
a right lower chest area;
a right axilla area;
a right upper back area;
a right mid back area;
a right lower back area;
a left upper chest area;
a left lower chest area;
a left axilla area;

a left upper back area;
a left mid back area;
a left lower back area; and
a suprastemal notch area.

10. A method of determining regional lung function of a living subject using the BAMS system of any of claims 1-9.

11. A method of monitoring bilateral lung function of a living subject using the BAMS system of any of claims 1-9.

12. A method of monitoring athletic performance of a living subject for conditioning using the BAMS system of any of claims 1-9.

13. A broadband acousto-mechanical sensing (BAMS) device for capturing physiological signals of a living subject, comprising:

a flexible printed circuit board (fPCB);

an inertial measurement unit (IMU) disposed on the fPCB, wherein the IMU functions as an accelerometer configured to capture 3-axis acceleration data from the living subject; and

two microphones, respectively disposed on a body-facing side and an ambient-facing side of the FPCB, configured to capture the body sounds from the living subject ambient sounds from the environment;

wherein the IMU and the microphones are time-synchronized.

14. The BAMS device of claim 13, further comprising a top elastomer layer and a bottom elastomer layer sandwiching the fPCB, wherein the bottom elastomer layer forms the body-facing surface attached to the living subject, and the top elastomer layer forms the ambient-facing surface.

15. The BAMS device of claim 13, further comprising a Bluetooth Low Energy (BLE)

system on a chip (SoC) disposed on the fPCB, configured to wirelessly communicate with the control device.

16. The BAMS device of claim 13, further comprising an embedded power supply disposed on the fPCB or a wireless charging power supply.

17. The BAMS device of claim 13, wherein each BAMS device is configured to generate the body sound by applying an adaptive filtering algorithm to perform sound separation to the body sounds and the ambient sounds in order to minimize contribution of the ambient sounds to the body sounds.

18. The BAMS device of claim 13, being disposed at one of the following locations of the living subject:

a right upper chest area;
a right lower chest area;
a right axilla area;
a right upper back area;
a right mid back area;
a right lower back area;
a left upper chest area;
a left lower chest area;
a left axilla area;
a left upper back area;
a left mid back area;
a left lower back area; and
a suprastemal notch area.

19. A BAMS system for monitoring physiological signals of a living subject, comprising:

one or more of wireless, skin-interfaced BAMS devices disposed on the living subject, being time-synchronized and wirelessly communicate with each other, wherein each BAMS device, wherein each BAMS device is the BAMS device of claim 13; and

a control device being time-synchronized and wirelessly communicate with the one or more BAMS devices, configured to manage and process the acceleration data and the body sounds from the one or more BAMS devices and to generate information of body movements and body sounds of the living subject based on the acceleration data and the body sounds obtained by the one or more BAMS devices.

20. A method of monitoring physiological signals of a living subject with a broadband acousto-mechanical sensing (BAMS) system, the method comprising:

managing and processing, by a control device being time-synchronized and wirelessly communicate with one or more, skin-interfaced BAMS devices, acceleration data and body sounds from the one or more BAMS devices, wherein the one or more BAMS device are disposed on the living subject, the one or more BAMS devices are time-synchronized and wirelessly communicate with each other, each BAMS device comprises an accelerometer configured to capture the acceleration data from the living subject and an acoustic mechanical device configured to capture the body sounds from the living subject, and the accelerometer and the acoustic mechanical device in each BAMS device are time-synchronized; and

generating, by the control device, information of body movements and body sounds of the living subject based on the acceleration data and the body sounds obtained by the one or more BAMS devices.

21. The method of claim 20, wherein the body movements include chest wall movements and abdominal wall excursions, and the body sounds include respiratory sound, lung sounds, gastro-intestinal sounds, bowel sound, and cardiac sounds.

22. The method of claim 20, wherein each BAMS device comprises:

a flexible printed circuit board (fPCB);

an inertial measurement unit (IMU) disposed on the fPCB, wherein the IMU functions as the accelerometer configured to capture 3-axis acceleration data from the living subject; and

two microphones functioning as the acoustic mechanical device, respectively

disposed on a body-facing side and an ambient-facing side of the FPCB, configured to capture the body sounds from the living subject ambient sounds from the environment.

23. The method of claim 22, wherein each BAMS device further comprises a top elastomer layer and a bottom elastomer layer sandwiching the fPCB, wherein the bottom elastomer layer forms the body-facing surface attached to the living subject, and the top elastomer layer forms the ambient-facing surface.

24. The method of claim 22, wherein each BAMS device further comprises a Bluetooth Low Energy (BLE) system on a chip (SoC) disposed on the fPCB, configured to wirelessly communicate with the control device.

25. The method of claim 22, wherein each BAMS device further comprises an embedded power supply disposed on the fPCB or a wireless charging power supply.

26. The method of claim 22, wherein each BAMS device is configured to generate the body sound by applying an adaptive filtering algorithm to perform sound separation to the body sounds and the ambient sounds in order to minimize contribution of the ambient sounds to the body sounds.

27. The method of claim 20, further comprising:

providing, by the control device, a graphical user interface (GUI); and

real-time displaying, by the GUI, quantitative information of the body movements and the body sounds of the living subject.

28. The method of claim 20, wherein the one or more BAMS devices are disposed at one or more of the following locations of the living subject:

a right upper chest area;

a right lower chest area;

a right axilla area;

a right upper back area;

a right mid back area;
a right lower back area;
a left upper chest area;
a left lower chest area;
a left axilla area;
a left upper back area;
a left mid back area;
a left lower back area; and
a suprastemal notch area.

29. A non-transitory tangible computer-readable medium storing instructions which, when executed by one or more processors, cause the method of any of claims 20-28 to be performed.

30. A method of detecting hypopnea and central apnea of a living subject with a broadband acousto-mechanical sensing (BAMS) system, the method comprising:

managing and processing, by a control device being time-synchronized and wirelessly communicate with one or more, skin-interfaced BAMS devices, acceleration data and body sounds from the one or more BAMS devices, wherein the one or more BAMS device are disposed on the living subject, the one or more BAMS devices are time-synchronized and wirelessly communicate with each other, each BAMS device comprises an accelerometer configured to capture the acceleration data from the living subject and an acoustic mechanical device configured to capture the body sounds from the living subject, and the accelerometer and the acoustic mechanical device in each BAMS device are time-synchronized;

generating, by the control device, information of body movements and body sounds of the living subject based on the acceleration data and the body sounds obtained by the one or more BAMS devices;

detecting, by the control device, whether the information of the body movements and the body sounds of the living subject show a partial reduction or an absence thereof; and

in response to detecting the information of the body movements and the body sounds of the living subject showing the partial reduction or the absence thereof, determining, by the control device, the living subject to have a hypopnea or a central apnea, wherein the partial reduction of the body movements and the body sounds of the living subject indicates the hypopnea, and the absence of the body movements and the body sounds of the living subject indicates the central apnea.

31. The method of claim 30, wherein the body movements include chest wall movements and abdominal wall excursions, and the body sounds include respiratory sounds and lung sounds.

32. The method of claim 31, further comprising displaying the information of the body movements and the body sounds of the living subject showing the partial reduction or the absence thereof.

33. A broadband acousto-mechanical sensing (BAMS) system for detecting hypopnea and central apnea of a living subject, comprising:

one or more wireless, skin-interfaced BAMS devices disposed on the living subject, being time-synchronized and wirelessly communicate with each other, wherein each BAMS device comprises an accelerometer configured to capture acceleration data from the living subject and an acoustic mechanical device configured to capture body sounds from the living subject, and the accelerometer and the acoustic mechanical device in each BAMS device are time-synchronized; and

a control device being time-synchronized and wirelessly communicate with the one or more BAMS devices, configured to

manage and process the acceleration data and the body sounds from the one or more BAMS devices and to generate information of body movements and body sounds of the living subject based on the acceleration data and the body sounds obtained by the one or more BAMS devices;

detect whether the information of the body movements and the body sounds of the living subject show a partial reduction or an absence thereof; and

determine, in response to detecting the information of the body movements and the body sounds of the living subject showing the partial reduction or the absence thereof, the living subject to have a hypopnea or a central apnea, wherein the partial reduction of the body movements and the body sounds of the living subject indicates the hypopnea, and the absence of the body movements and the body sounds of the living subject indicates the central apnea.

34. The BAMS system of claim 33, wherein each BAMS device is configured to generate the body sound by applying an adaptive filtering algorithm to perform sound separation to the body sounds and the ambient sounds in order to minimize contribution of the ambient sounds to the body sounds.

35. The BAMS system of claim 33, wherein each BAMS device further comprises a Bluetooth Low Energy (BLE) system on a chip (SoC), configured to wirelessly communicate with the control device.

36. The BAMS system of claim 33, wherein the body movements include chest wall movements and abdominal wall excursions, and the body sounds include respiratory sounds and lung sounds.

37. The BAMS system of claim 33, wherein the control device comprises a graphical user interface (GUI) configured to real-time display quantitative information of the body movements and the body sounds of the living subject.

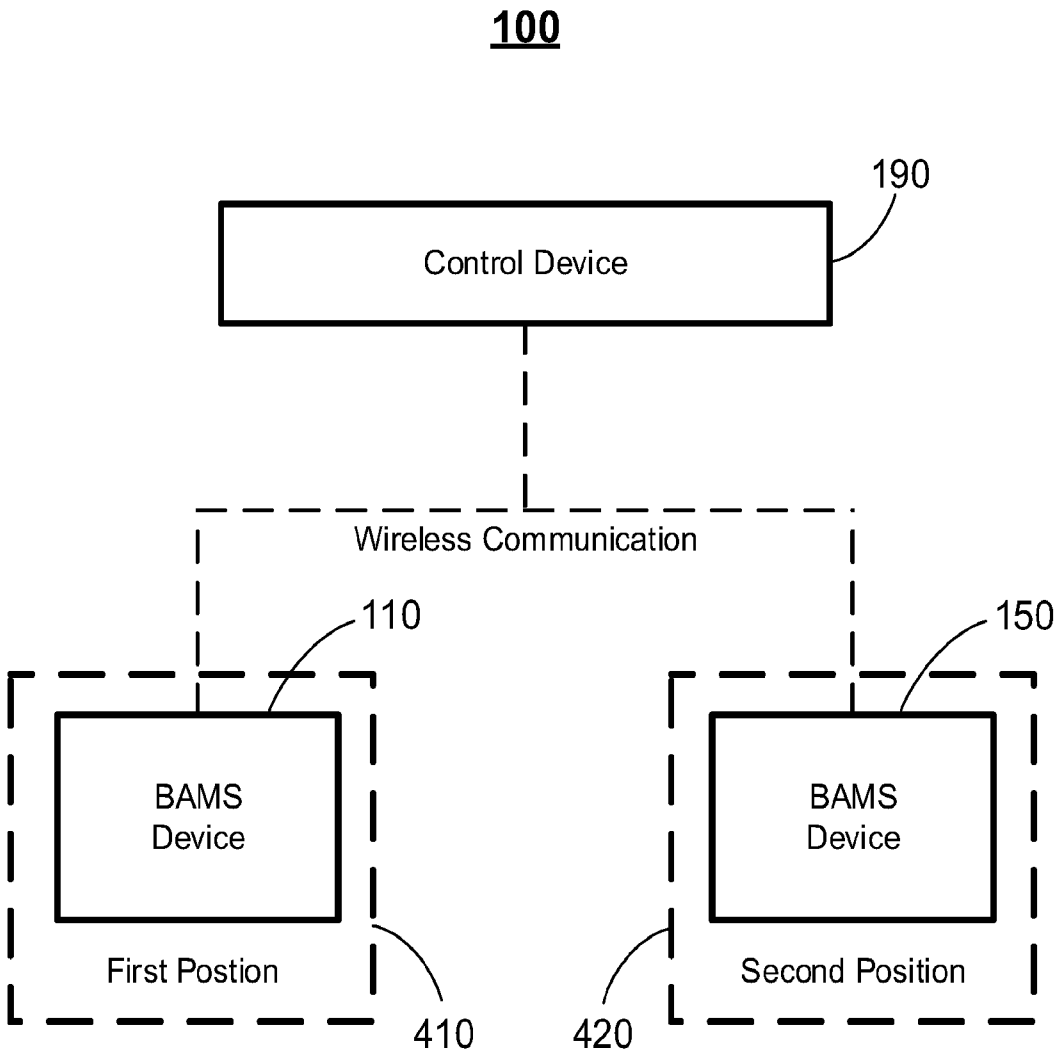
100
190
Control Device
Wireless Communication
110
150
BAMS
Device
BAMS
Device
First Postion
Second Position
410
420

FIG. 1A

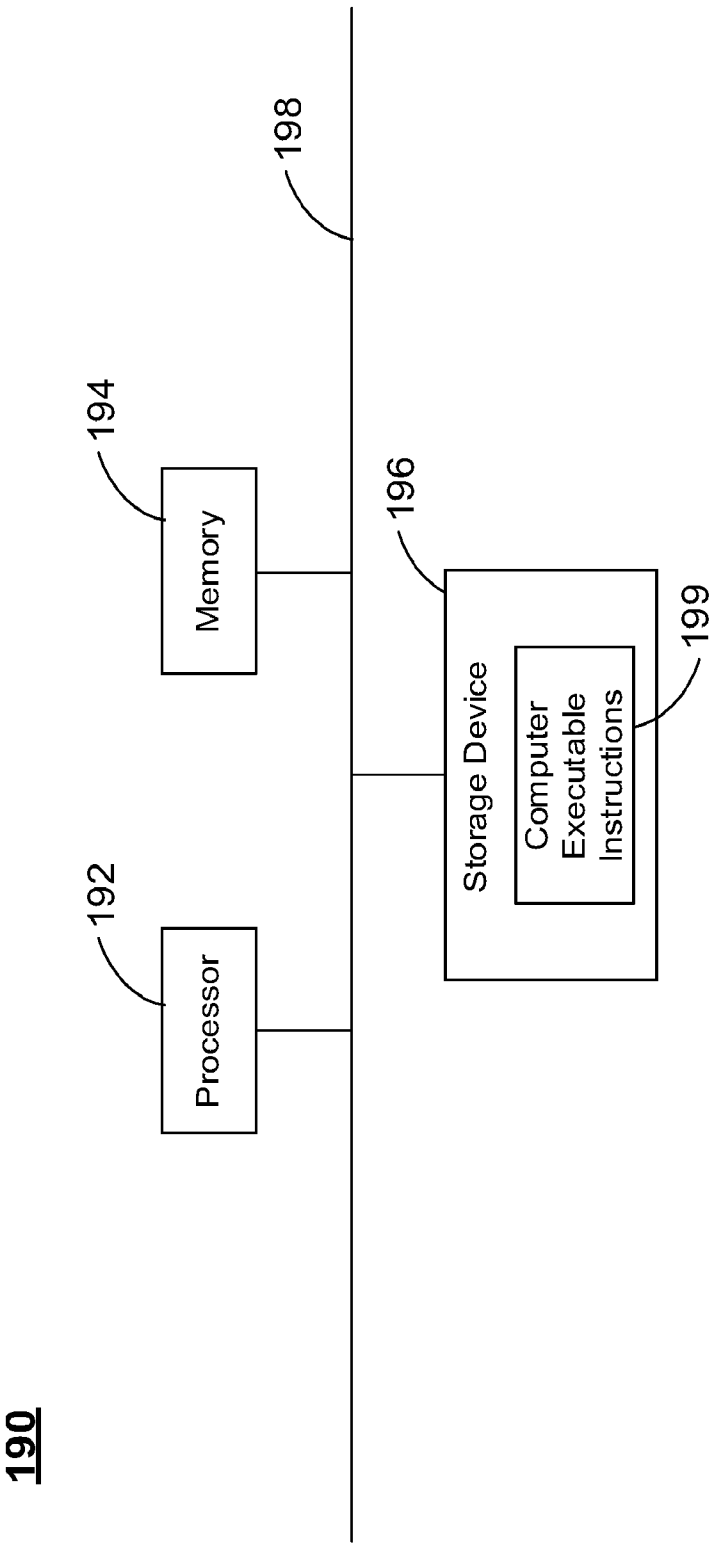
190
192
Processor
194
Memory
196
Storage Device
199
Computer Executable Instructions
198

FIG. 1B

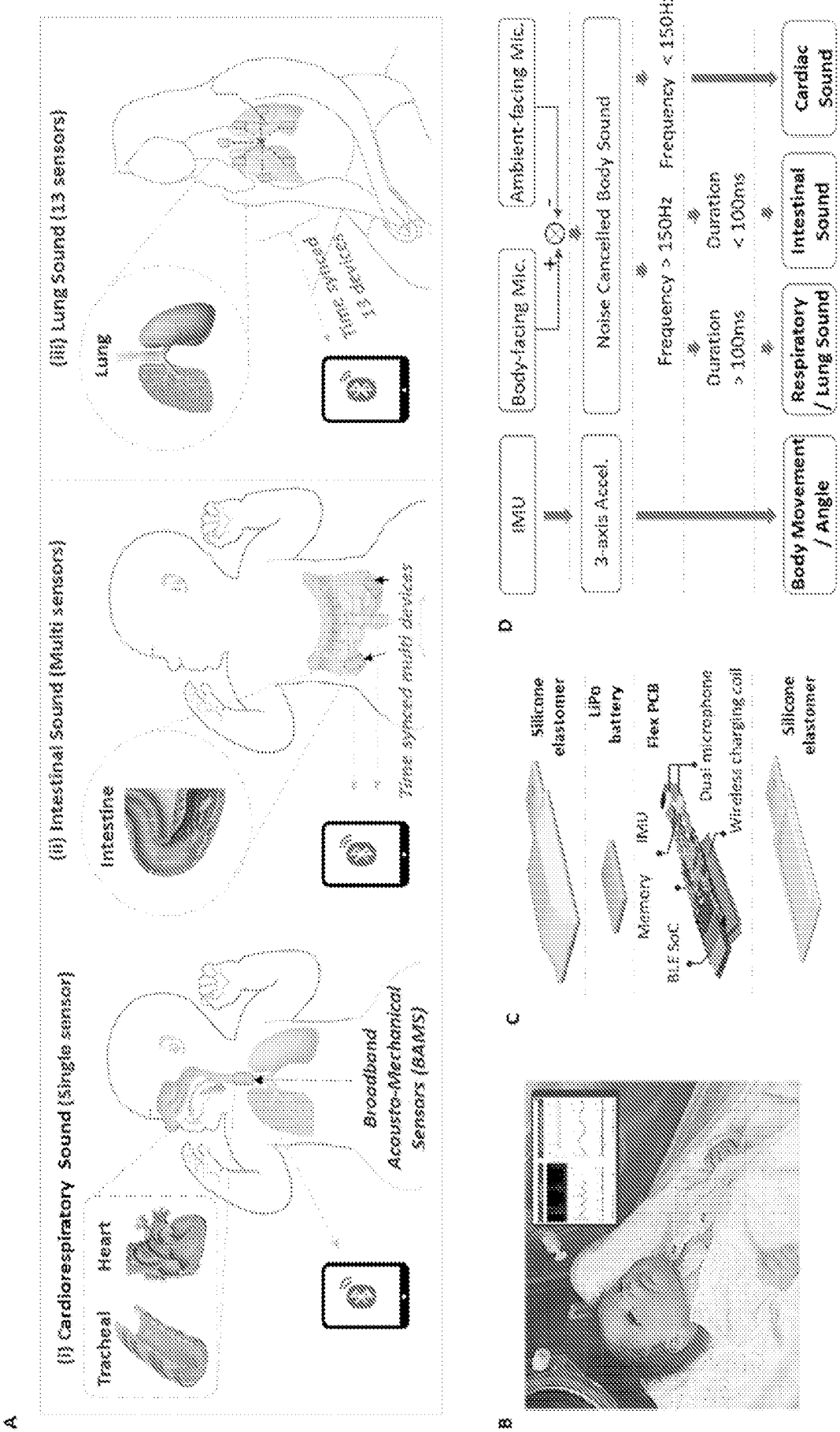
A
(i) Cardiorespiratory Sound (Single sensor)
Tracheal
Heart
Broadband Acousto-Mechanical Sensors (BAMS)
(ii) Intestinal Sound (Multi sensors)
Intestine
Time synced multi devices
(iii) Lung Sound (13 sensors)
Lung
Time synced 13 devices
B
C
Silicone elastomer
LiPo battery
Memory
IMU
Flex PCB
BLE SoC
Dual microphone
Wireless charging coil
Silicone elastomer
D
IMU
Body-facing Mic.
Ambient-facing Mic.
3-axis Accel.
Noise Cancelled Body Sound
Frequency > 150Hz
Frequency < 150Hz
Duration > 100ms
Duration < 100ms
Body Movement / Angle
Respiratory / Lung Sound
Intestinal Sound
Cardiac Sound

FIG. 2A

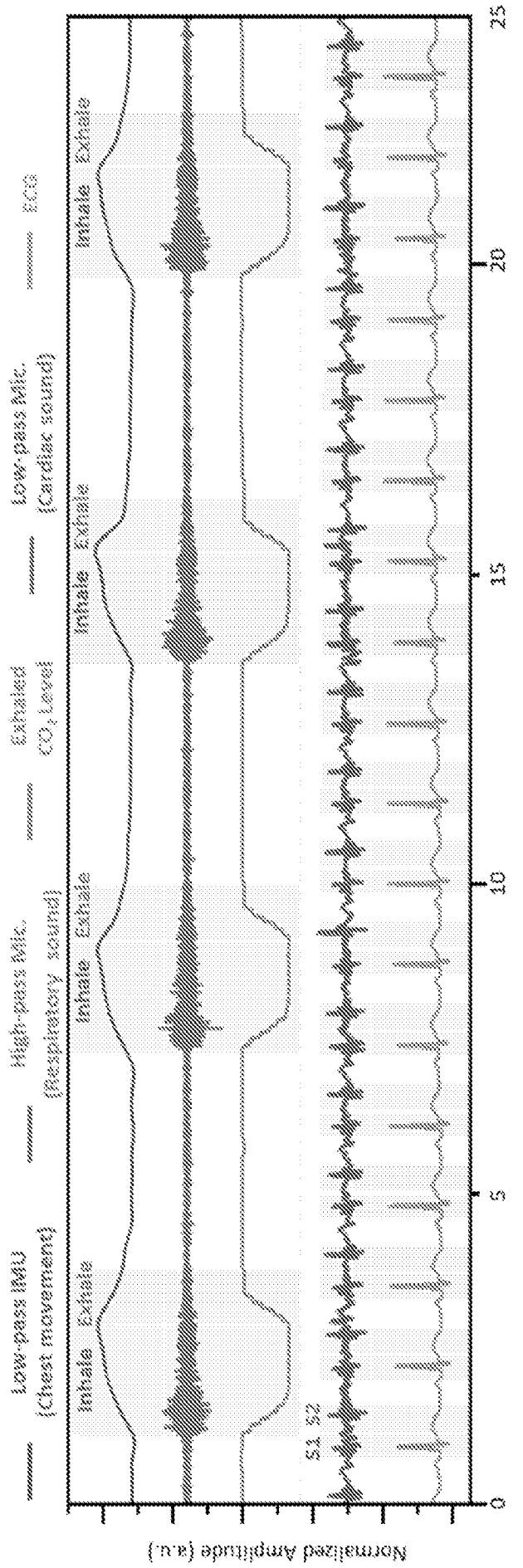
Low-pass IMU (Chest movement)
High-pass Mic. (Respiratory sound)
Exhaled CO_2 Level
Low-pass Mic. (Cardiac sound)
ECG
Inhale
Exhale
S1 S2
Normalized Amplitude (a.u.)
Time (s)
0
5
10
15
20
25

FIG. 2B

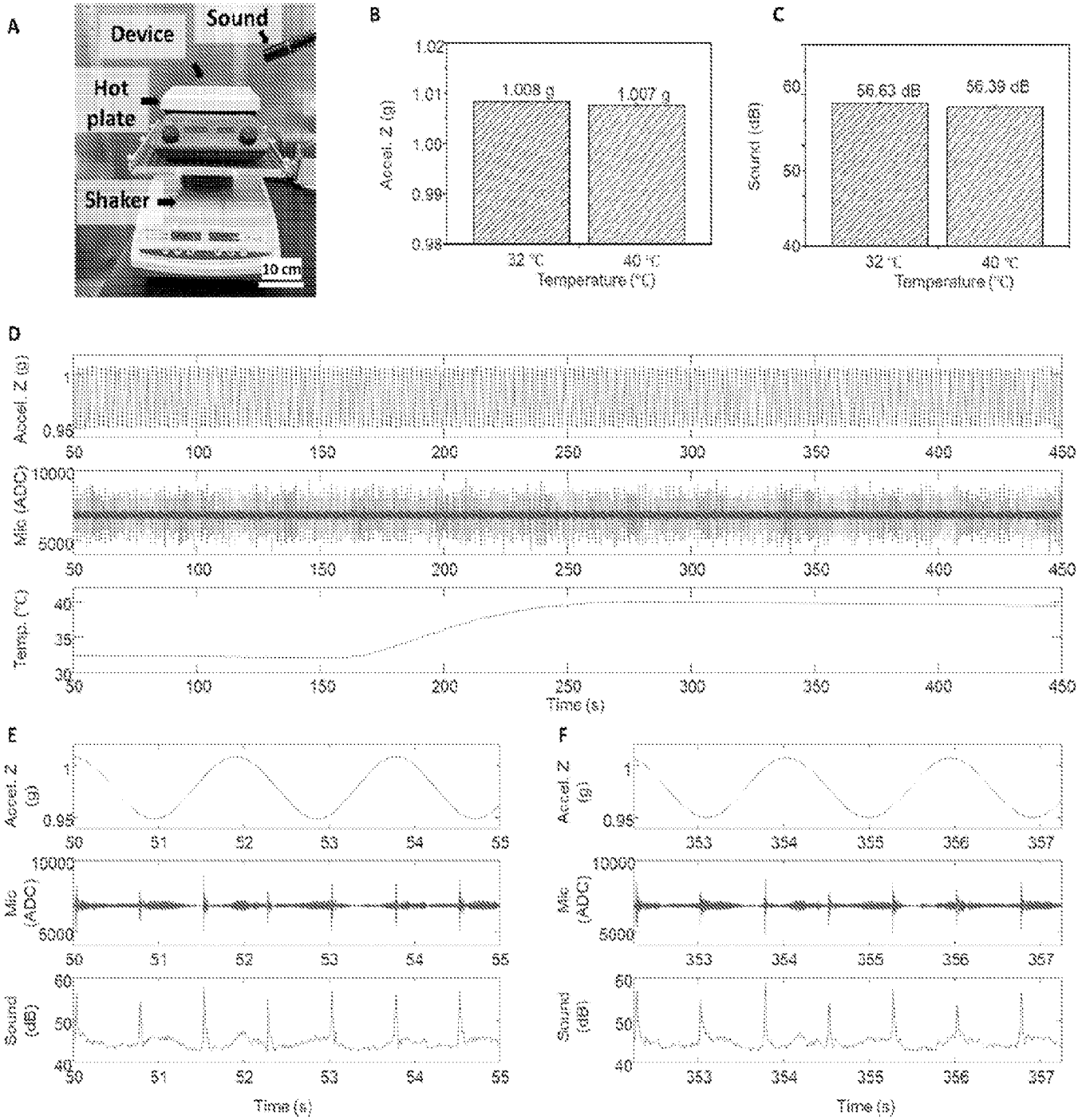
A
Device
Sound
Hot plate
Shaker
10 cm
B
Accel. Z (g)
1.008 g
1.007 g
32 °C
40 °C
Temperature (°C)
C
Sound (dB)
56.63 dB
56.39 dB
32 °C
40 °C
Temperature (°C)
D
Accel. Z (g)
Mic (ADC)
Temp. (°C)
Time (s)
E
Accel. Z (g)
Mic (ADC)
Sound (dB)
Time (s)
F
Accel. Z (g)
Mic (ADC)
Sound (dB)
Time (s)

FIG. 3

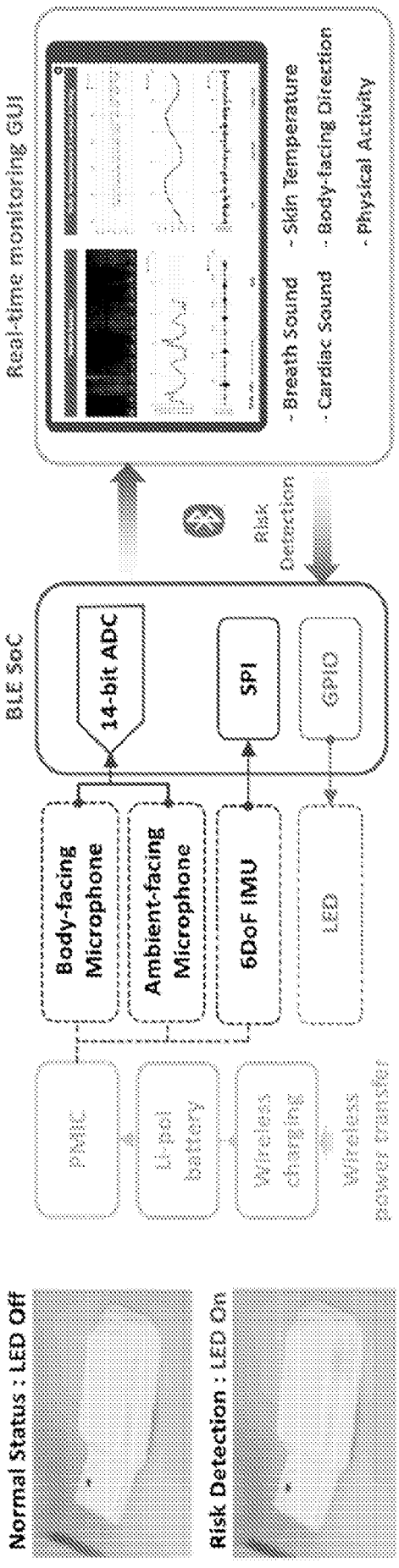
Real-time monitoring GUI
- Breath Sound
- Cardiac Sound
- Skin Temperature
- Body-facing Direction
- Physical Activity
Risk Detection
BLE SoC
14-bit ADC
SPI
GPIO
Body-facing Microphone
Ambient-facing Microphone
6DoF IMU
LED
PMIC
Li-pol battery
Wireless charging
Wireless power transfer
Normal Status : LED Off
Risk Detection : LED On

FIG. 4

Ref	Data Communication	Size (Weight)	Collected Data	Noise cancellation	SNR of cardiac signal (dB)	number of devices in the system	Clinical study
This work	Bluetooth	40 x 20 x 8 mm (6 g)	- Body sound - Ambient sound - Physical activity - Skin temperature	Yes	37 dB	13 devices	- NICU vital monitoring - Multichannel Bowel sound - Multichannel lung sound
3M™ Littmann® CORE	Bluetooth	175 x 45 x 30 mm (127.3 g)	Body sound	Yes	35 dB	Single device	-
[1]	Bluetooth	-	Lung sound	No	14.8 dB	Single device	Single channel lung sound
[2]	Bluetooth	-	Lung sound	No	10.0 dB	Single device	Pneumonia monitoring
[3]	Bluetooth	41.9 x 30.2 x 7.8 mm (6.5 g)	Bowel sound	No	7.0 dB	Single device	Single channel bowel sound
[4]	Bluetooth	-	Heart sound	No	10.0 dB	Single device	-
[5]	Wire communication	-	Lung sound	No	-	7 devices	Multichannel lung sound
[6]	Wire communication	-	Lung sound	No	-	4 devices	Multichannel lung sound

FIG. 5

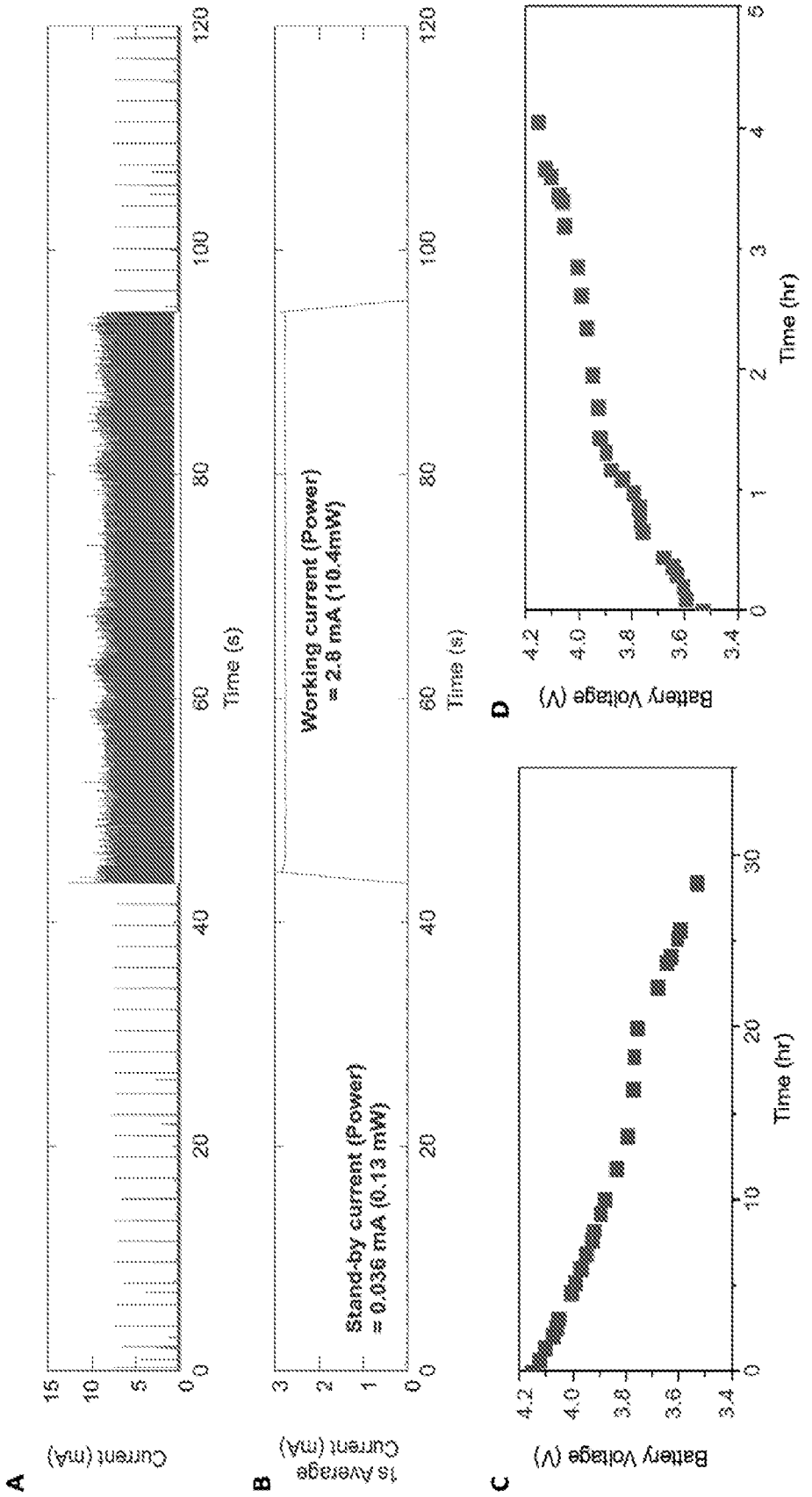
A
Current (mA)
Time (s)
B
1s Average Current (mA)
Working current (Power) = 2.8 mA (10.4mW)
Stand-by current (Power) = 0.036 mA (0.13 mW)
Time (s)
C
Battery Voltage (V)
Time (hr)
D
Battery Voltage (V)
Time (hr)

FIG. 6

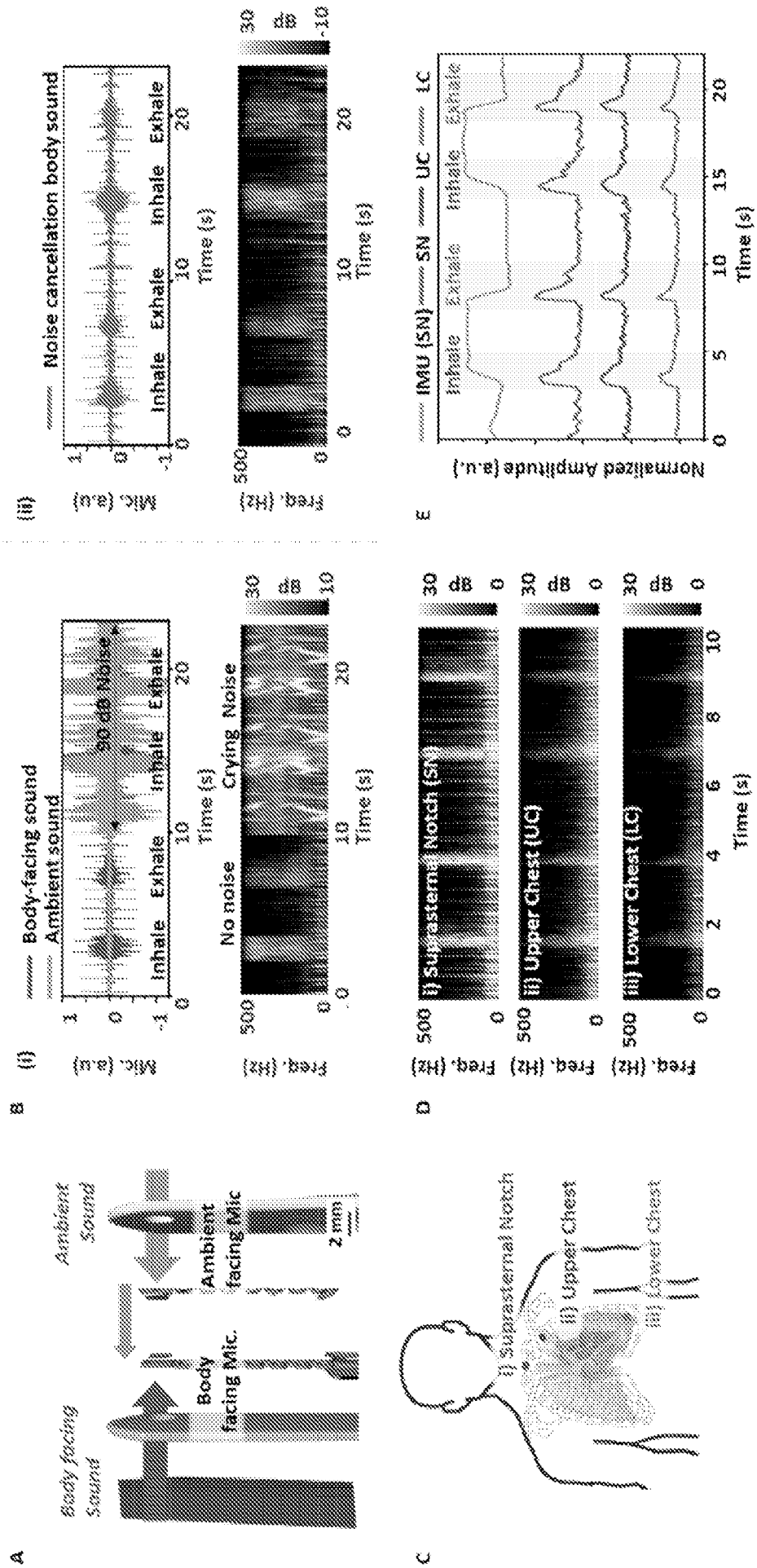
A
Body facing Sound
Ambient Sound
Body facing Mic.
Ambient facing Mic
2 mm
B
(i)
Body-facing sound
Ambient sound
Mic. (a.u)
Inhale
Exhale
Inhale
Exhale
30 dB Noise
Time (s)
No noise
Crying Noise
Freq. (Hz)
dB
(ii)
Noise cancellation body sound
(iii)
C
i) Suprasternal Notch
ii) Upper Chest
iii) Lower Chest
D
i) Suprasternal Notch (SN)
ii) Upper Chest (UC)
iii) Lower Chest (LC)
Freq. (Hz)
Time (s)
E
IMU (SN)
SN
UC
LC
Inhale
Exhale
Normalized Amplitude (a.u.)
Time (s)

FIG. 7A

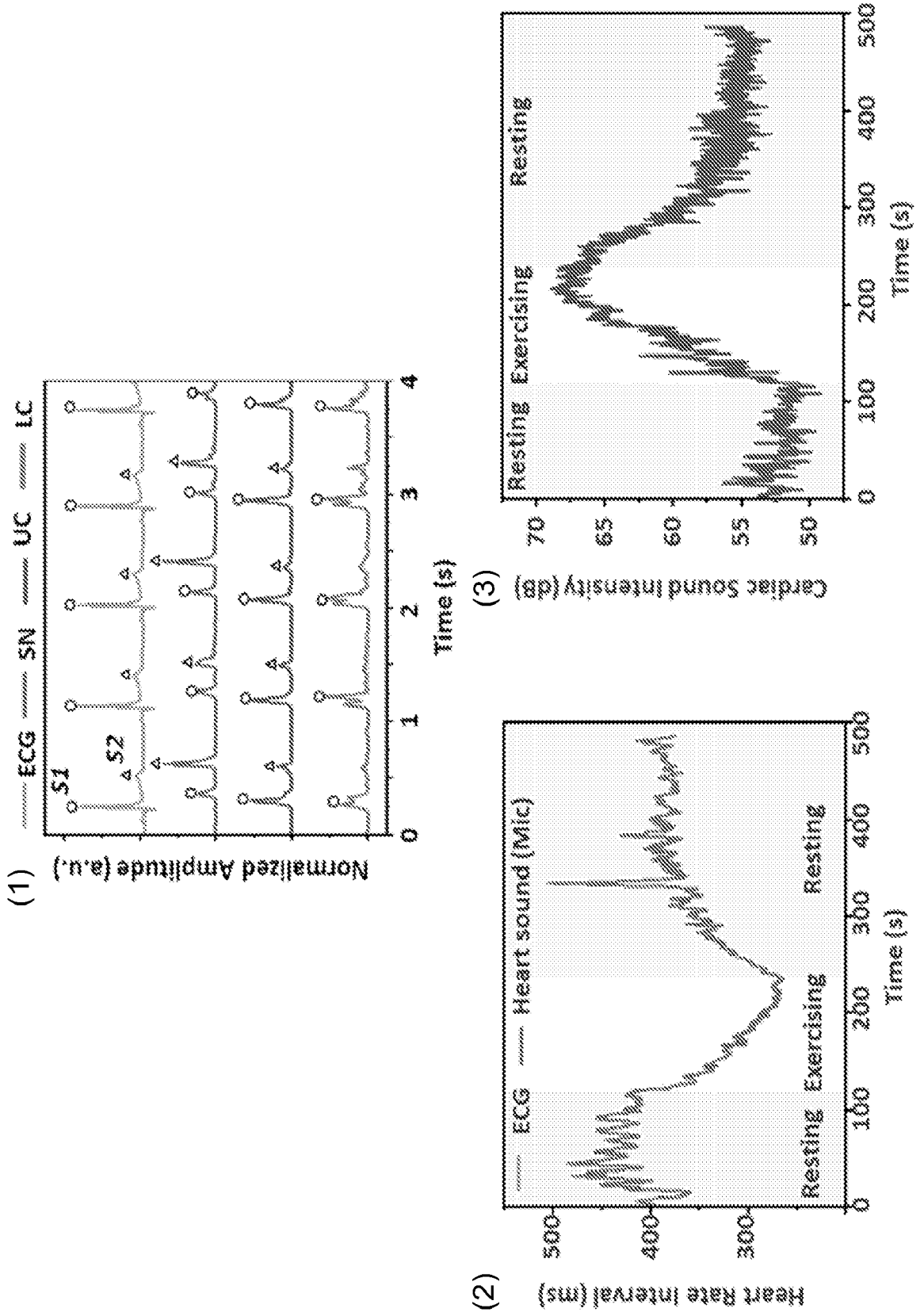
(1)
ECG
SN
UC
LC
S1
S2
Normalized Amplitude (a.u.)
Time (s)
(2)
ECG
Heart sound (Mic)
Resting
Exercising
Resting
Heart Rate Interval (ms)
Time (s)
(3)
Resting
Exercising
Resting
Cardiac Sound Intensity (dB)
Time (s)

FIG. 7B

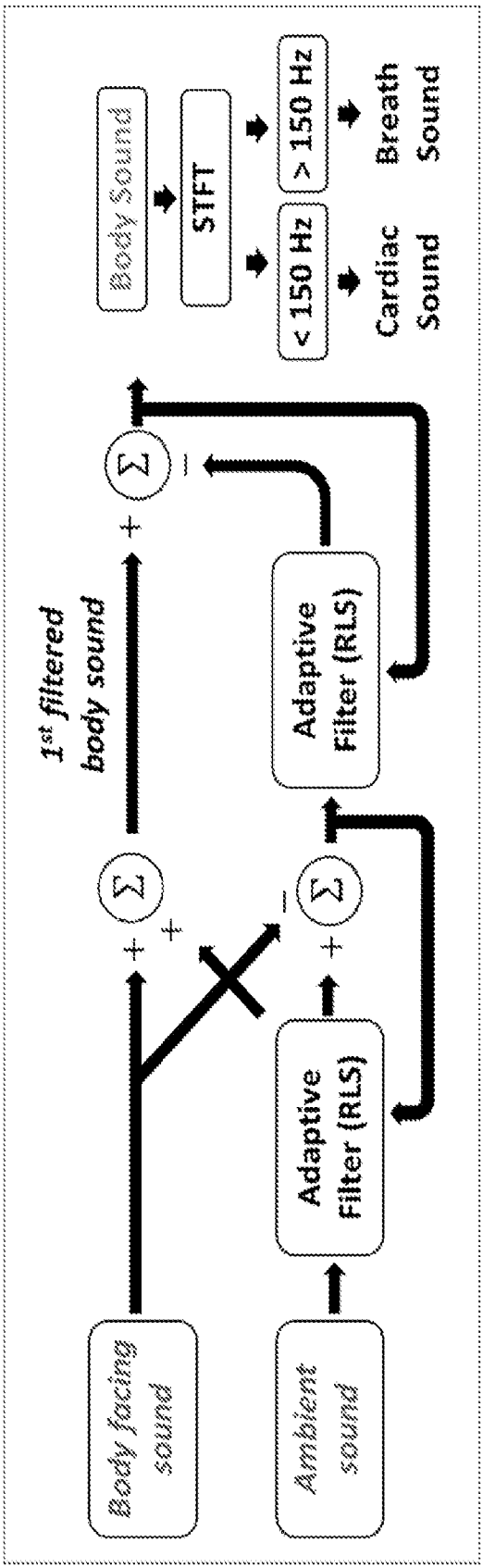
Body facing sound
Ambient sound
Adaptive Filter (RLS)
Adaptive Filter (RLS)
1st filtered body sound
Body Sound
STFT
< 150 Hz
> 150 Hz
Cardiac Sound
Breath Sound

FIG. 8

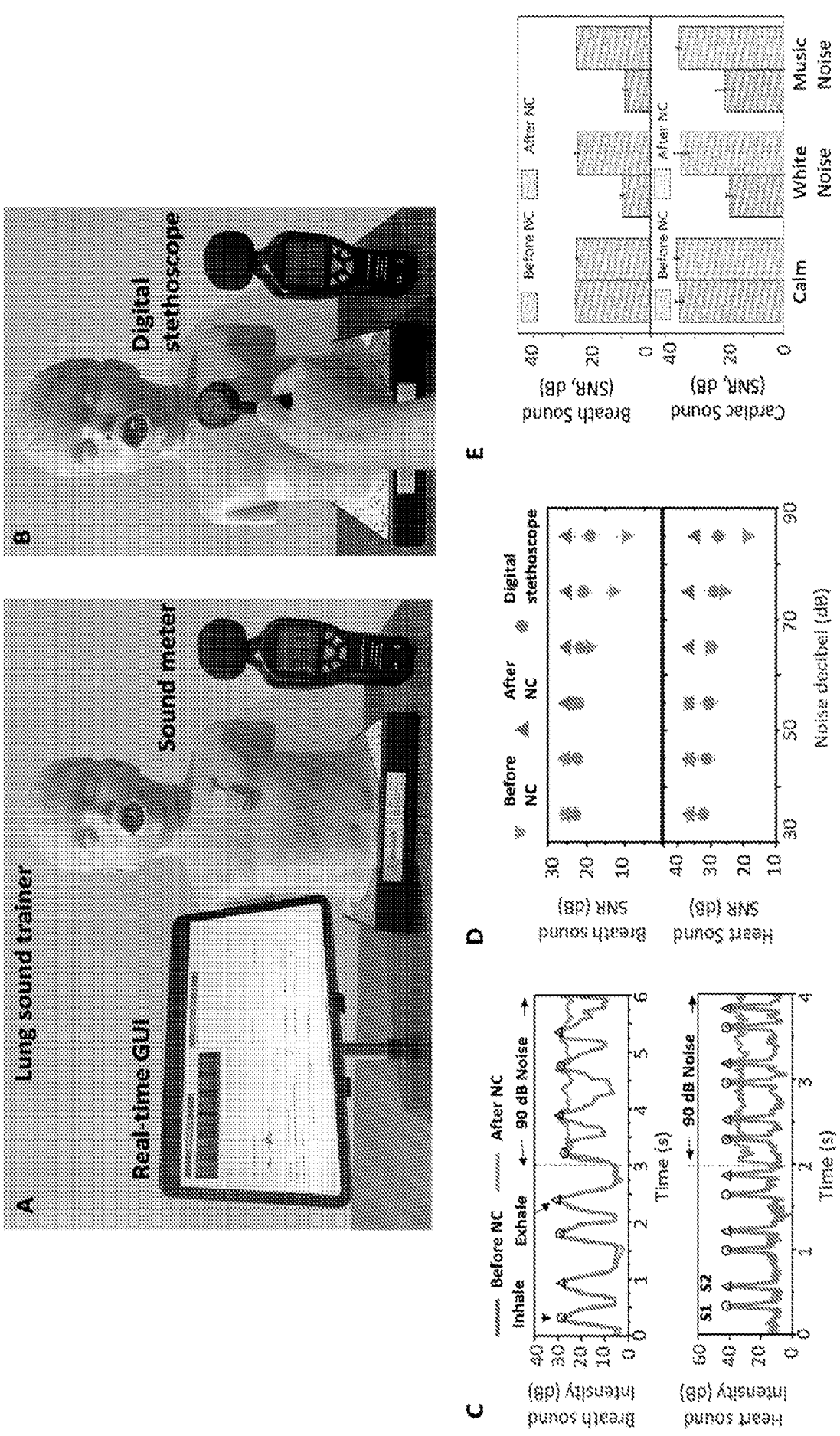
A
Lung sound trainer
Real-time GUI
Sound meter
B
Digital stethoscope
C
Before NC
After NC
Inhale
Exhale
90 dB Noise
Breath sound Intensity (dB)
Heart sound Intensity (dB)
S1 S2
Time (s)
D
Before NC
After NC
Digital stethoscope
Breath sound SNR (dB)
Heart Sound SNR (dB)
Noise decibel (dB)
E
Before NC
After NC
Cardiac Sound (SNR, dB)
Breath Sound (SNR, dB)
Calm
White Noise
Music Noise

FIG. 9

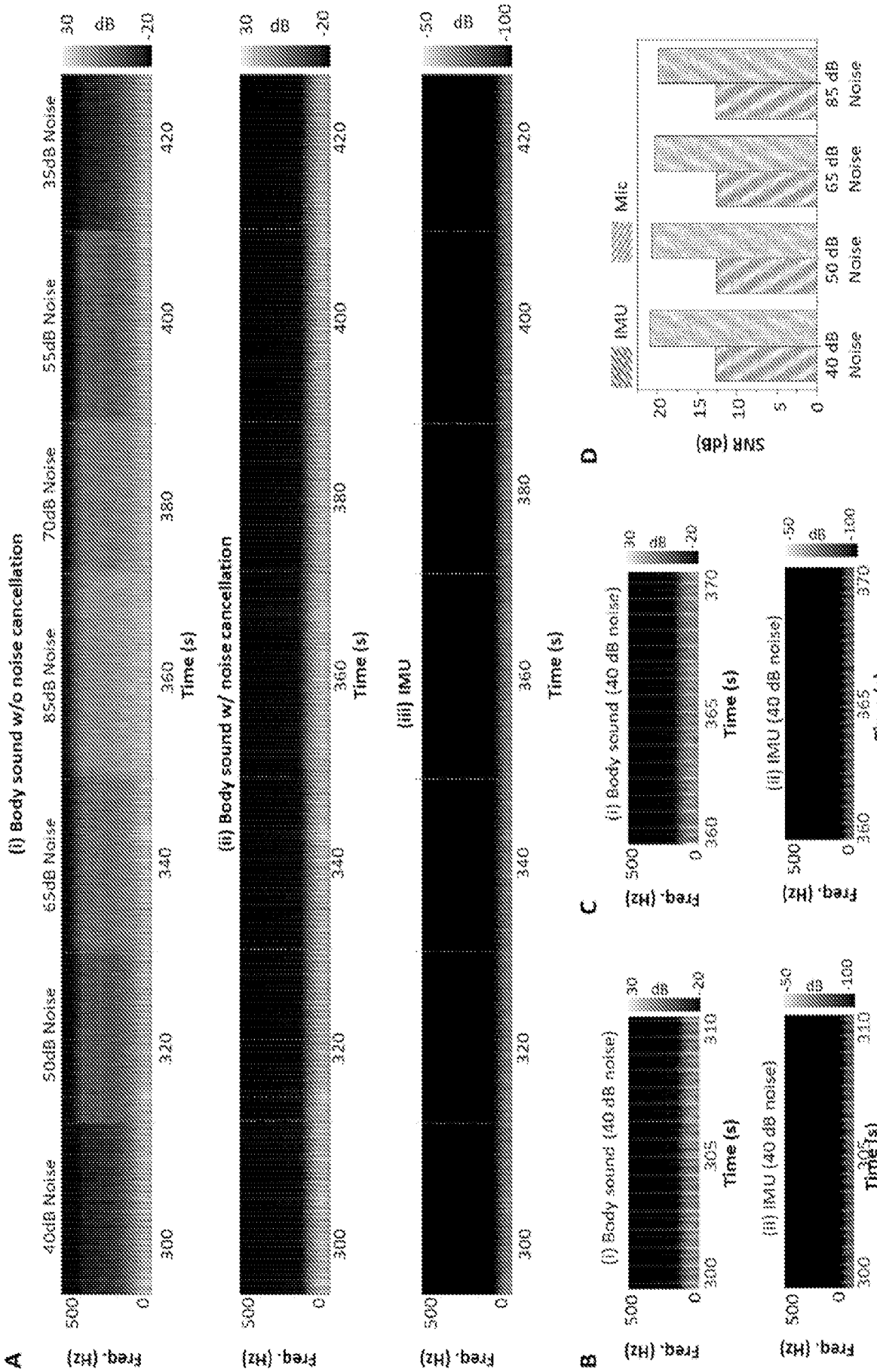
A
(i) Body sound w/o noise cancellation
40dB Noise
50dB Noise
65dB Noise
85dB Noise
70dB Noise
55dB Noise
35dB Noise
Freq. (Hz)
Time (s)
dB
(ii) Body sound w/ noise cancellation
(iii) IMU
B
(i) Body sound (40 dB noise)
(ii) IMU (40 dB noise)
C
(i) Body sound (40 dB noise)
(ii) IMU (40 dB noise)
D
IMU
Mic
SNR (db)
40 dB Noise
50 dB Noise
65 dB Noise
85 dB Noise

FIG. 10

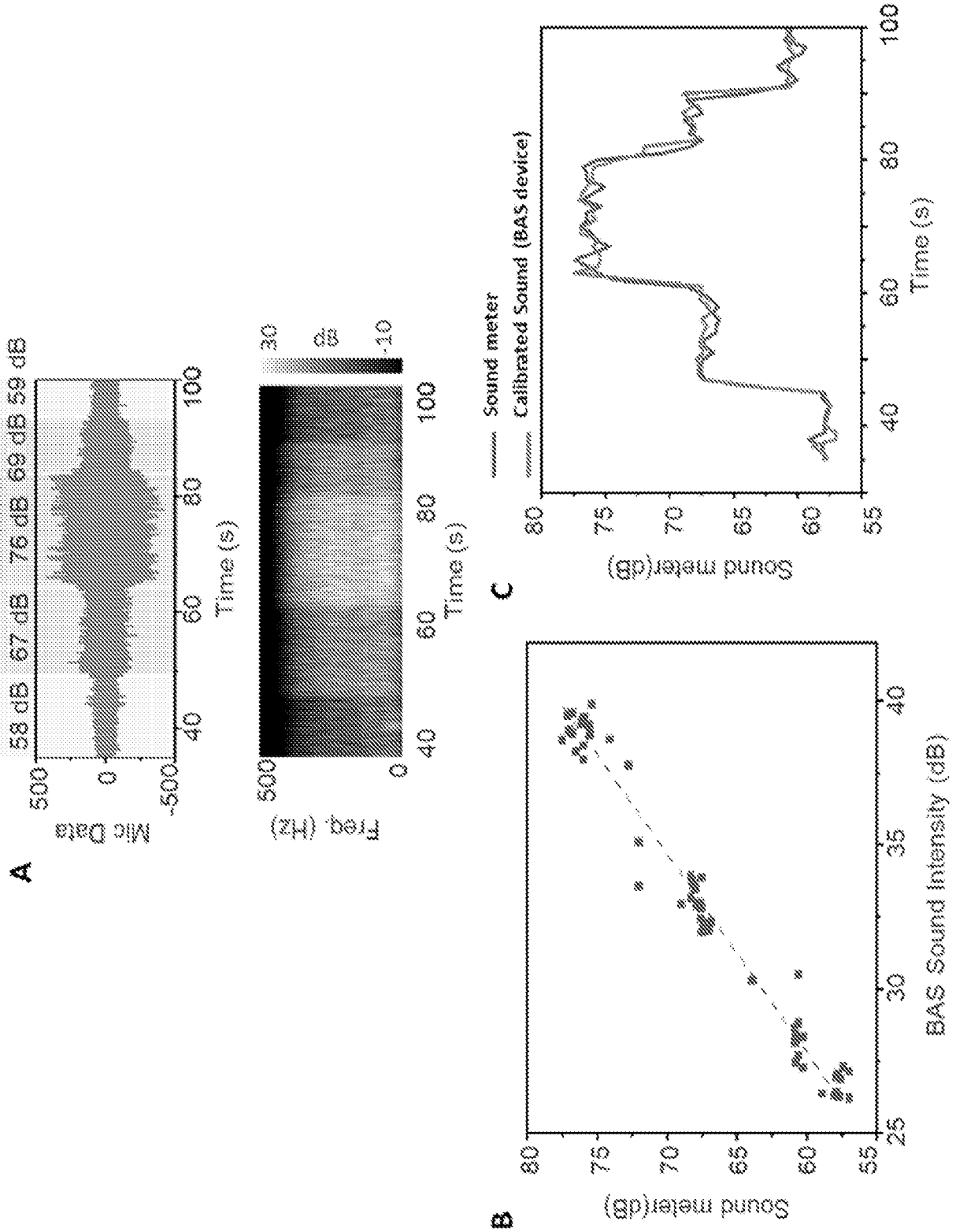
A
Mic Data
500
0
-500
58 dB
67 dB
76 dB
69 dB
59 dB
40
60
80
100
Time (s)
Freq. (Hz)
500
0
30
dB
-10
40
60
80
100
Time (s)
C
Sound meter
Calibrated Sound (BAS device)
Sound meter(dB)
80
75
70
65
60
55
40
60
80
100
Time (s)
B
Sound meter(dB)
80
75
70
65
60
55
25
30
35
40
BAS Sound Intensity (dB)

FIG. 11

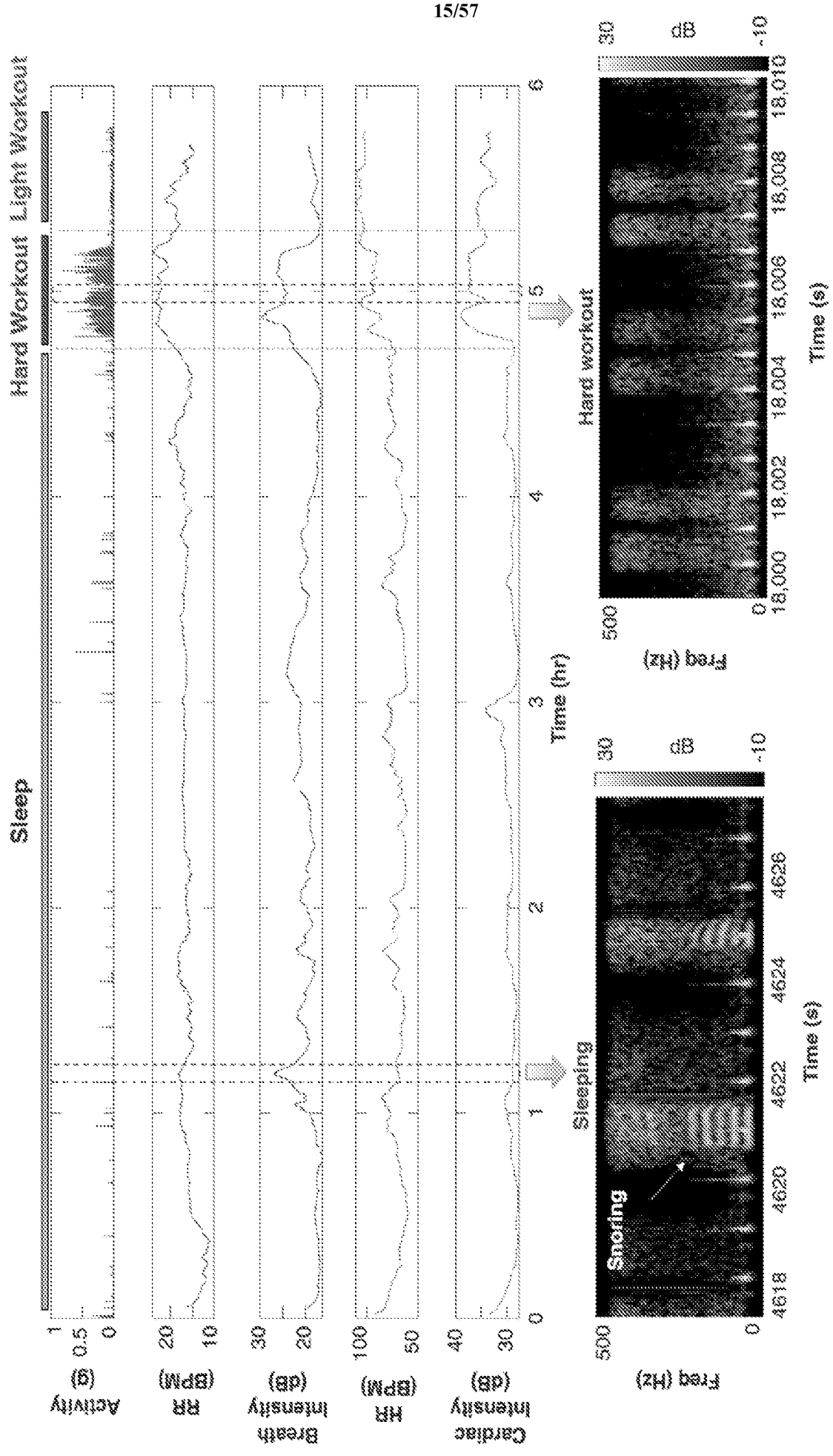
Sleep
Light Workout
Hard Workout
Activity (g)
RR (BPM)
Breath Intensity (dB)
HR (BPM)
Cardiac Intensity (dB)
Time (hr)
Hard workout
Freq (Hz)
Time (s)
dB
Sleeping
Snoring

FIG. 12

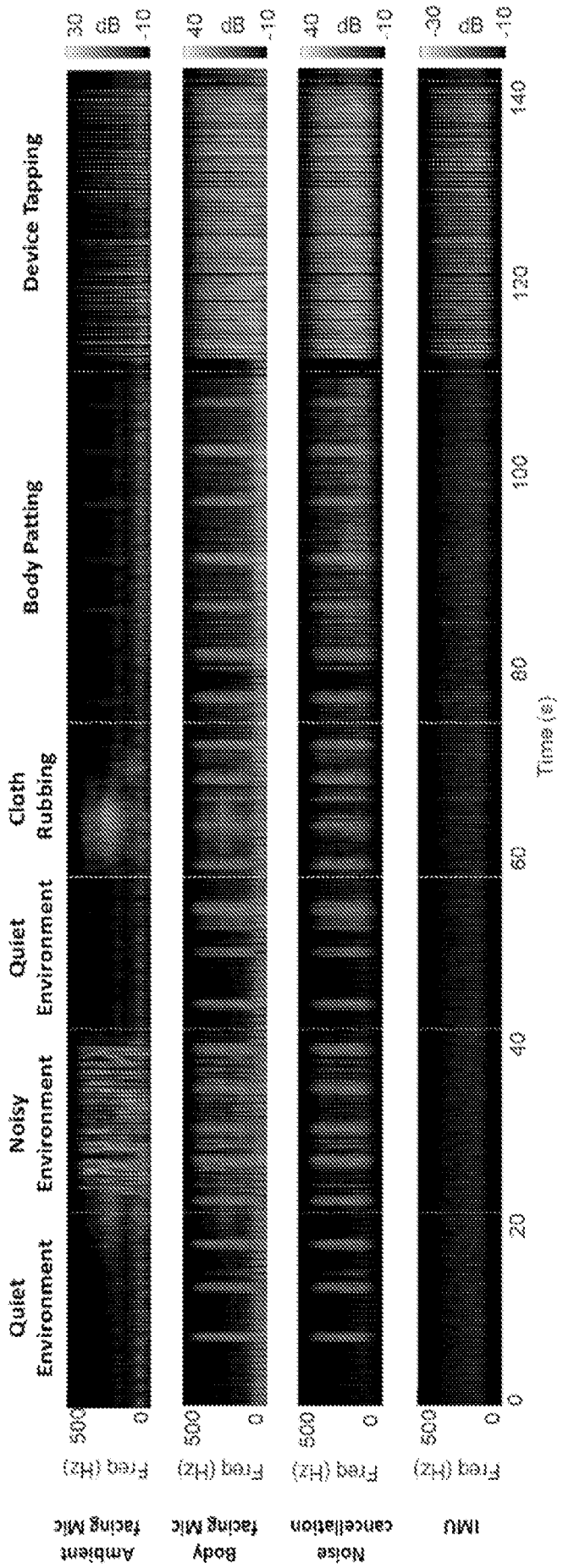
Quiet Environment
Noisy Environment
Quiet Environment
Cloth Rubbing
Body Patting
Device Tapping
Ambient facing Mic
Body facing Mic
Noise cancellation
IMU
Freq (Hz)
500
0
30
dB
-10
40
-30
20
60
80
100
120
140
Time (s)

FIG. 13

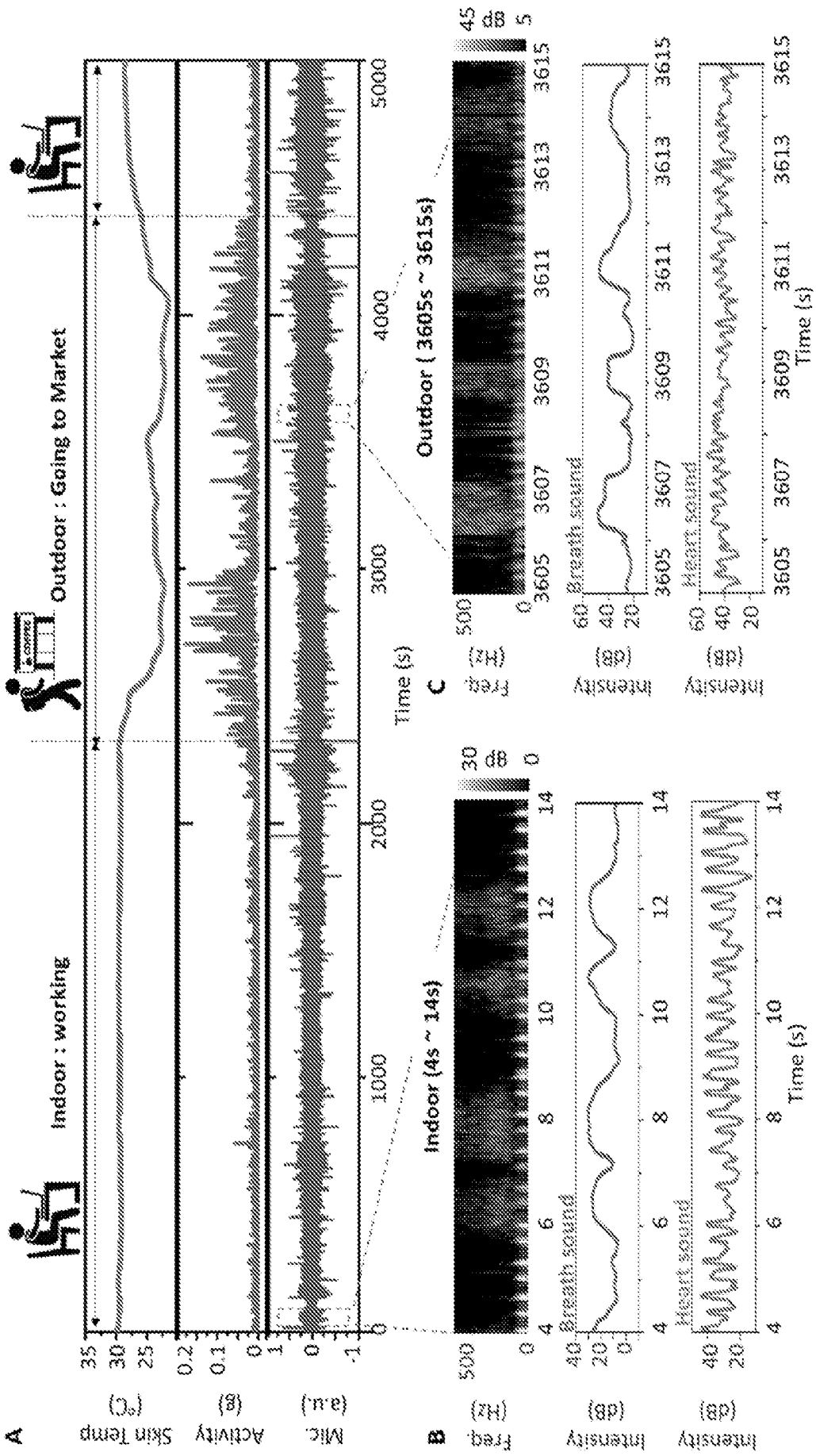
A
Indoor : working
Outdoor : Going to Market
Skin Temp (°C)
Activity (g)
Mic. (a.u.)
Time (s)
B
Indoor (4s ~ 14s)
Freq. (Hz)
Intensity (dB)
Breath sound
Heart sound
Time (s)
C
Outdoor (3605s ~ 3615s)
Freq. (Hz)
Intensity (dB)
Breath sound
Heart sound
Time (s)

FIG. 14A

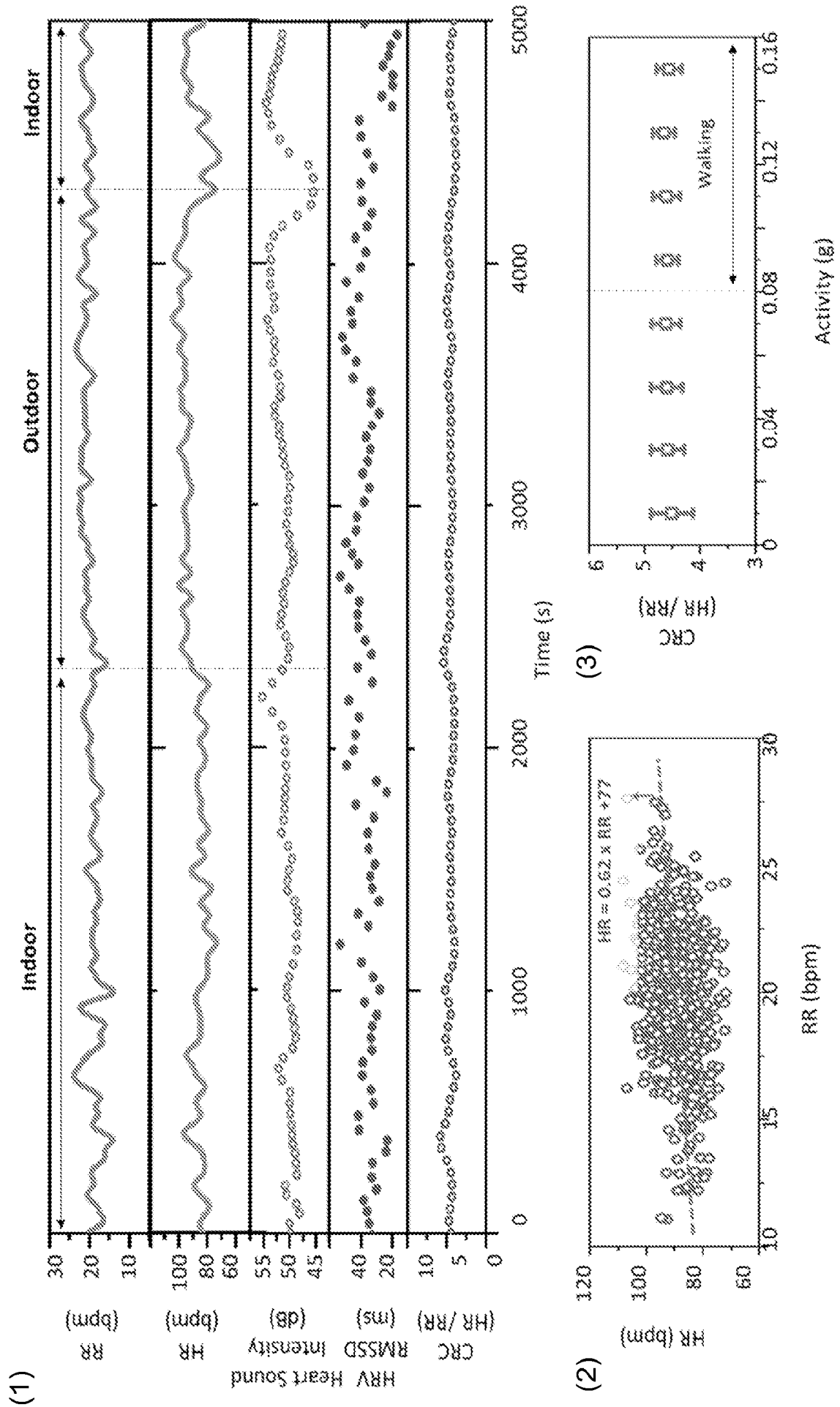
(1)
Indoor
Outdoor
Indoor
RR (bpm)
HR (bpm)
Heart Sound Intensity (dB)
HRV RMSSD (ms)
CRC (HR /RR)
Time (s)
(2)
HR = 0.62 x RR +77
HR (bpm)
RR (bpm)
(3)
CRC (HR /RR)
Walking
Activity (g)

FIG. 14B

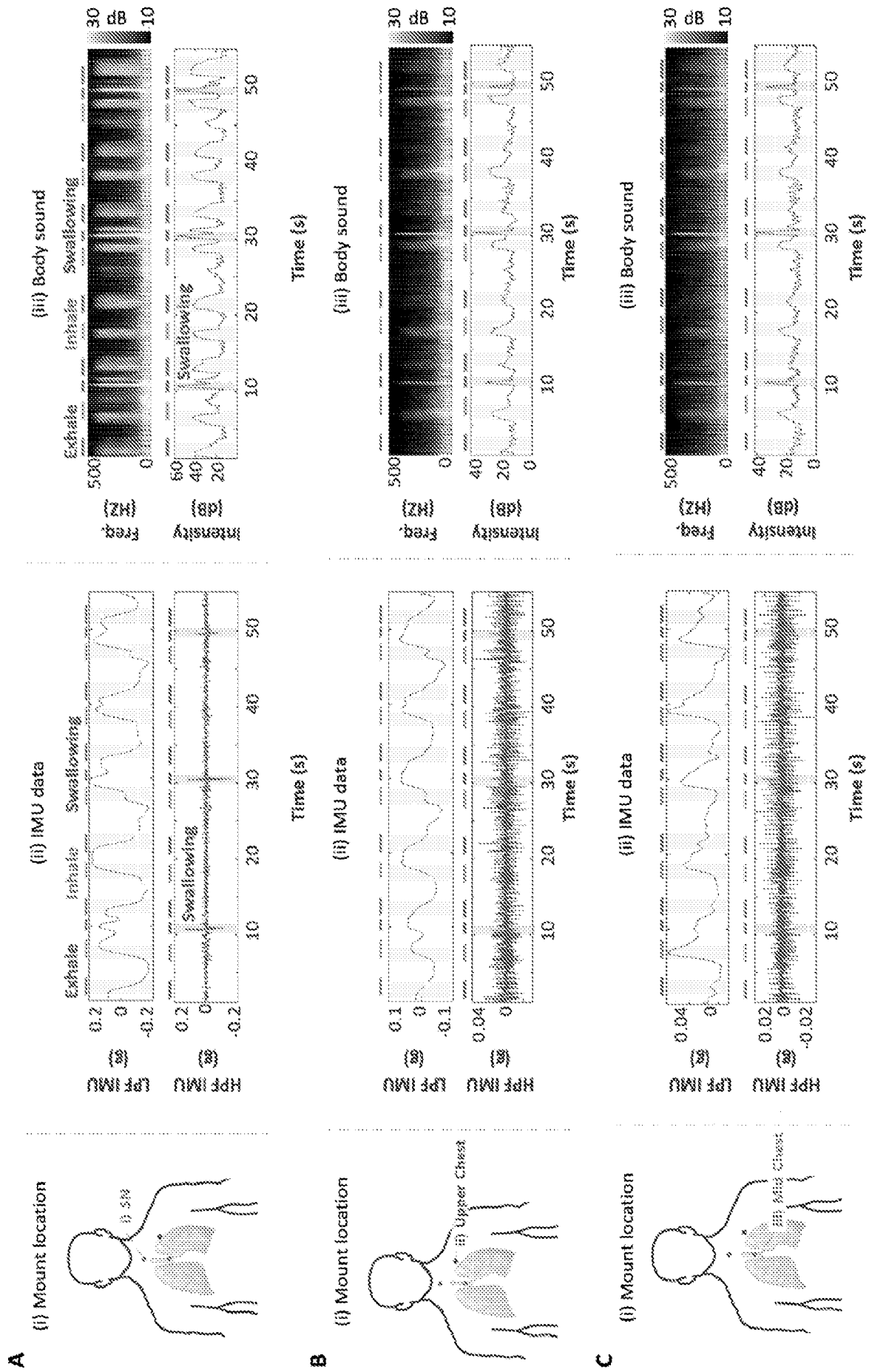
A
(i) Mount location
i) Sternum
(ii) IMU data
Exhale
Inhale
Swallowing
LPF IMU (g)
HPF IMU (g)
Swallowing
Time (s)
(iii) Body sound
Freq. (HZ)
Intensity (dB)
dB
Swallowing
Time (s)
B
(i) Mount location
ii) Upper Chest
(ii) IMU data
LPF IMU (g)
HPF IMU (g)
Time (s)
(iii) Body sound
Freq. (HZ)
Intensity (dB)
Time (s)
C
(i) Mount location
iii) Mid Chest
(ii) IMU data
LPF IMU (g)
HPF IMU (g)
Time (s)
(iii) Body sound
Freq. (HZ)
Intensity (dB)
Time (s)

FIG. 15

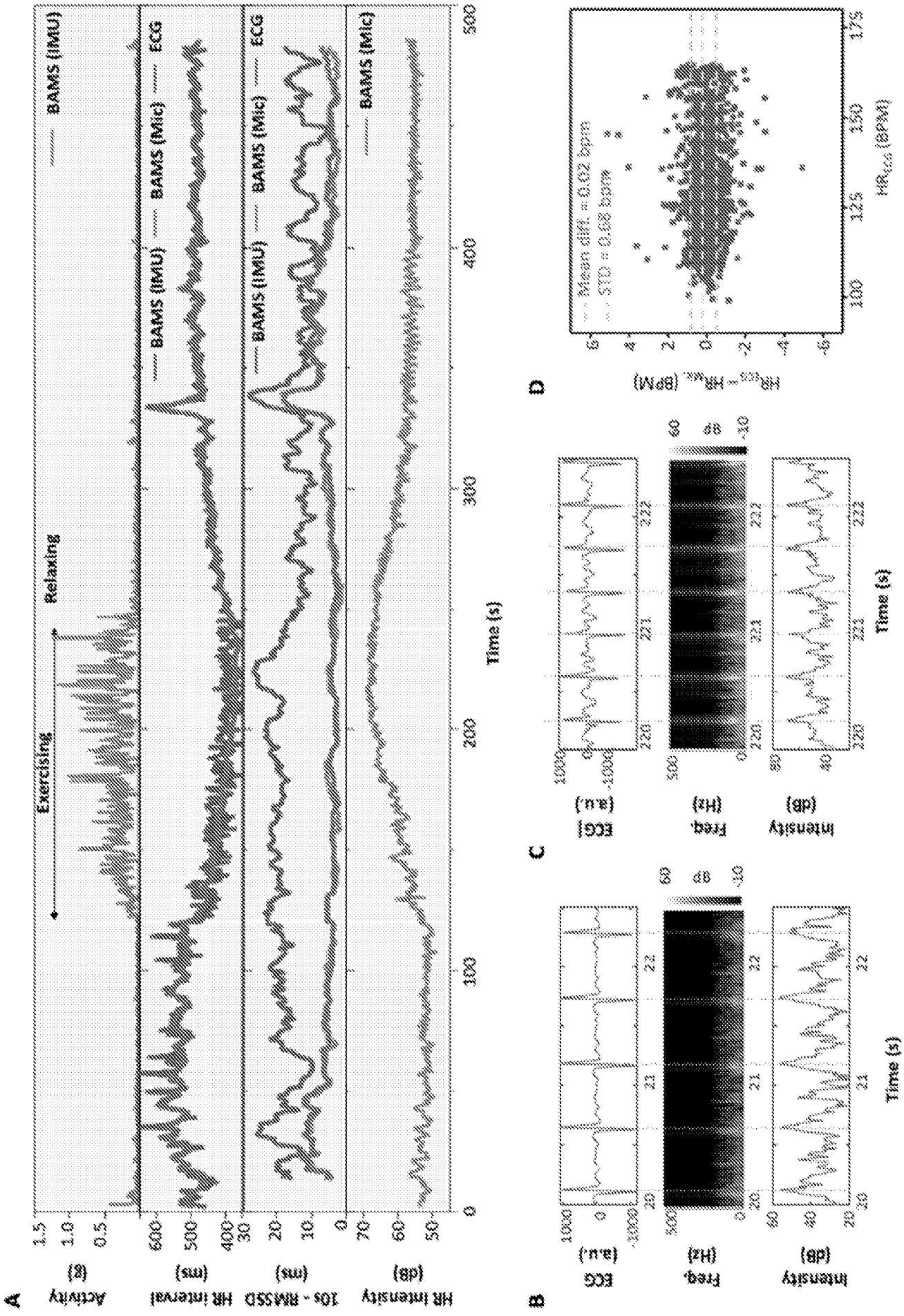
A
Activity (g)
HR interval (ms)
10s - RMSSD (ms)
HR intensity (dB)
Exercising
Relaxing
BAMS (IMU)
BAMS (Mic)
ECG
Time (s)
B
ECG (a.u.)
Freq. (Hz)
Intensity (dB)
Time (s)
C
ECG (a.u.)
Freq. (Hz)
Intensity (dB)
Time (s)
D
Mean diff. = 0.02 bpm
STD = 0.68 bpm
HR_ECG − HR_IMU (BPM)
HR_ECG (BPM)

FIG. 16

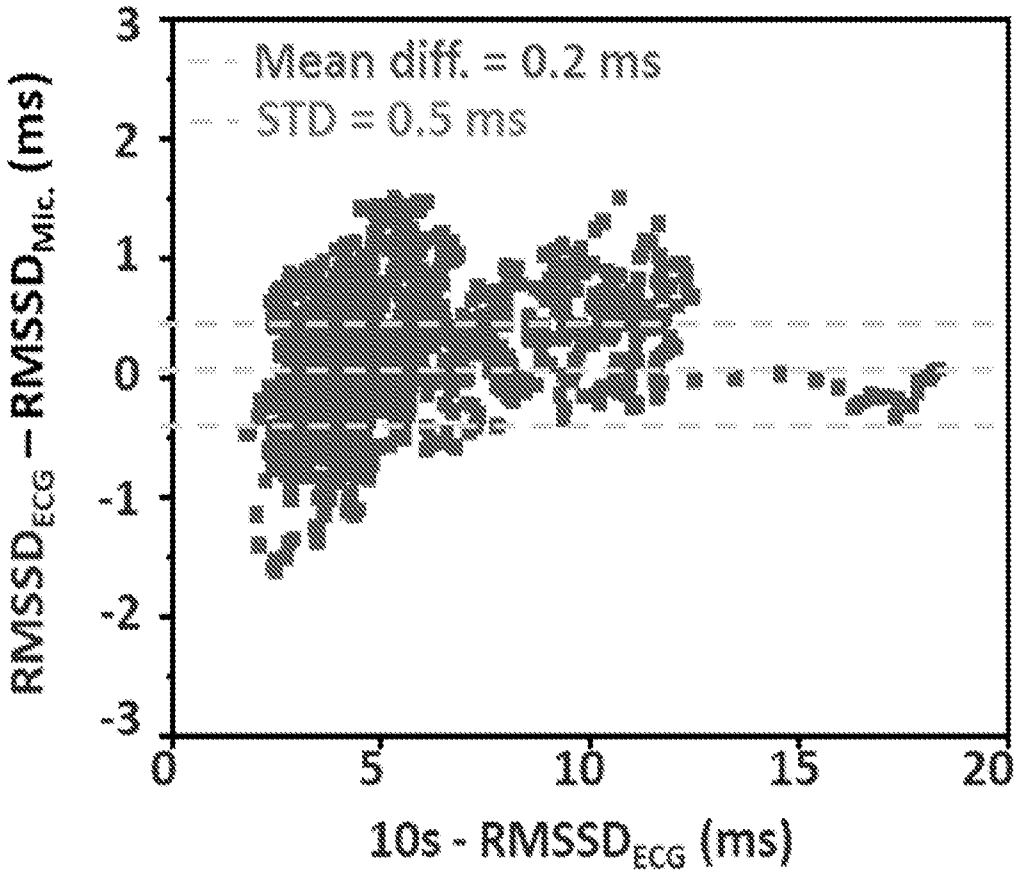
Mean diff. = 0.2 ms
STD = 0.5 ms
RMSSD$_{ECG}$ − RMSSD$_{Mic.}$ (ms)
10s - RMSSD$_{ECG}$ (ms)
3
2
1
0
-1
-2
-3
0
5
10
15
20

FIG. 17

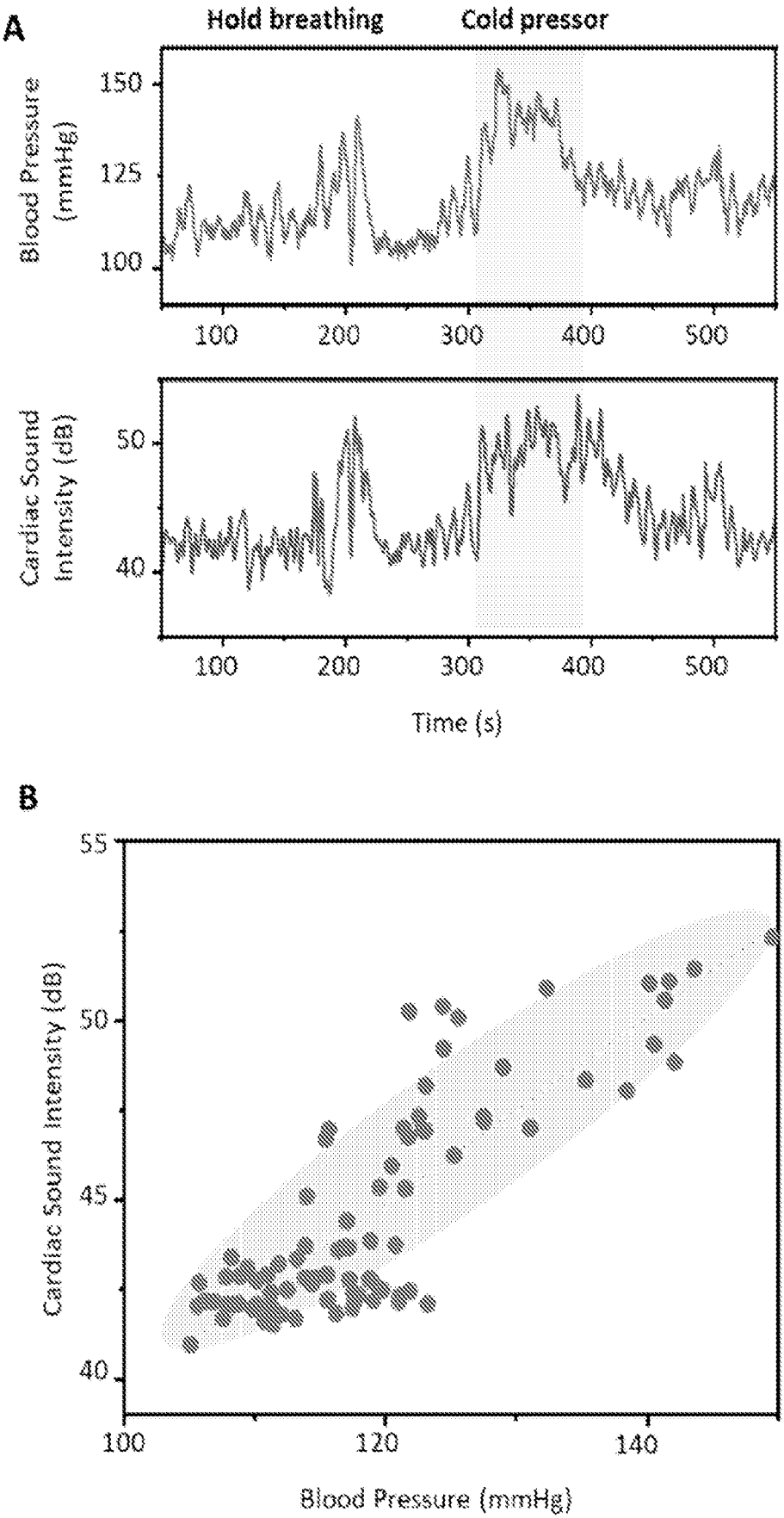
A
Hold breathing
Cold pressor
Blood Pressure (mmHg)
150
125
100
100
200
300
400
500
Cardiac Sound Intensity (dB)
50
40
100
200
300
400
500
Time (s)
B
Cardiac Sound Intensity (dB)
55
50
45
40
100
120
140
Blood Pressure (mmHg)

FIG. 18

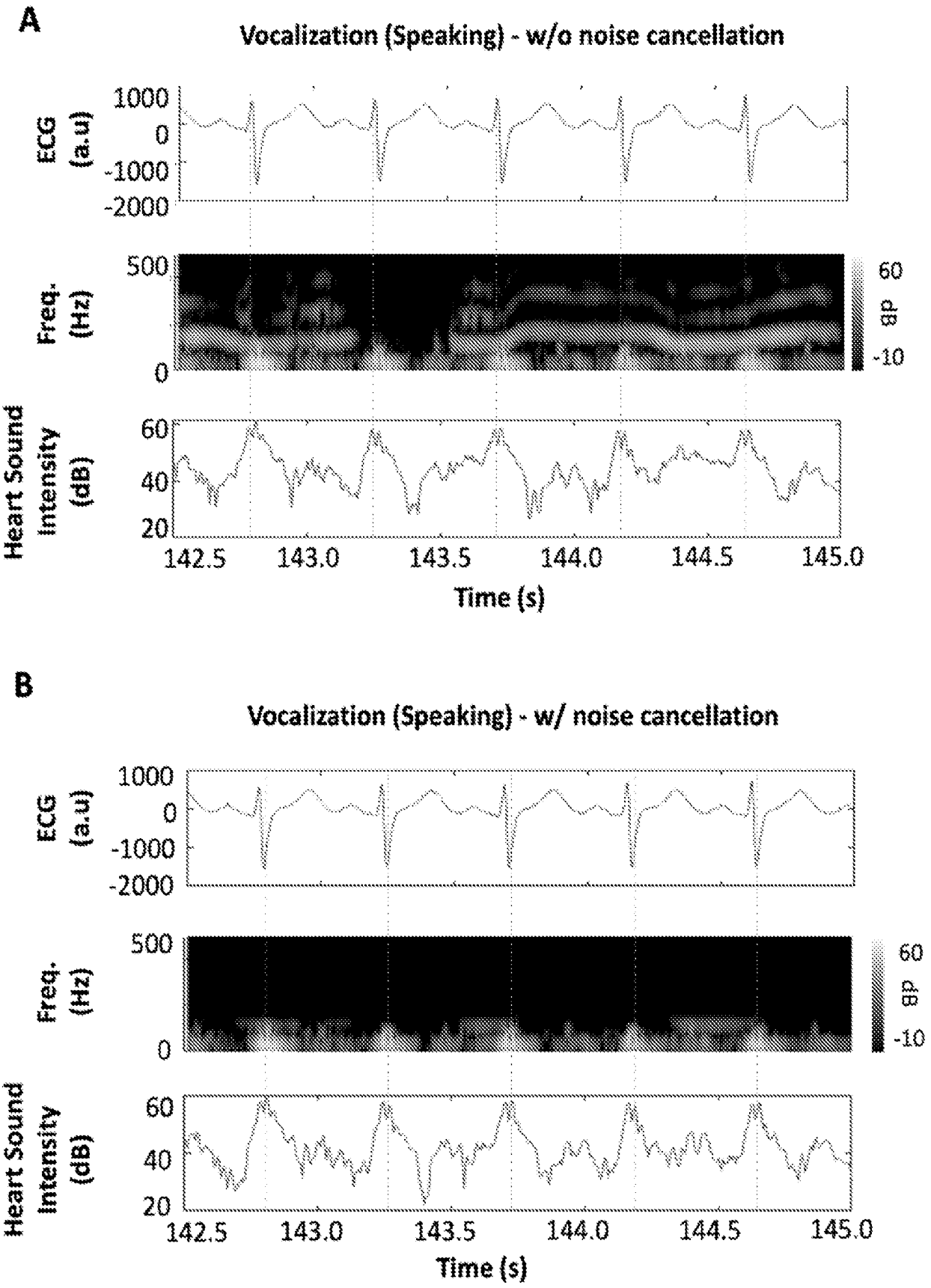
A
Vocalization (Speaking) - w/o noise cancellation
ECG (a.u)
1000
0
-1000
-2000
Freq. (Hz)
500
0
60
dB
-10
Heart Sound Intensity (dB)
60
40
20
142.5
143.0
143.5
144.0
144.5
145.0
Time (s)
B
Vocalization (Speaking) - w/ noise cancellation
ECG (a.u)
1000
0
-1000
-2000
Freq. (Hz)
500
0
60
dB
-10
Heart Sound Intensity (dB)
60
40
20
142.5
143.0
143.5
144.0
144.5
145.0
Time (s)

FIG. 19

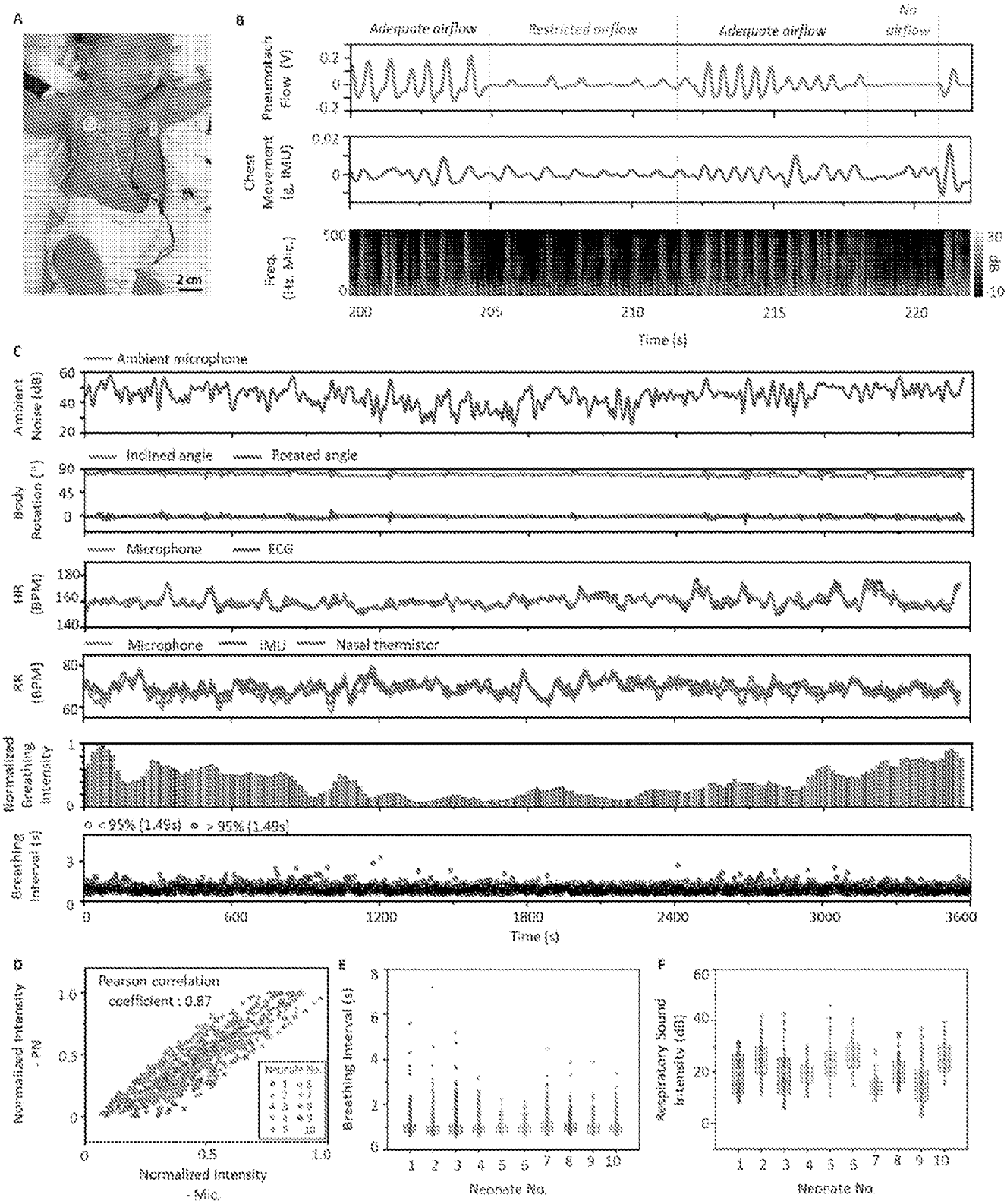
A
2 cm
B
Adequate airflow
Restricted airflow
Adequate airflow
No airflow
Pneumotach Flow (V)
Chest Movement (g, IMU)
Freq. (Hz, Mic.)
Time (s)
C
Ambient microphone
Ambient Noise (dB)
Inclined angle
Rotated angle
Body Rotation (°)
Microphone
ECG
HR (BPM)
Microphone
IMU
Nasal thermistor
RR (BPM)
Normalized Breathing Intensity
< 95% (1.49s)
> 95% (1.49s)
Breathing Interval (s)
Time (s)
D
Pearson correlation coefficient : 0.87
Normalized Intensity - PM
Normalized Intensity - Mic.
Neonate No.
E
Breathing Interval (s)
Neonate No.
F
Respiratory Sound Intensity (dB)
Neonate No.

FIG. 20



FIG. 21

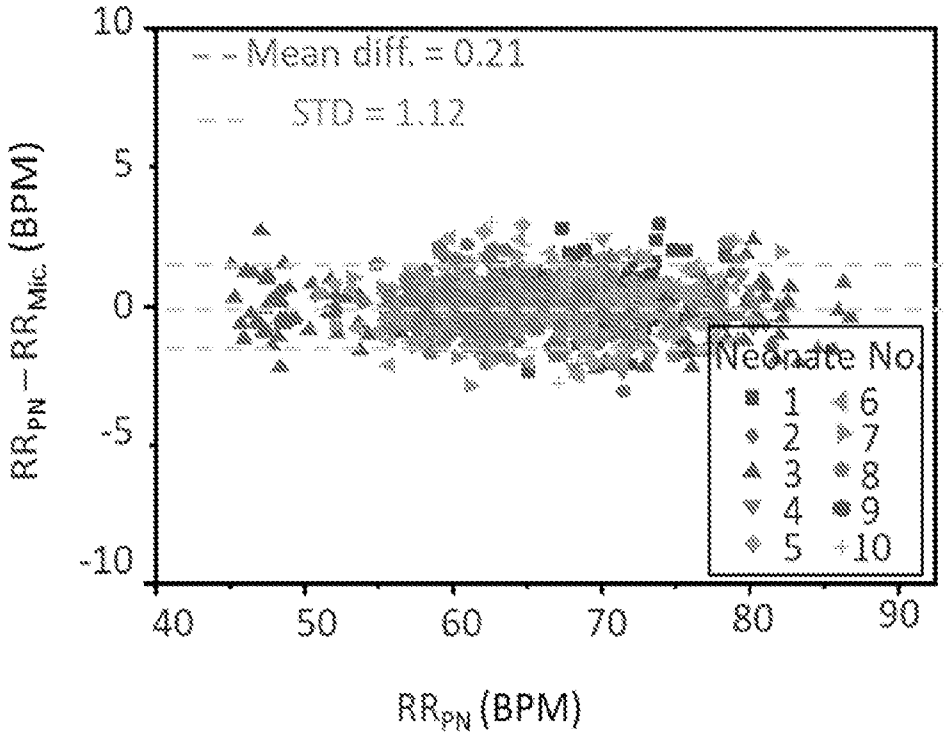
10
5
0
-5
-10
40
50
60
70
80
90
Mean diff. = 0.21
STD = 1.12
Neonate No.
1
2
3
4
5
6
7
8
9
10
RR_PN − RR_Mic. (BPM)
RR_PN (BPM)

FIG. 22

Study	Sensor (Communication)	Participants	Correlation value (Acoustic power)
This study	**MEMS microphones (Bluetooth)**	**10 preterm infants**	**0.87**
Kraman (1984)	Electret microphones (Wired)	4 adults	0.83
Lessard & Wong (1986)	Electronic stethoscope (Wired)	12 adults	0.74
Nakano et al. (1994)	Tie-clip microphones (Wired)	19 adults	0.85
Blowes et al. (1995)	Piezoelectric accelerometer (Wired)	16 term infants	0.73
Ciftci & Kahya (2008)	Air-coupled electret microphones (Wired)	18 adults	0.88
Montazeri Ghahjaverestan et al. (2021)	Microphone (unspecified) (Wireless, unspecified)	61 adults	0.36
Fu et al. (2022)	Microphone (unspecified) (Unspecified)	9 adults	0.66

FIG. 23

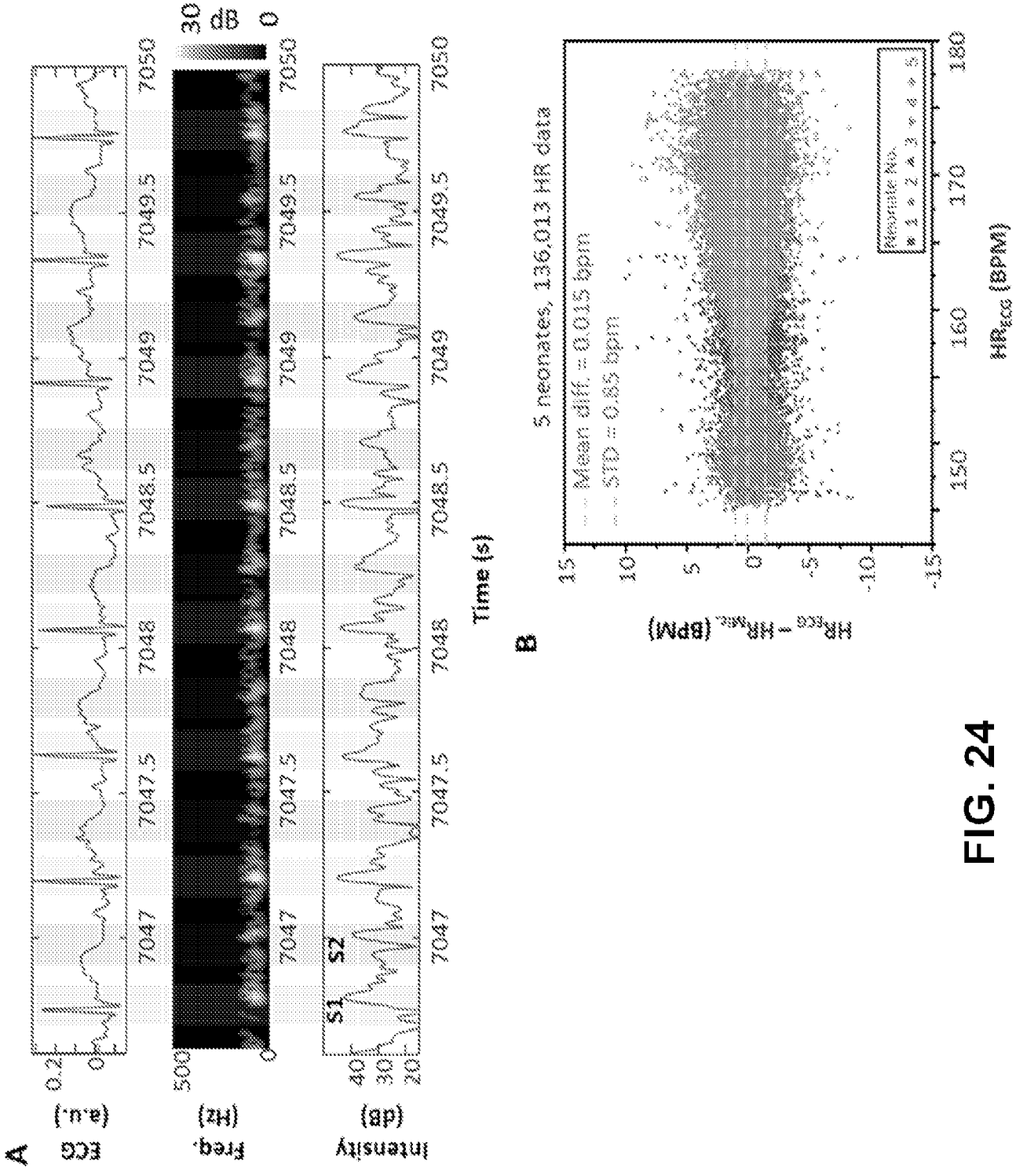
A
ECG (a.u.)
Freq. (Hz)
Intensity (dB)
S1
S2
Time (s)
B
5 neonates, 136,013 HR data
Mean diff. = 0.015 bpm
STD = 0.85 bpm
Neonate No.
HR_ECG − HR_Acc. (BPM)
HR_ECG (BPM)

FIG. 24

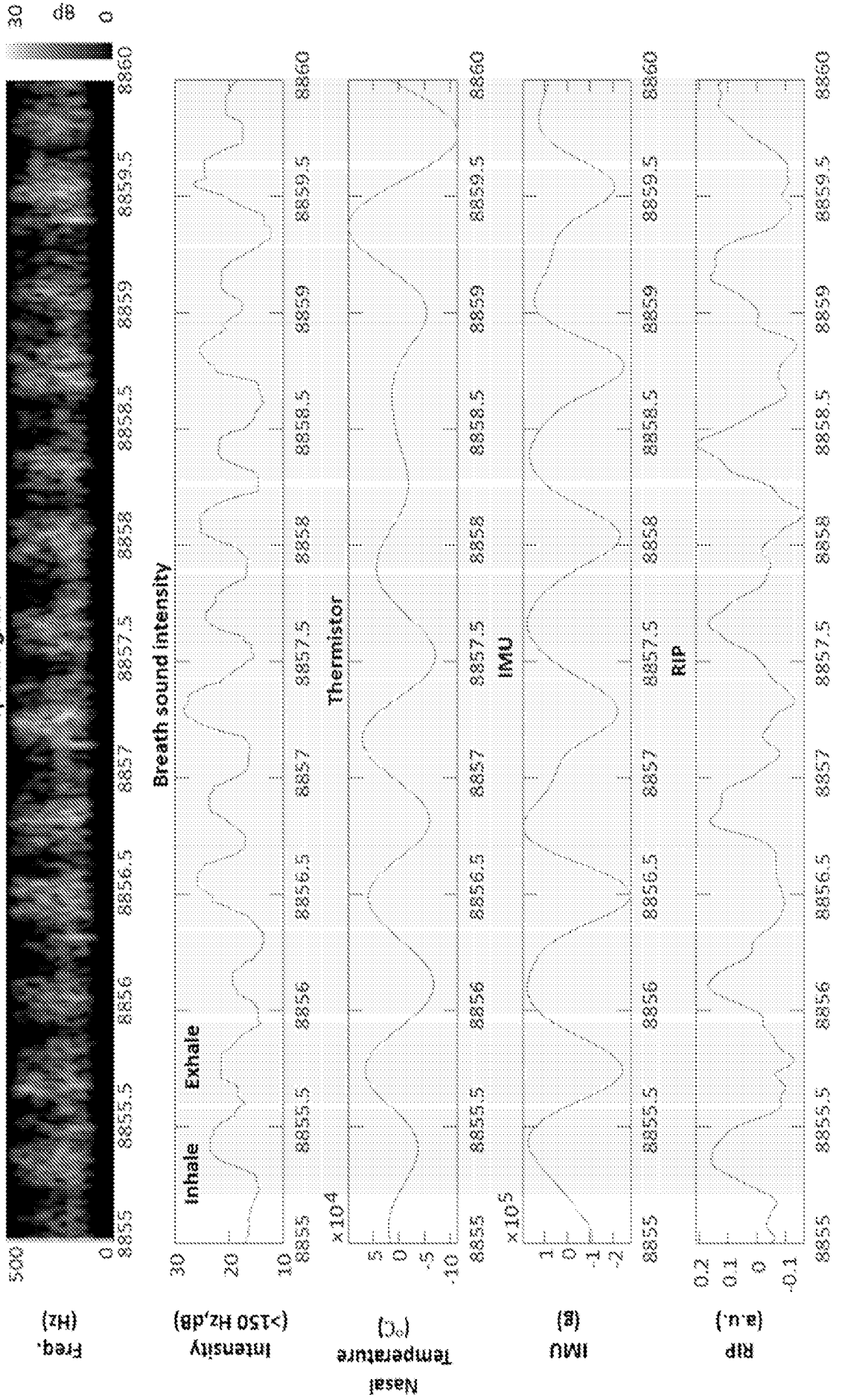
Spectrogram
Freq. (Hz)
Breath sound intensity
Intensity (>150 Hz,dB)
Inhale
Exhale
Thermistor
Nasal Temperature (°C)
IMU
IMU (g)
RIP
RIP (a.u.)
Time (s)

FIG. 25

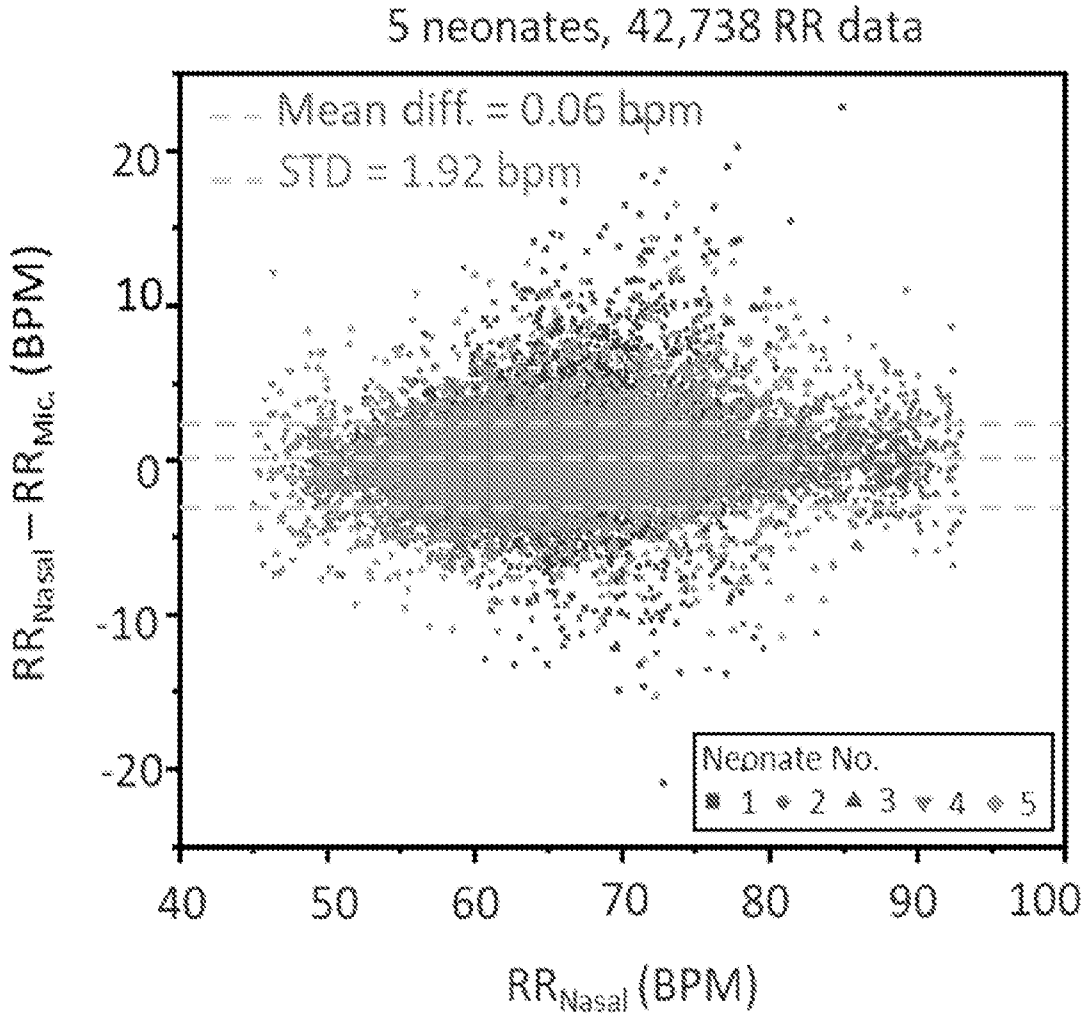
5 neonates, 42,738 RR data
Mean diff. = 0.06 bpm
STD = 1.92 bpm
20
10
0
-10
-20
40
50
60
70
80
90
100
RR_Nasal − RR_Mic. (BPM)
RR_Nasal (BPM)
Neonate No.
1 2 3 4 5

FIG. 26

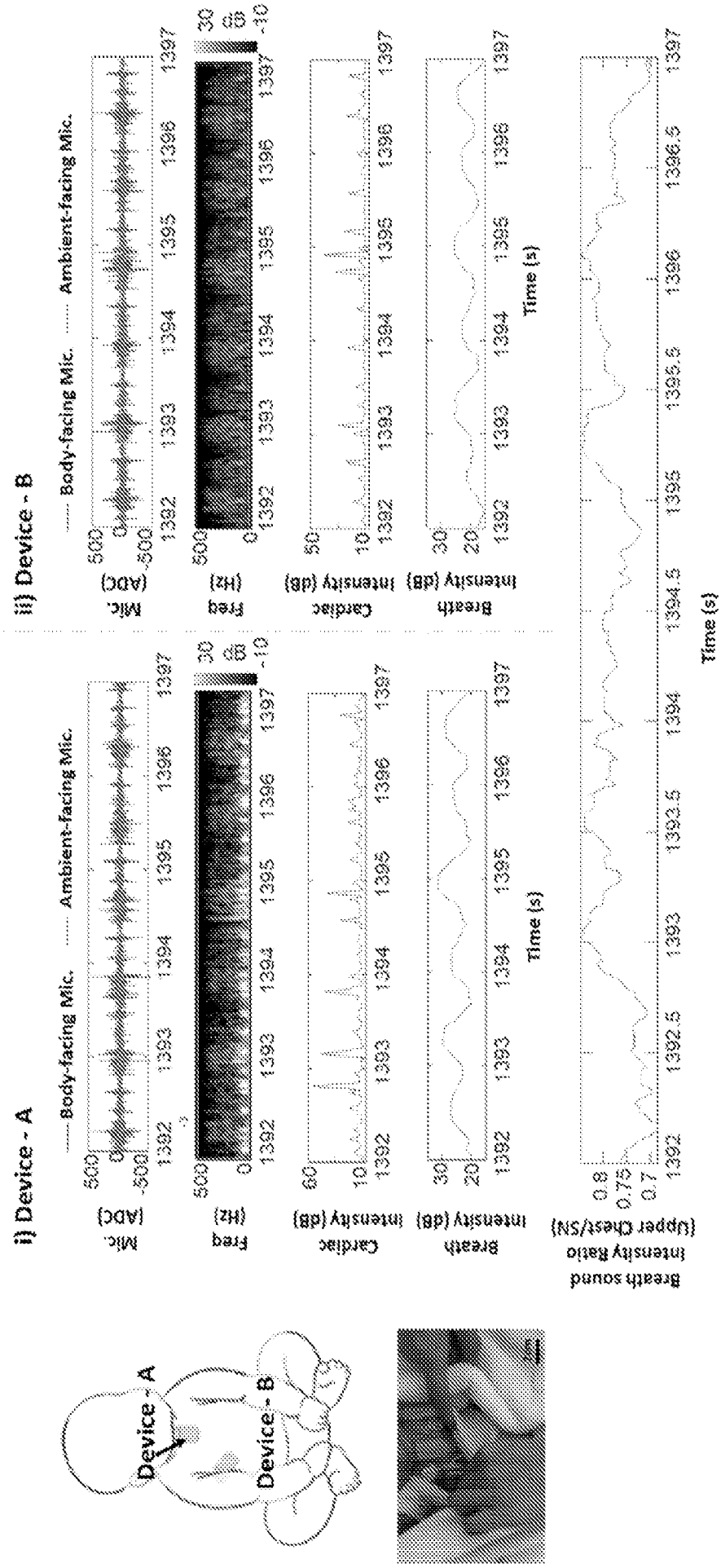
i) Device - A
ii) Device - B
Body-facing Mic.
Ambient-facing Mic.
Mic. (ADC)
Freq (Hz)
Cardiac intensity (dB)
Breath intensity (dB)
Breath sound intensity Ratio (Upper Chest/SN)
Time (s)
Device - A
Device - B

FIG. 27

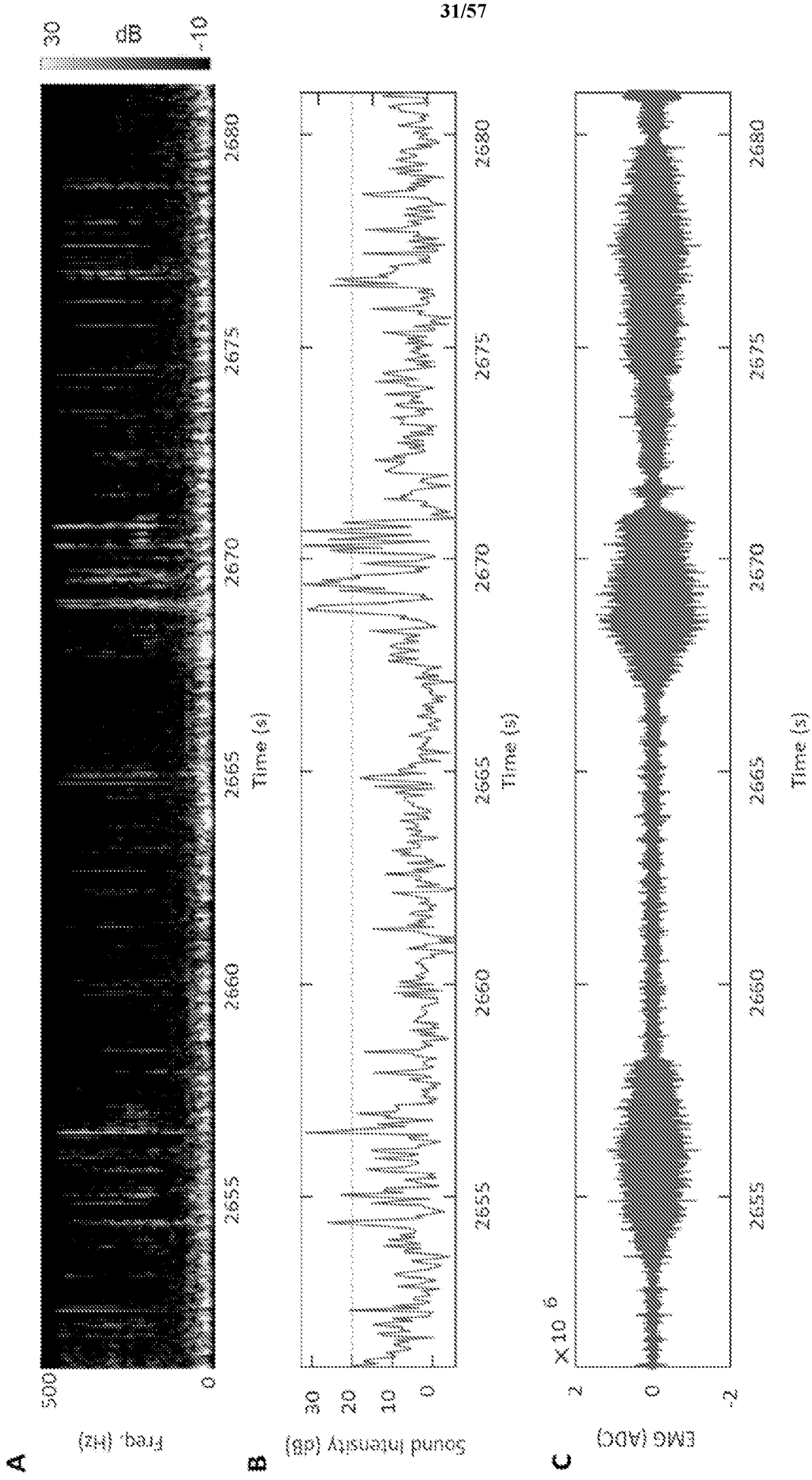
A
B
C
30
dB
-10
500
0
Freq. (Hz)
2655
2660
2665
2670
2675
2680
Time (s)
30
20
10
0
Sound Intensity (dB)
X 10^6
2
0
-2
EMG (ADC)

FIG. 28

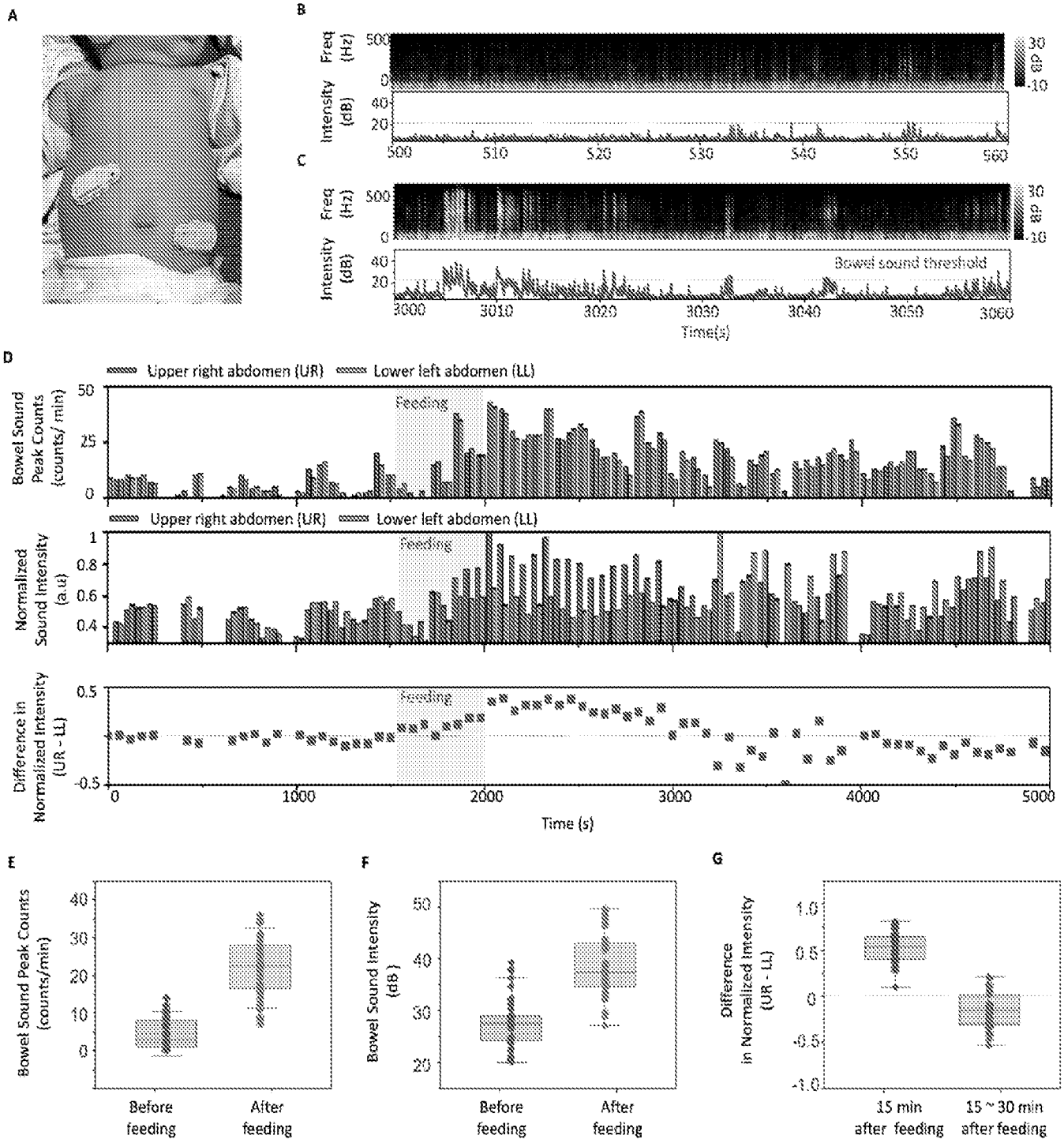
A
B
Freq (Hz)
Intensity (dB)
C
Bowel sound threshold
Time(s)
D
Upper right abdomen (UR)
Lower left abdomen (LL)
Bowel Sound Peak Counts (counts/ min)
Feeding
Normalized Sound Intensity (a.u)
Difference in Normalized Intensity (UR - LL)
Time (s)
E
Bowel Sound Peak Counts (counts/min)
Before feeding
After feeding
F
Bowel Sound Intensity (dB)
G
Difference in Normalized Intensity (UR - LL)
15 min after feeding
15 ~ 30 min after feeding

FIG. 29

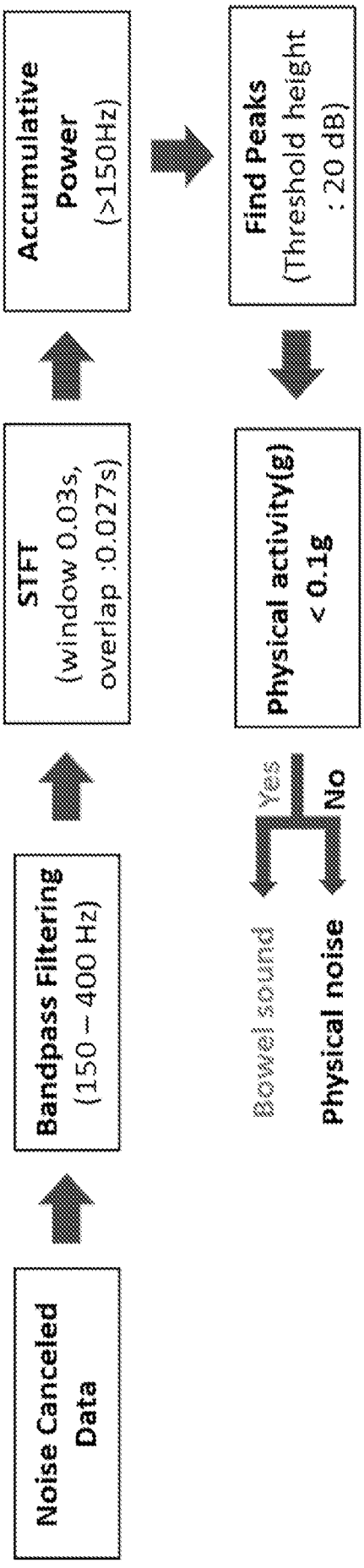
Noise Canceled Data
Bandpass Filtering (150 – 400 Hz)
STFT (window 0.03s, overlap :0.027s)
Accumulative Power (>150Hz)
Find Peaks (Threshold height : 20 dB)
Physical activity(g) < 0.1g
Yes
No
Bowel sound
Physical noise

FIG. 30

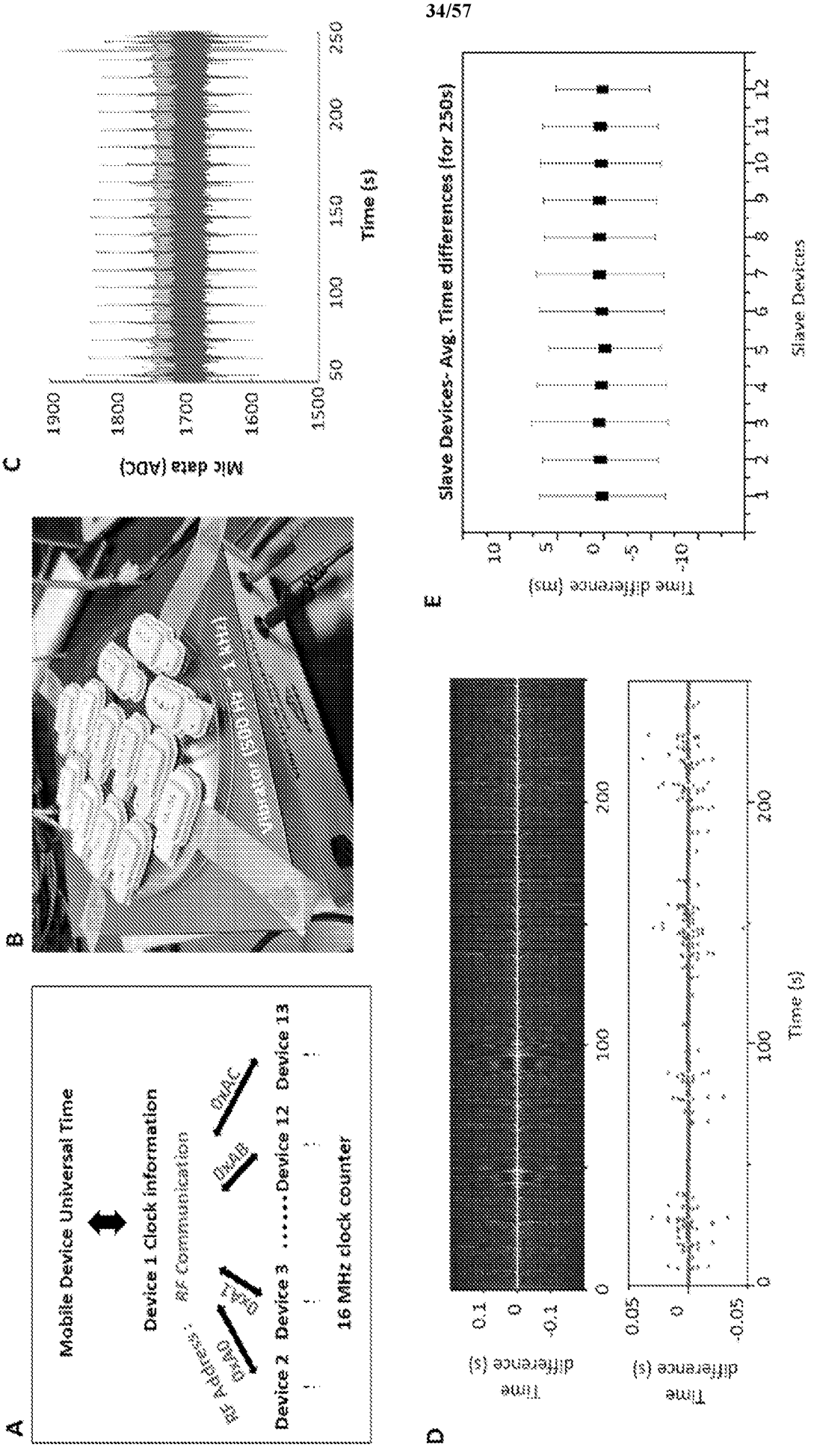
A
Mobile Device Universal Time
Device 1 Clock information
RF Communication
RF Address:
0xA0
0xA1
0xAB
0xAC
Device 2
Device 3
Device 12
Device 13
16 MHz clock counter
B
Vibrator (500 Hz - 1 kHz)
C
Mic data (ADC)
1900
1800
1700
1600
1500
50
100
150
200
250
Time (s)
D
Time difference (s)
0.1
0
-0.1
0
100
200
Time difference (s)
0.05
0
-0.05
0
100
200
Time (s)
E
Slave Devices- Avg. Time differences (for 250s)
Time difference (ms)
10
5
0
-5
-10
1
2
3
4
5
6
7
8
9
10
11
12
Slave Devices

FIG. 31

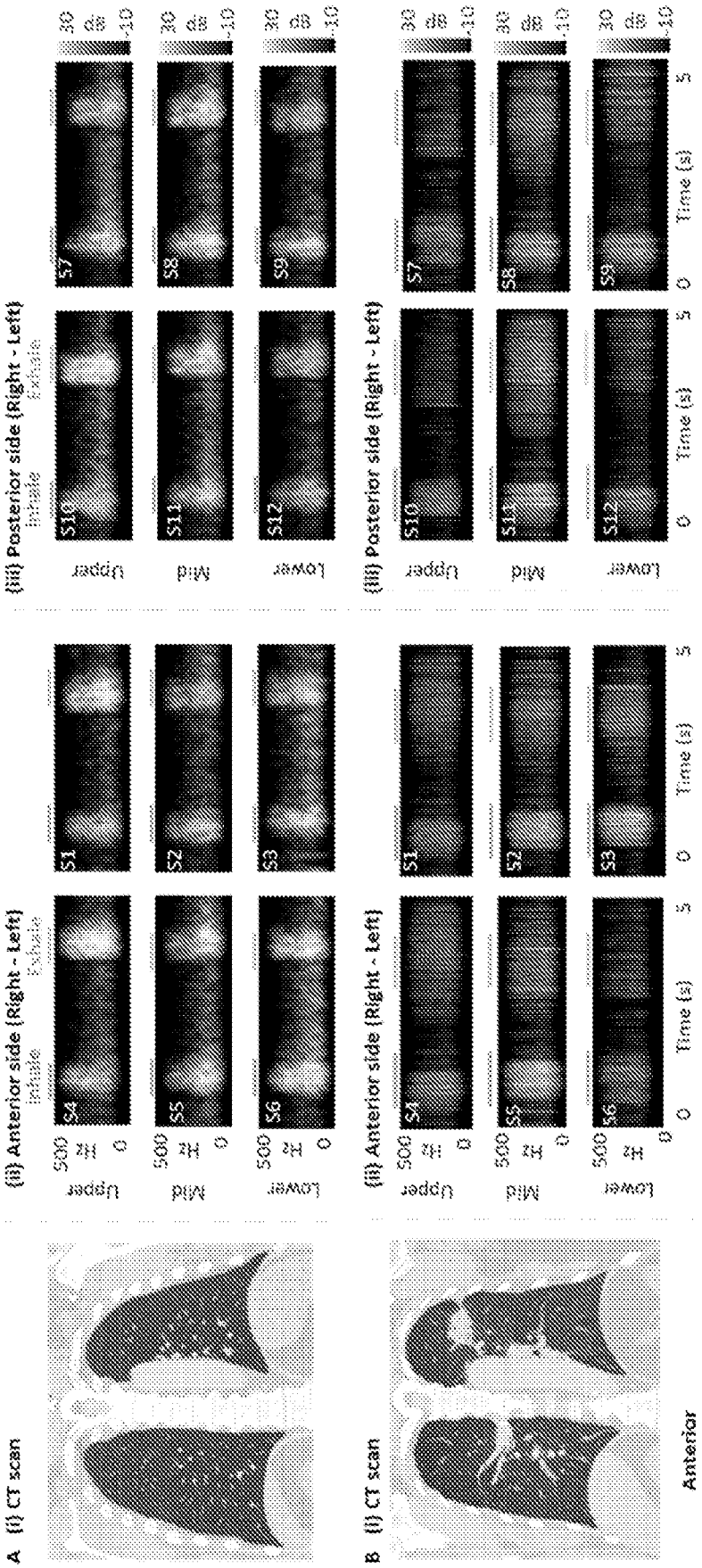
A (i) CT scan
B (i) CT scan
Anterior
(ii) Anterior side (Right - Left)
Inhale
Exhale
(iii) Posterior side (Right - Left)
Upper
Mid
lower
S1
S2
S3
S4
S5
S6
S7
S8
S9
S10
S11
S12
500 Hz 0
30 dB 10
0 Time (s) 5

FIG. 32A

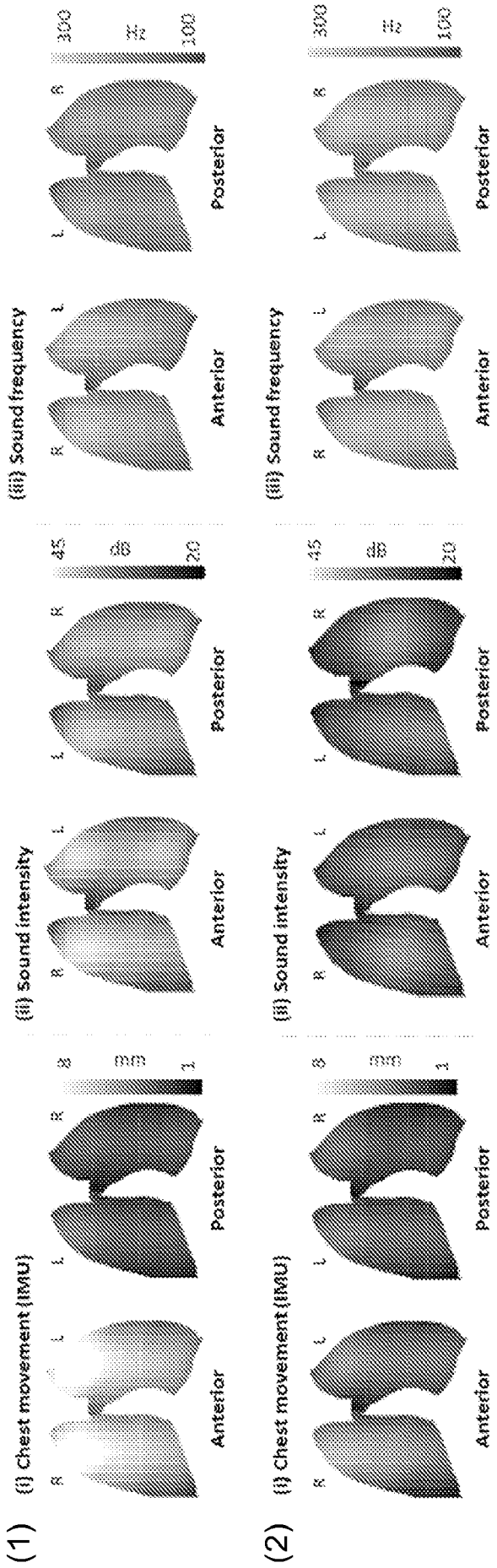
(1)
(2)
(i) Chest movement (IMU)
(ii) Sound intensity
(iii) Sound frequency
Anterior
Posterior
R
L
dB
Hz

FIG. 32B

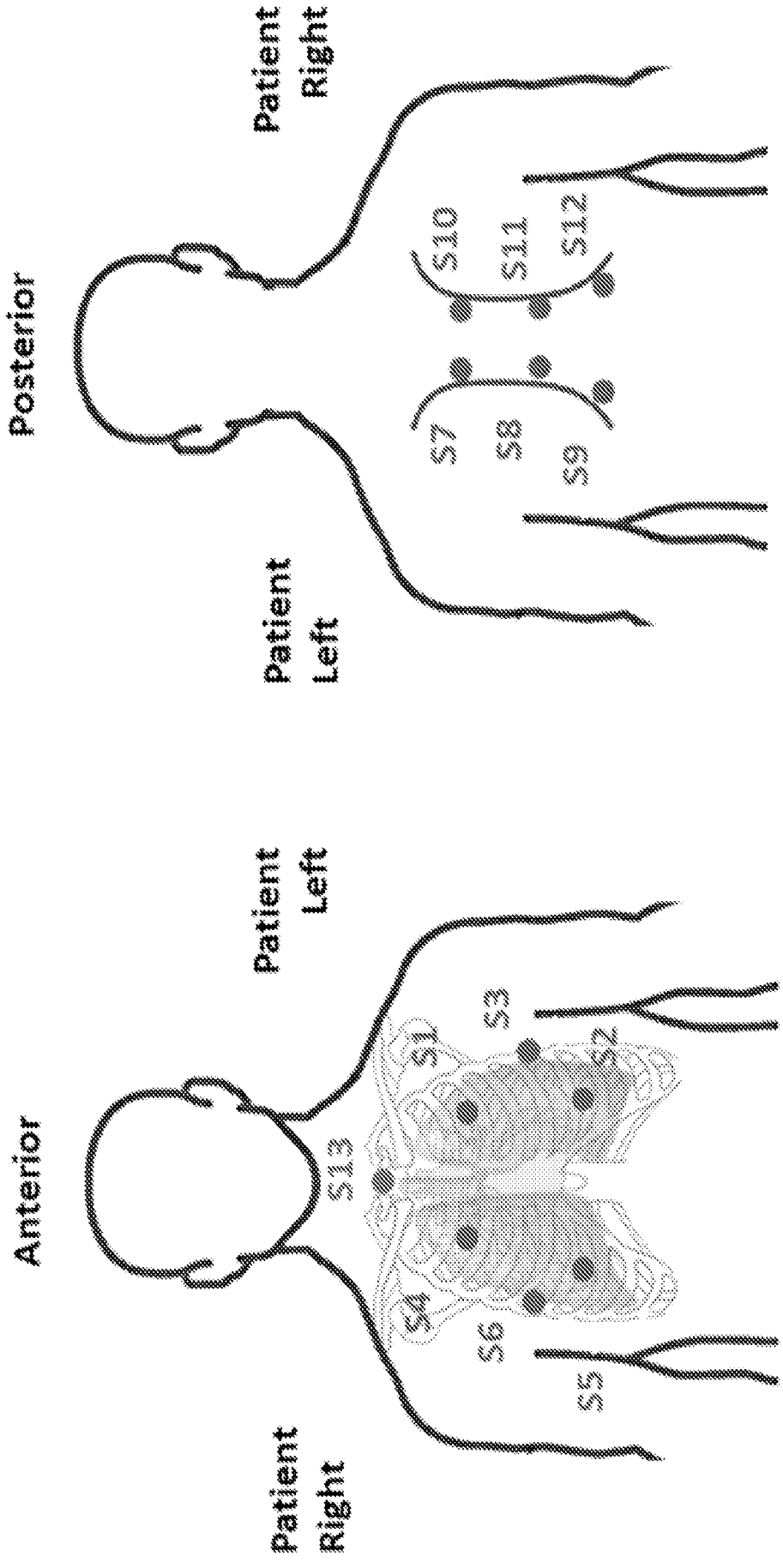
Posterior
Patient Right
Patient Left
S10
S11
S12
S7
S8
S9
Anterior
Patient Left
S13
S1
S3
S2
S4
S6
S5
Patient Right

FIG. 33

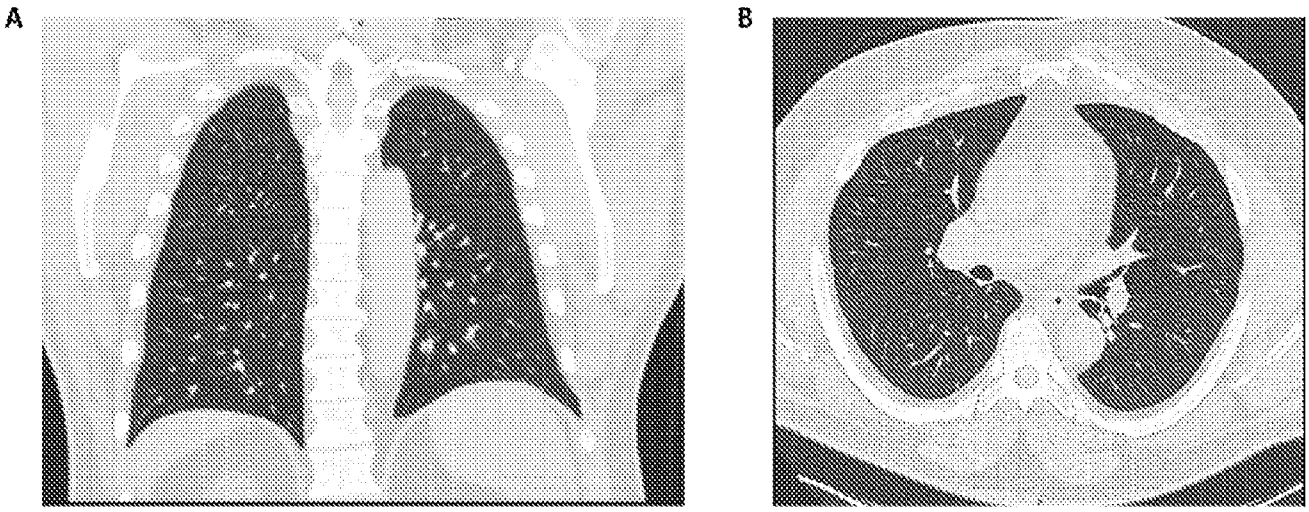

FIG. 34

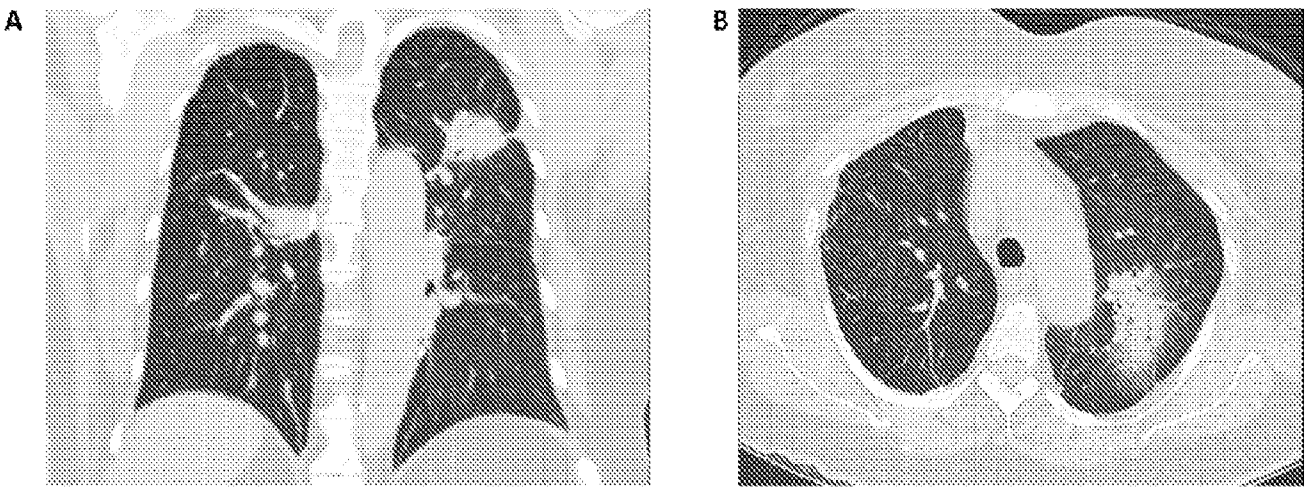

FIG. 35

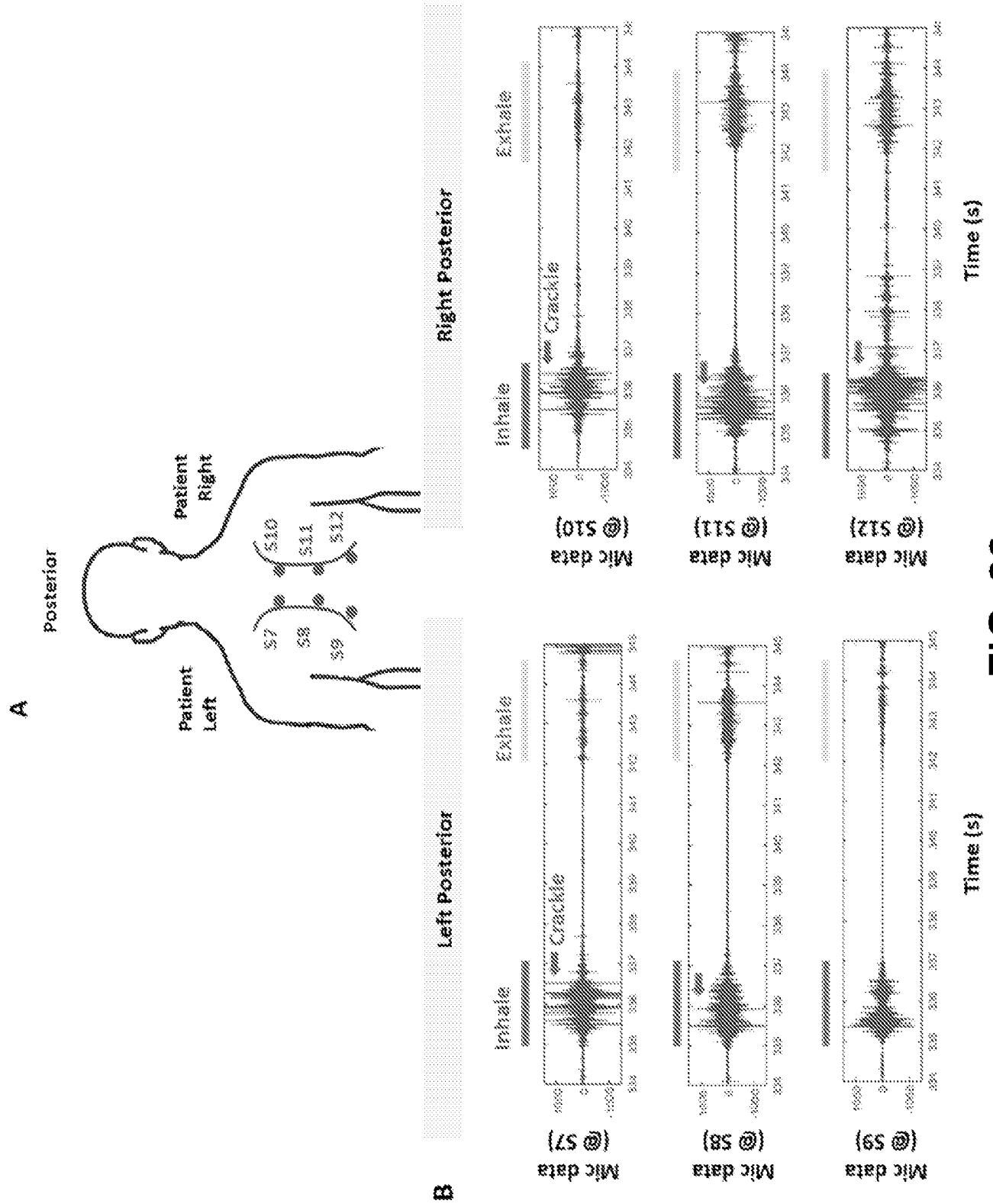
A
Posterior
Patient Left
Patient Right
S7
S8
S9
S10
S11
S12
B
Left Posterior
Right Posterior
Inhale
Exhale
Crackle
Mic data (@ S7)
Mic data (@ S8)
Mic data (@ S9)
Mic data (@ S10)
Mic data (@ S11)
Mic data (@ S12)
Time (s)

FIG. 36

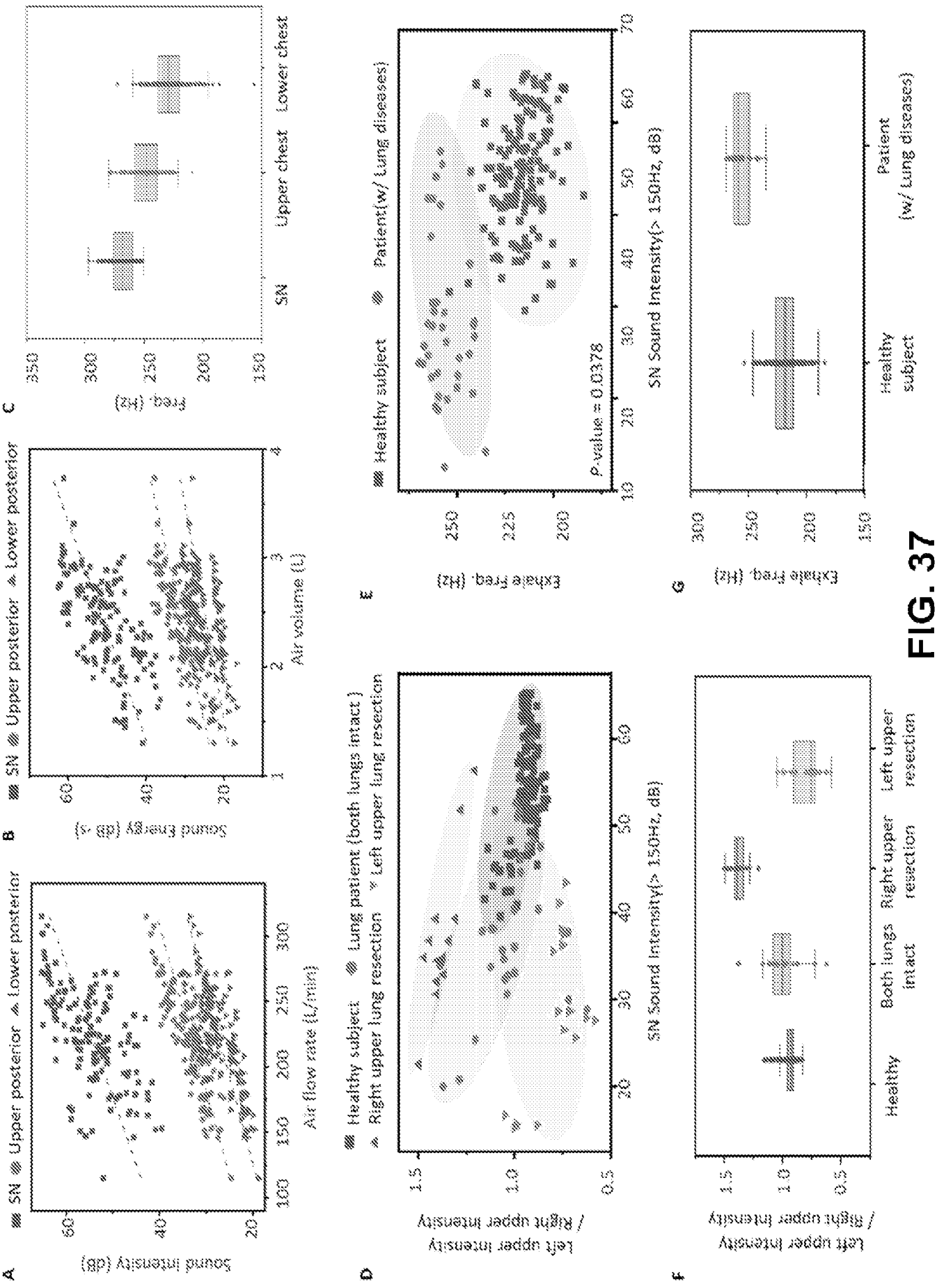
A
SN
Upper posterior
Lower posterior
Sound intensity (dB)
Air flow rate (L/min)
B
SN
Upper posterior
Lower posterior
Sound Energy (dB·s)
Air volume (L)
C
Freq. (Hz)
SN
Upper chest
Lower chest
D
Healthy subject
Lung patient (both lungs intact)
Right upper lung resection
Left upper lung resection
Left upper intensity / Right upper intensity
SN Sound Intensity(> 150Hz, dB)
E
Healthy subject
Patient(w/ Lung diseases)
Exhale Freq. (Hz)
P-value = 0.0378
SN Sound Intensity(> 150Hz, dB)
F
Left upper intensity / Right upper intensity
Healthy
Both lungs intact
Right upper resection
Left upper resection
G
Exhale Freq. (Hz)
Healthy subject
Patient (w/ Lung diseases)

FIG. 37

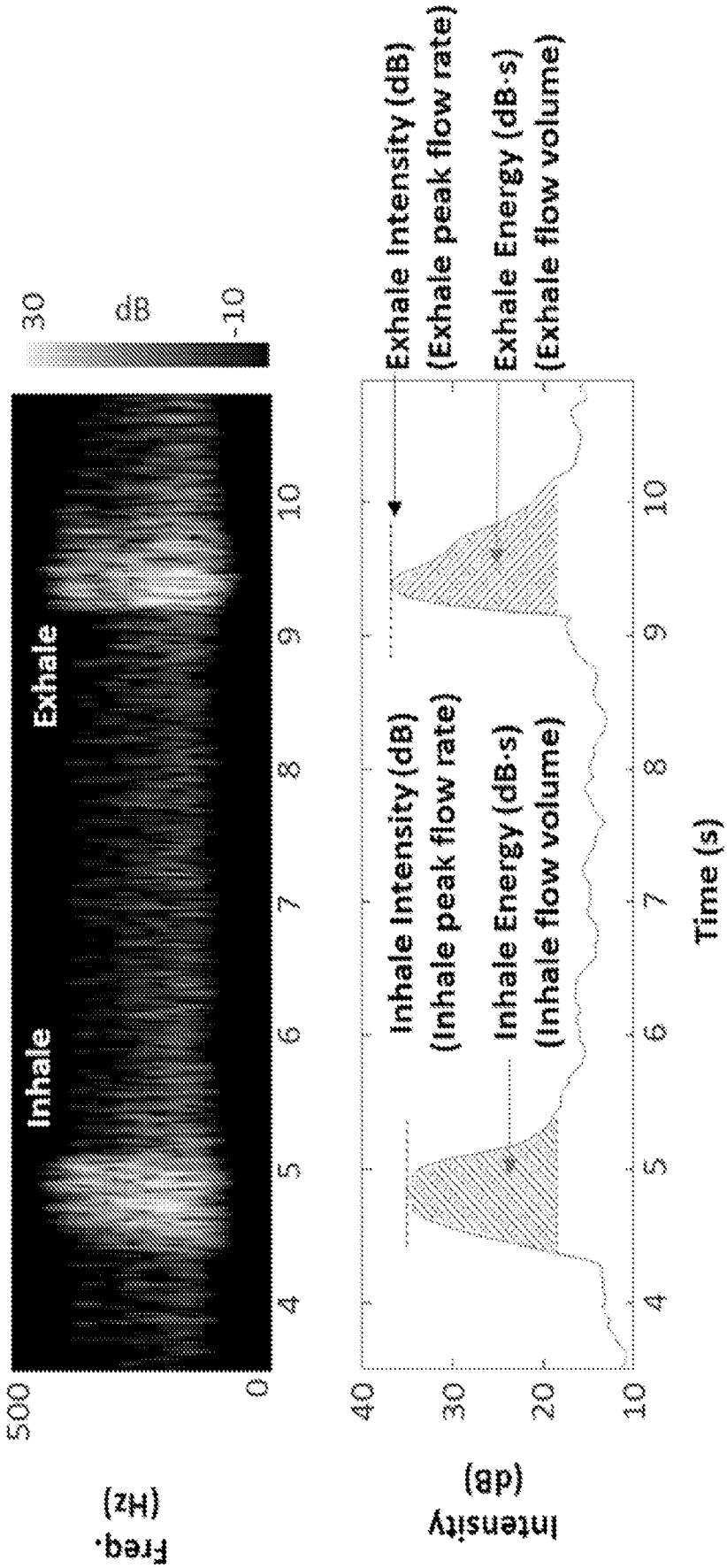
30
dB
-10
Inhale
Exhale
500
0
Freq.
(Hz)
4
5
6
7
8
9
10
Time (s)
40
30
20
10
Intensity
(dB)
Inhale Intensity (dB)
(Inhale peak flow rate)
Inhale Energy (dB·s)
(Inhale flow volume)
Exhale Intensity (dB)
(Exhale peak flow rate)
Exhale Energy (dB·s)
(Exhale flow volume)

FIG. 38

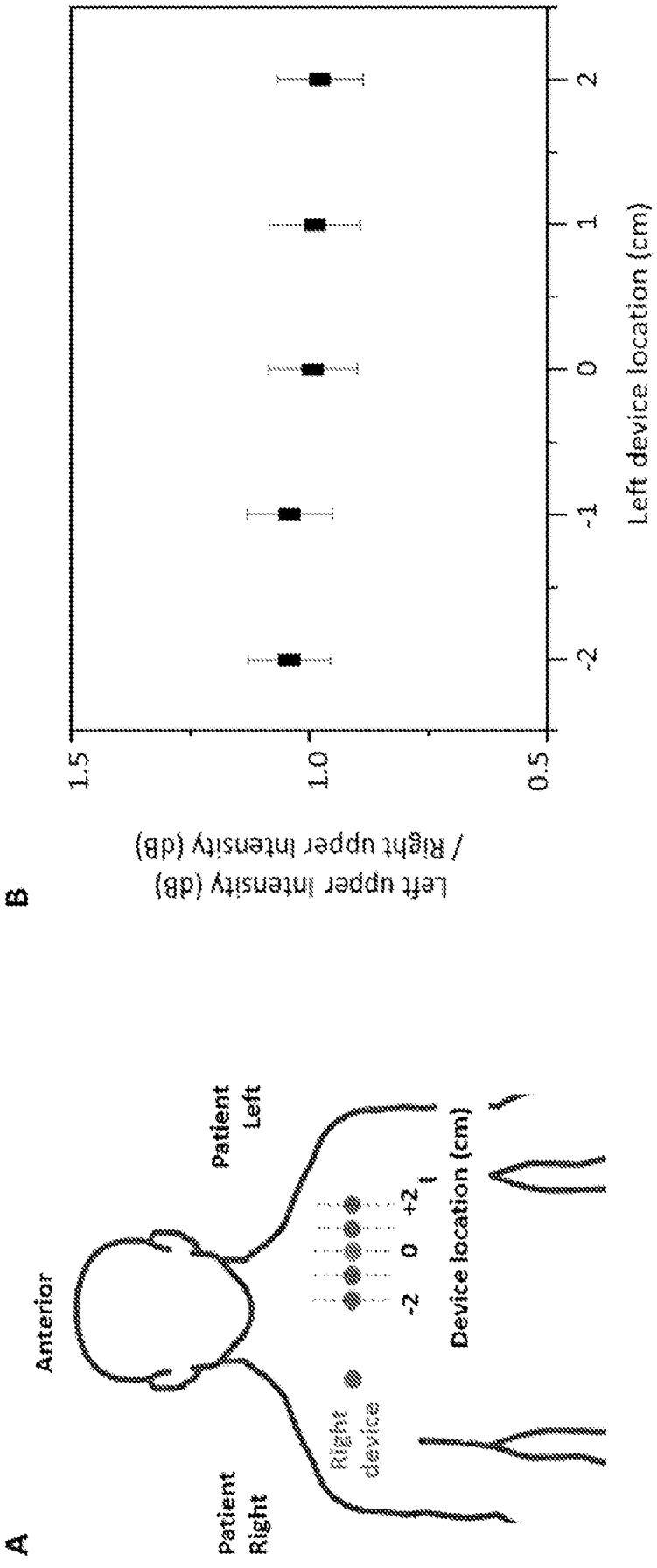
A
Patient Left
Anterior
Patient Right
Right device
-2
0
+2
Device location (cm)
B
Left upper intensity (dB)
/ Right upper intensity (dB)
1.5
1.0
0.5
-2
-1
0
1
2
Left device location (cm)

FIG. 39

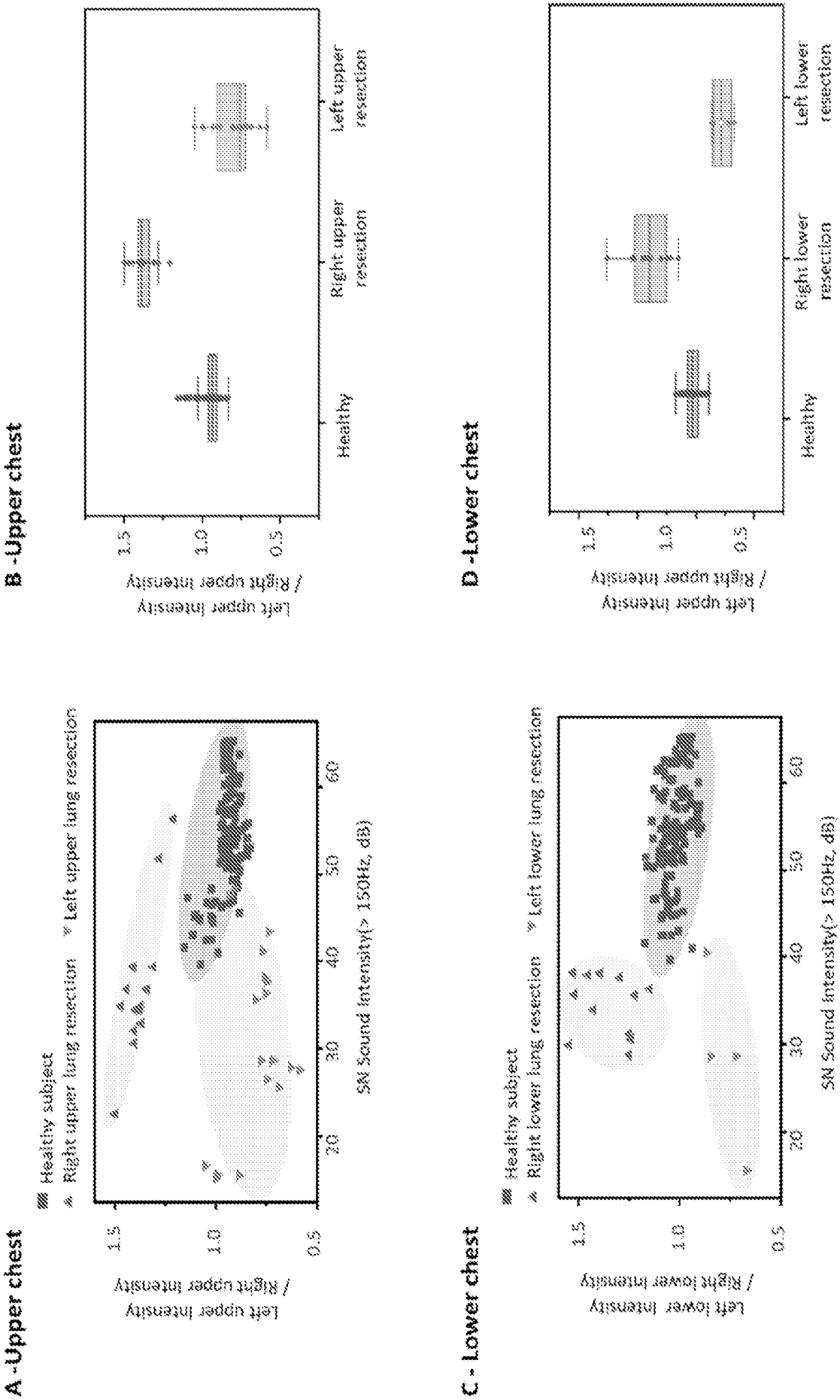
A -Upper chest
Healthy subject
Right upper lung resection
Left upper lung resection
Left upper intensity / Right upper intensity
SN Sound intensity(> 150Hz, dB)
B -Upper chest
Left upper intensity / Right upper intensity
Healthy
Right upper resection
Left upper resection
C - Lower chest
Healthy subject
Right lower lung resection
Left lower lung resection
Left lower intensity / Right lower intensity
SN Sound intensity(> 150Hz, dB)
D -Lower chest
Left upper intensity / Right upper intensity
Healthy
Right lower resection
Left lower resection

FIG. 40

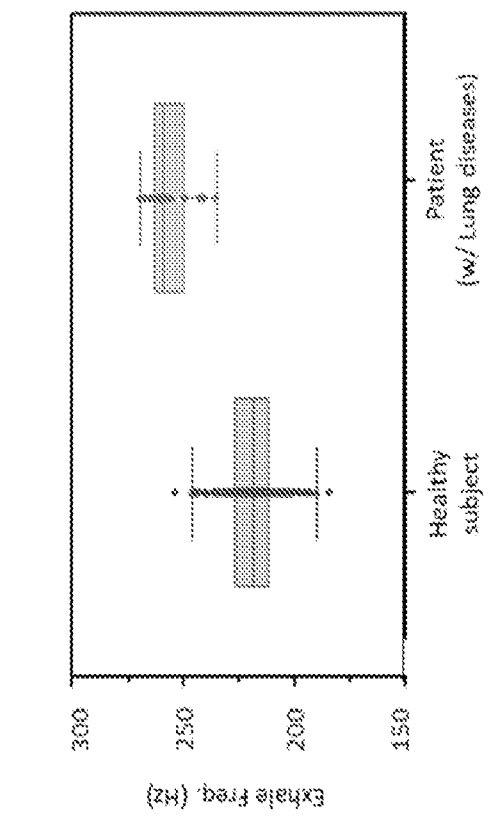
Exhale freq. (Hz)
300
250
200
150
Healthy subject
Patient (w/ Lung diseases)

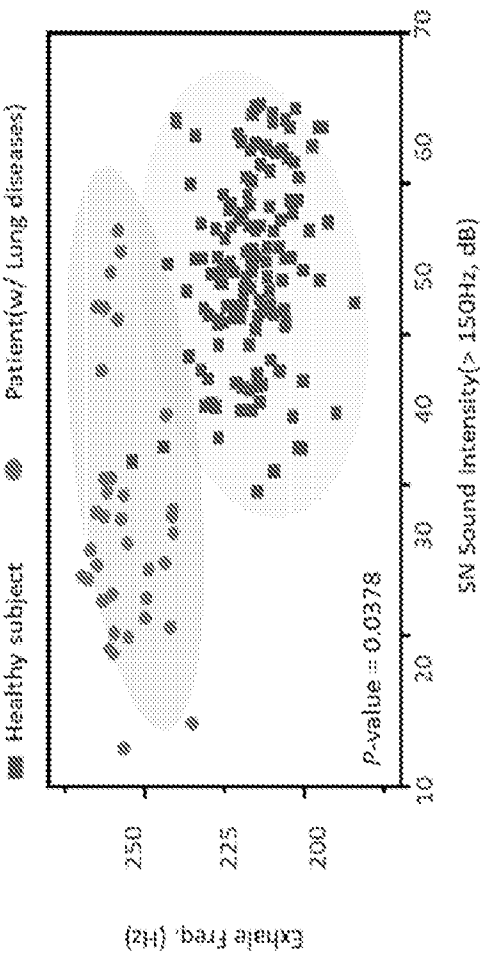
Exhale freq. (Hz)
250
225
200
Healthy subject
Patient(w/ Lung diseases)
P-value = 0.0378
SN Sound intensity(> 150Hz, dB)
10
20
30
40
50
60
70

FIG. 41A

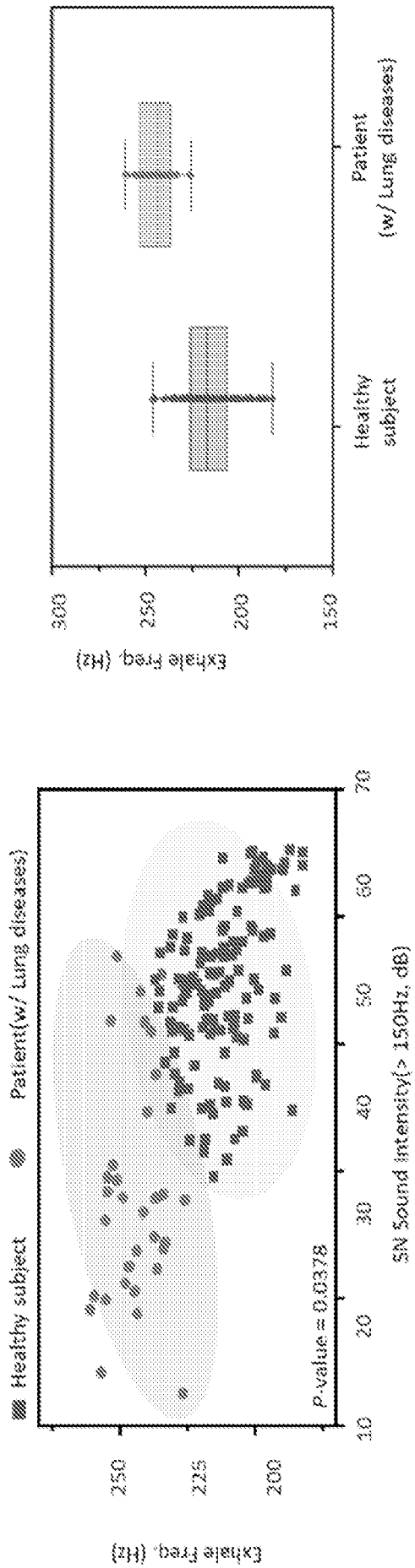
Exhale freq. (Hz)
300
250
200
150
Healthy subject
Patient (w/ Lung diseases)
Exhale freq. (Hz)
250
225
200
Healthy subject
Patient(w/ Lung diseases)
P-value = 0.0378
10
20
30
40
50
60
70
SN Sound intensity(> 150Hz, dB)

FIG. 41B

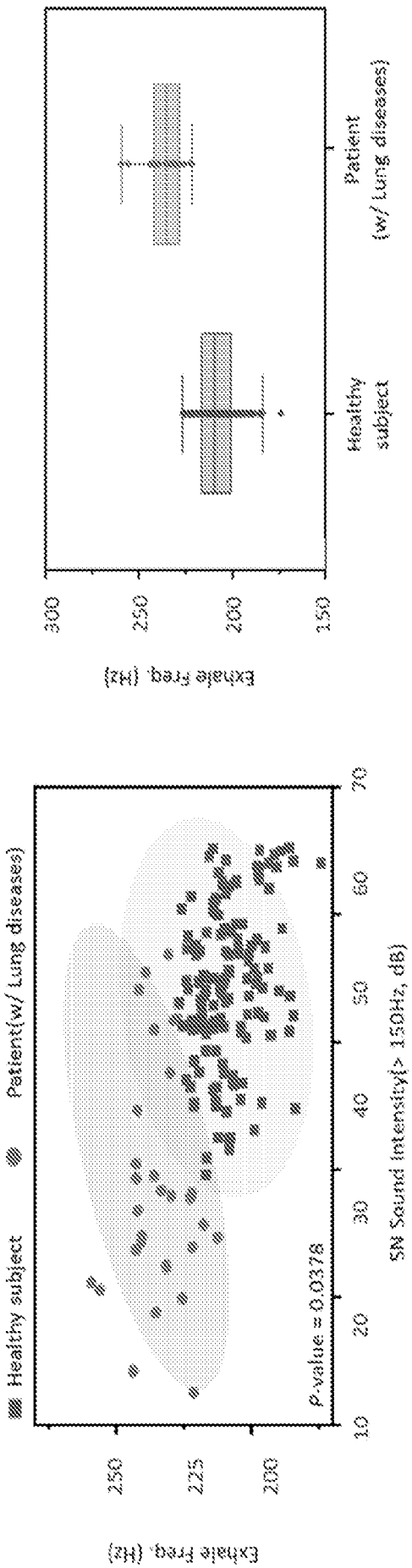
Exhale Freq. (Hz)
300
250
200
150
Healthy subject
Patient (w/ Lung diseases)
Exhale Freq. (Hz)
250
225
200
Healthy subject
Patient(w/ Lung diseases)
P-value = 0.0378
10
20
30
40
50
60
70
SN Sound Intensity(> 150Hz, dB)

FIG. 41C

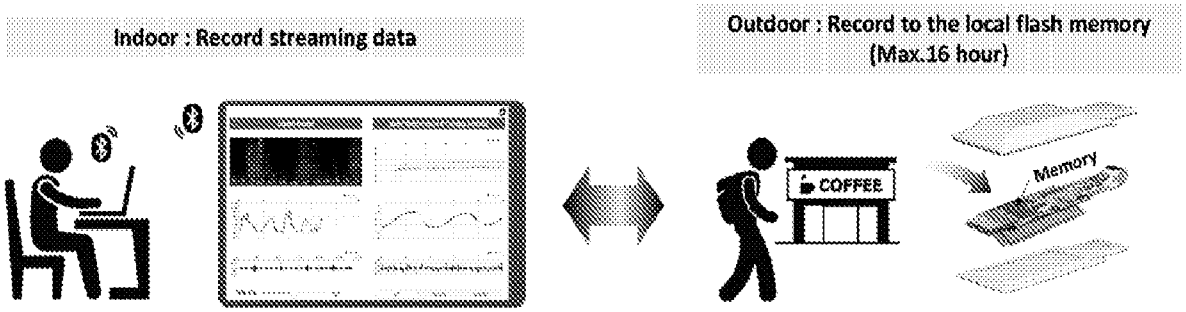
Indoor : Record streaming data
Outdoor : Record to the local flash memory
(Max.16 hour)
COFFEE
Memory

FIG. 42

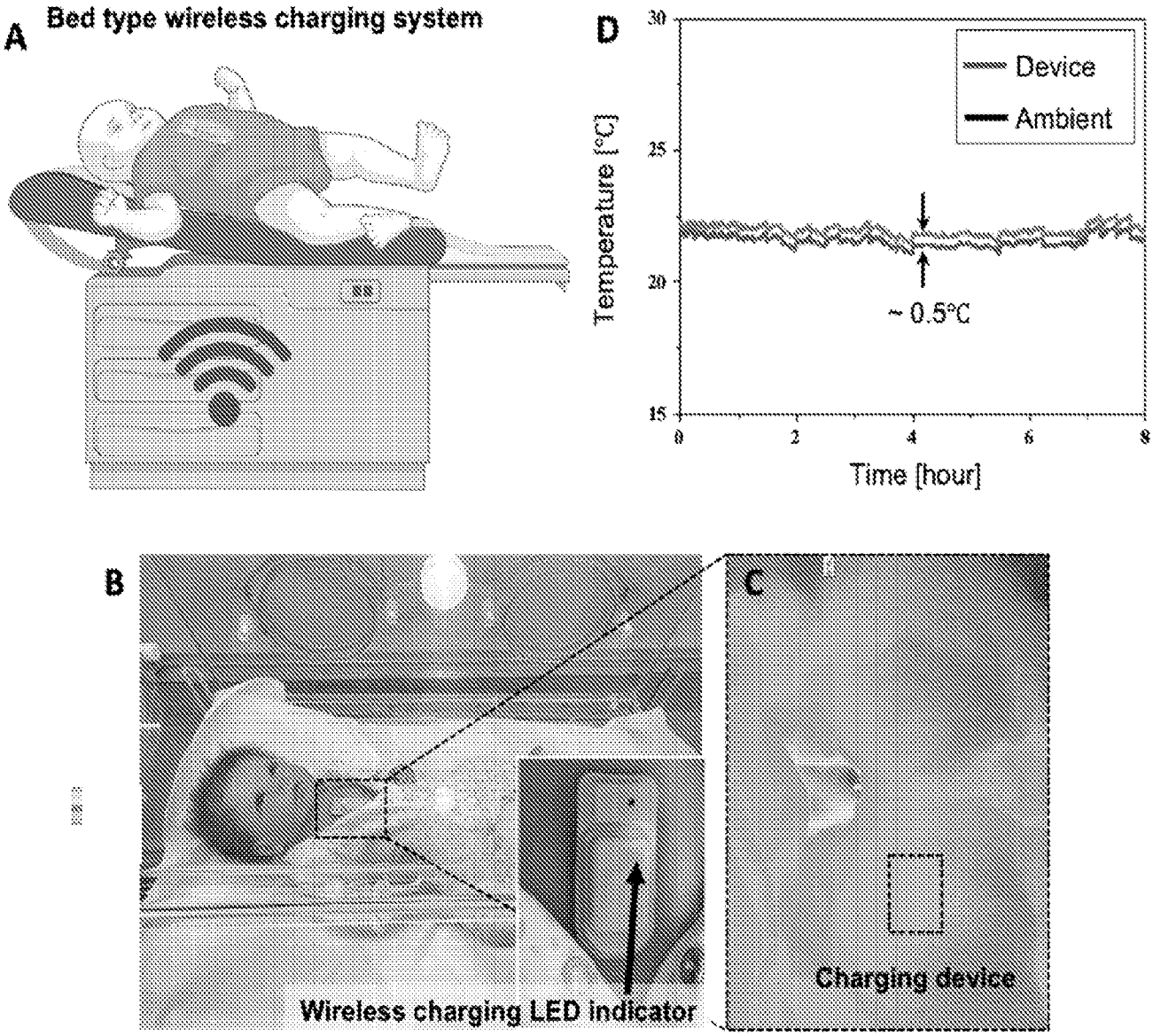
A
Bed type wireless charging system
D
Device
Ambient
Temperature [°C]
~ 0.5°C
Time [hour]
B
C
Wireless charging LED indicator
Charging device

FIG. 43

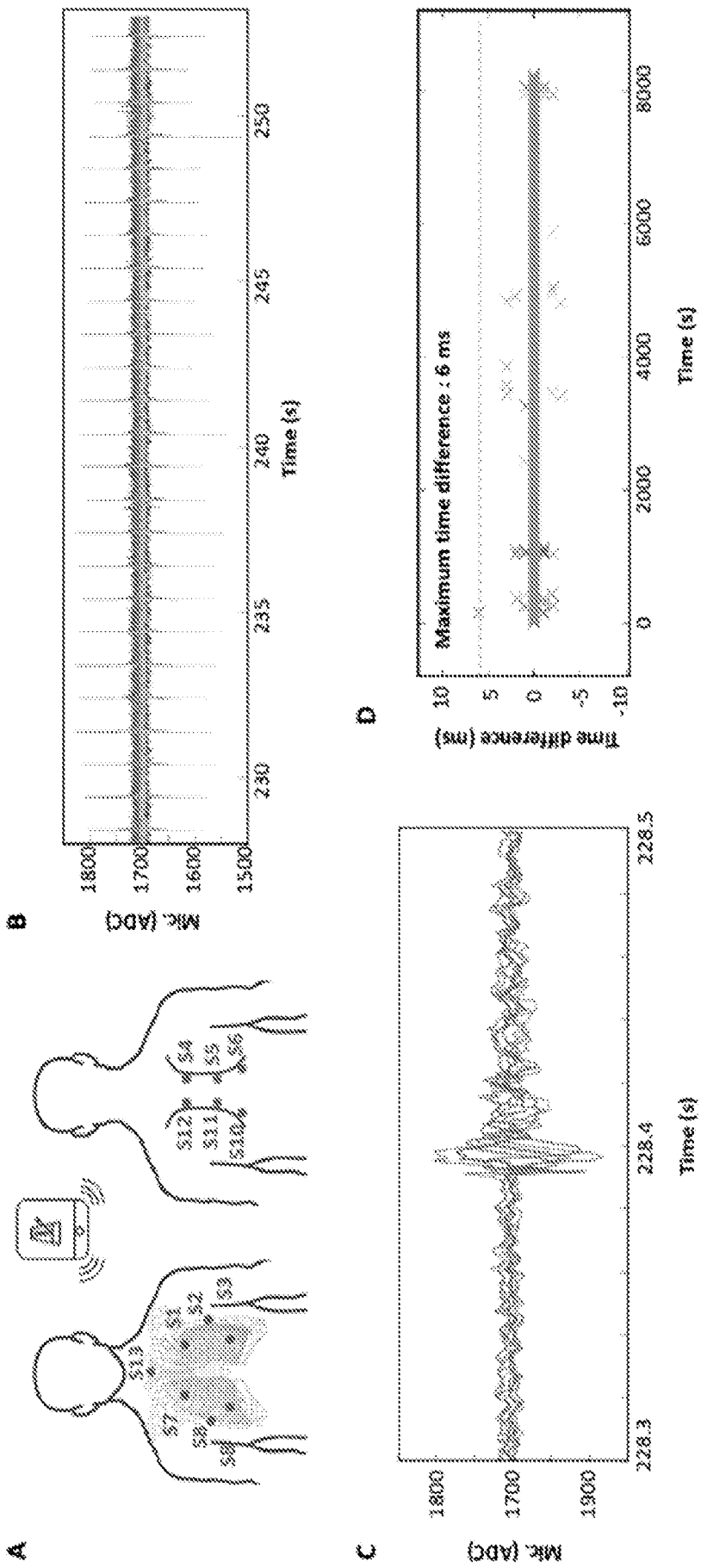
A
S18
S1
S2
S3
S7
S8
S9
S12
S11
S10
S4
S5
S6
B
Mic. (ADC)
1800
1700
1600
1500
230
235
240
245
250
Time (s)
C
Mic. (ADC)
1800
1700
1900
228.3
228.4
228.5
Time (s)
D
Maximum time difference : 6 ms
Time difference (ms)
10
5
0
-5
-10
0
2000
4000
6000
8000
Time (s)

FIG. 44

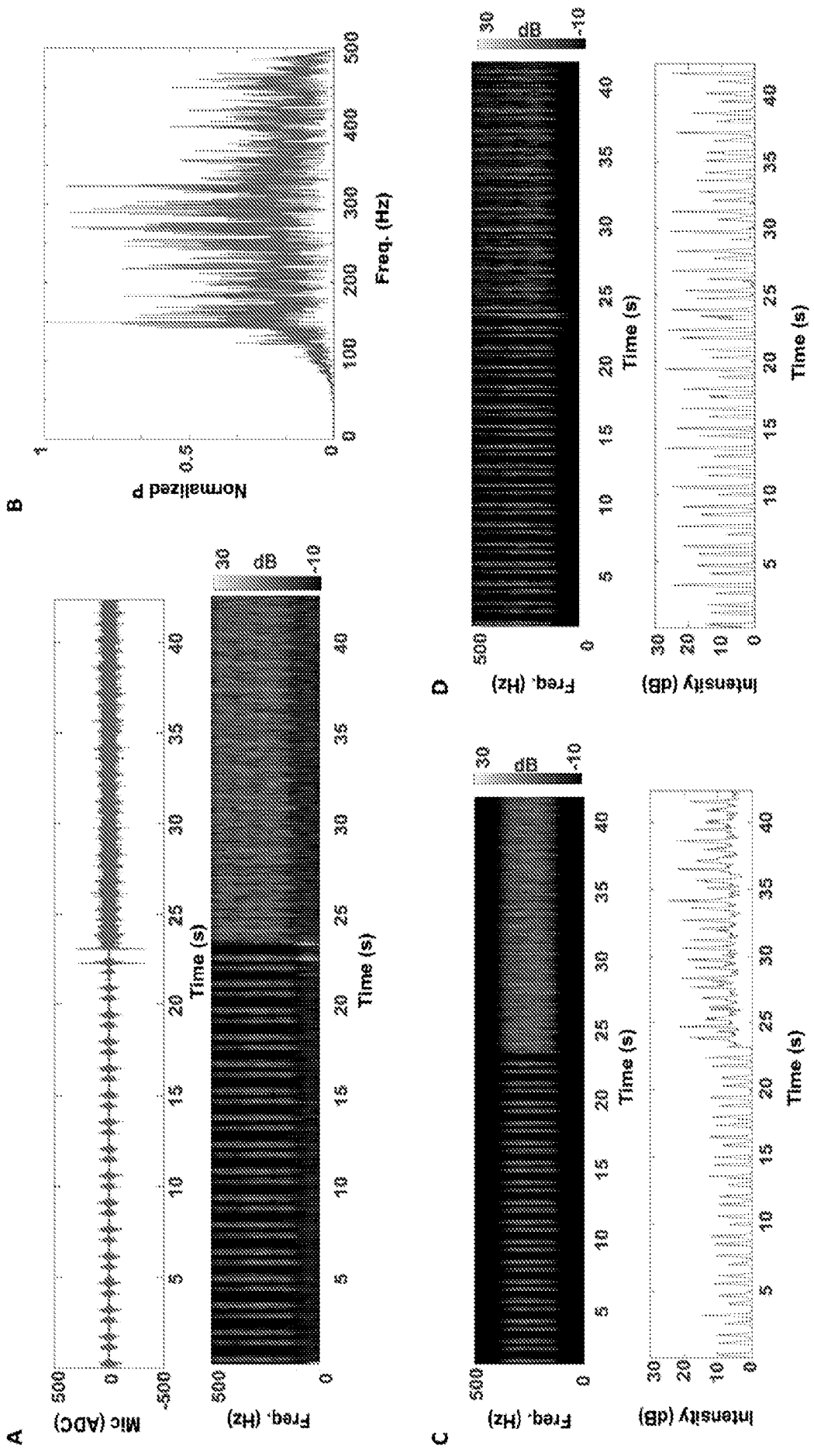
A
Mic (ADC)
Freq. (Hz)
Time (s)
B
Normalized P
Freq. (Hz)
C
Intensity (dB)
D
dB

FIG. 45

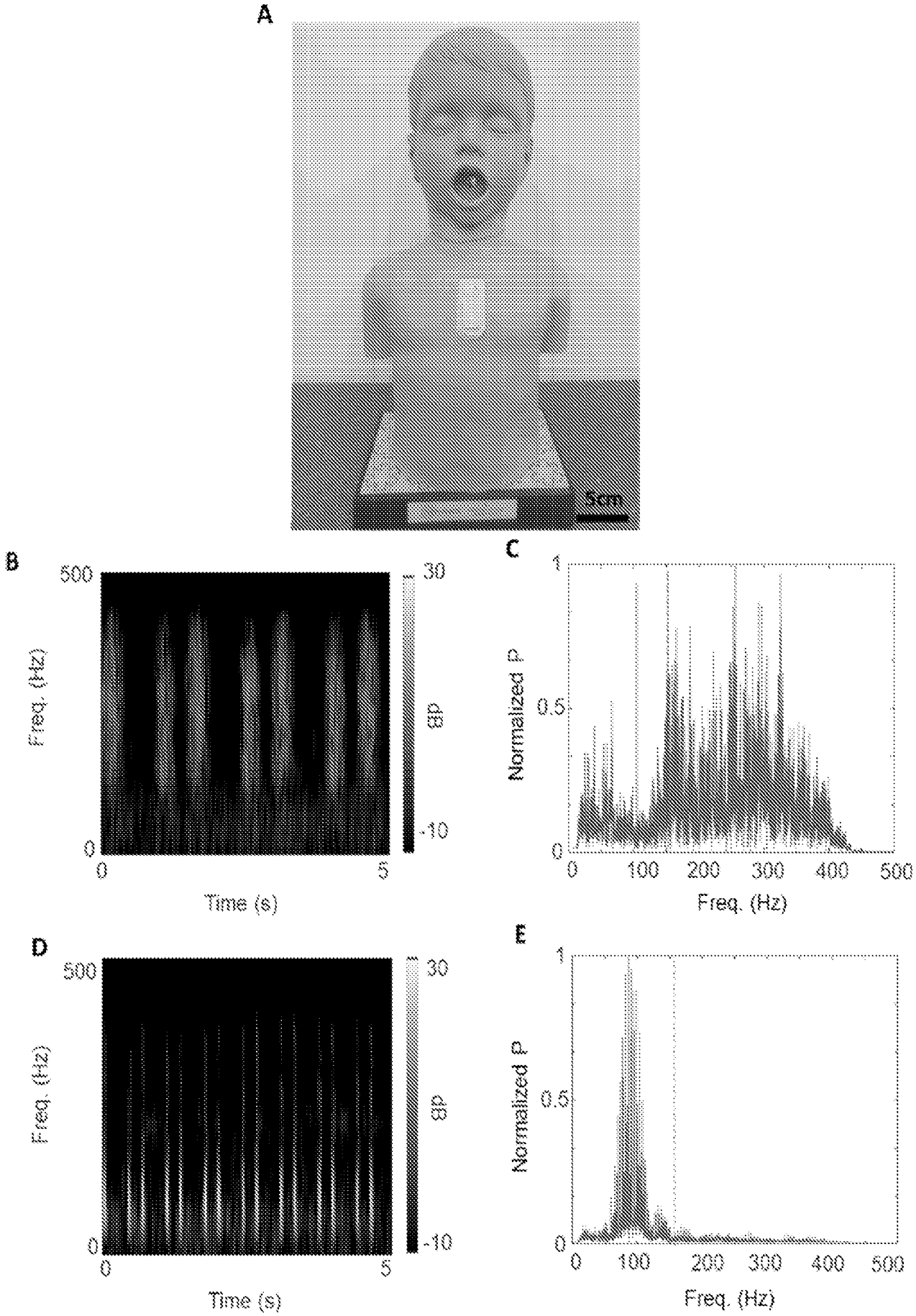
A
5cm
B
500
Freq. (Hz)
0
0
5
Time (s)
30
dB
-10
C
1
Normalized P
0.5
0
0
100
200
300
400
500
Freq. (Hz)
D
500
Freq. (Hz)
0
0
5
Time (s)
30
dB
-10
E
1
Normalized P
0.5
0
0
100
200
300
400
500
Freq. (Hz)

FIG. 46

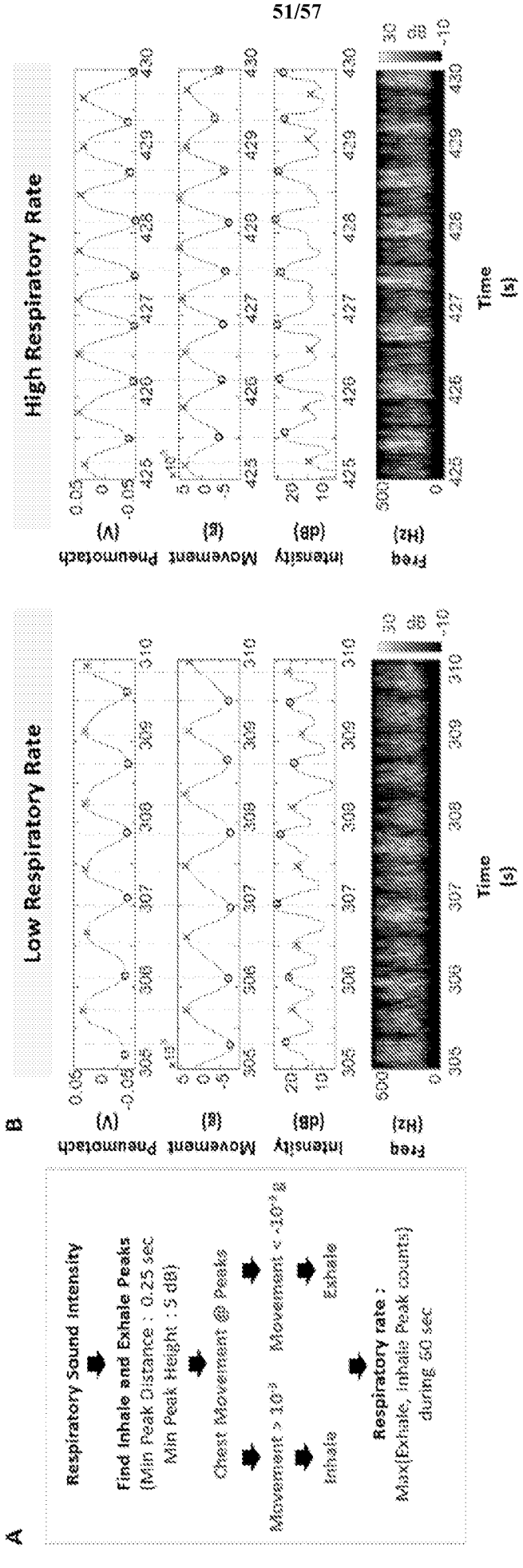
A
Respiratory Sound Intensity
Find Inhale and Exhale Peaks
(Min Peak Distance : 0.25 sec
Min Peak Height : 5 dB)
Chest Movement @ Peaks
Movement > 10^-3
Movement < -10^-3
Inhale
Exhale
Respiratory rate :
Max(Exhale, Inhale Peak counts)
during 60 sec
B
Low Respiratory Rate
High Respiratory Rate
Pneumotach (V)
Movement (g)
Intensity (dB)
Freq (Hz)
Time (s)

FIG. 47

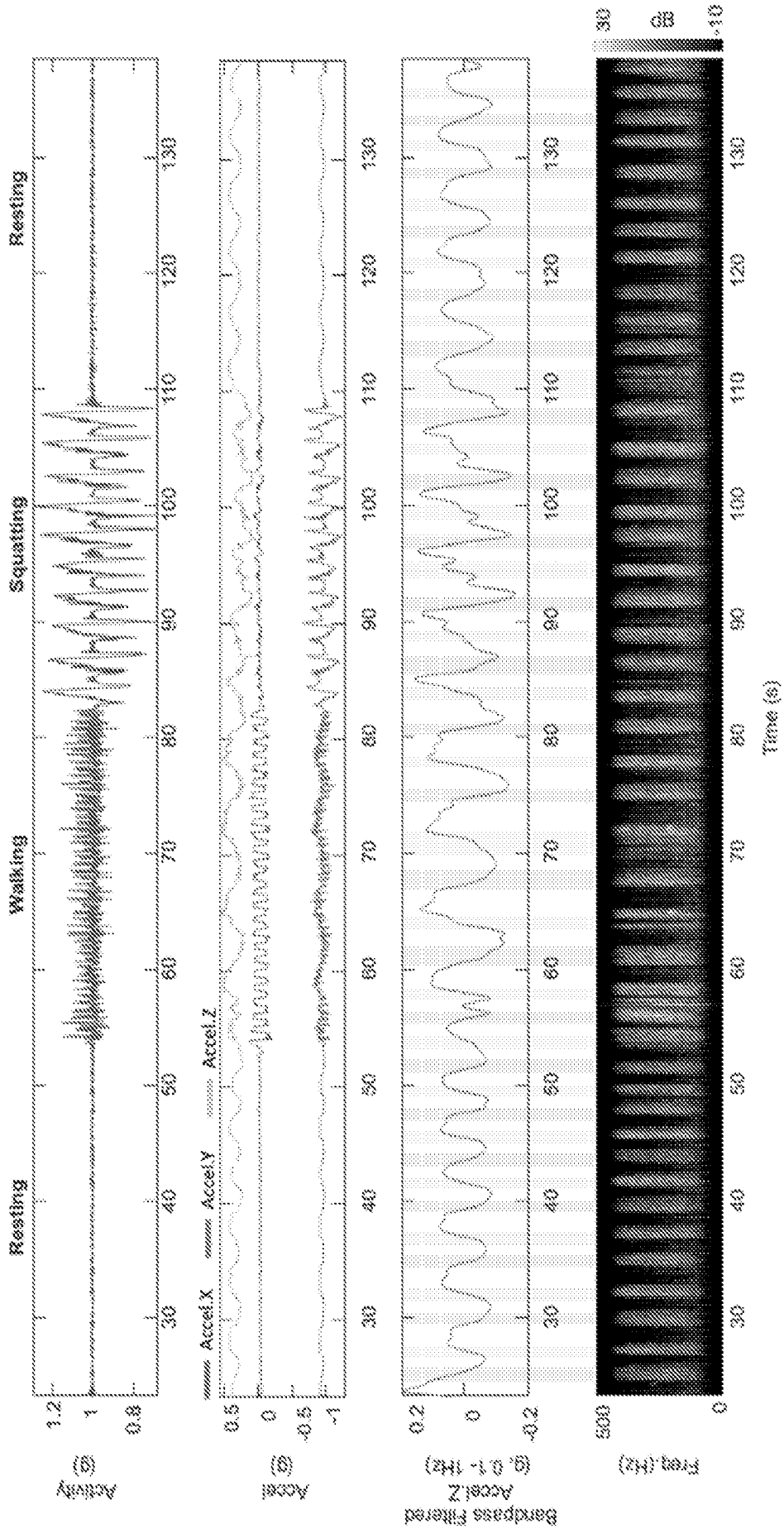
Resting
Walking
Squatting
Resting
Activity (g)
Accel (g)
Accel.X
Accel.Y
Accel.Z
Bandpass Filtered Accel.Z (g, 0.1- 1Hz)
Freq (Hz)
dB
Time (s)

FIG. 48

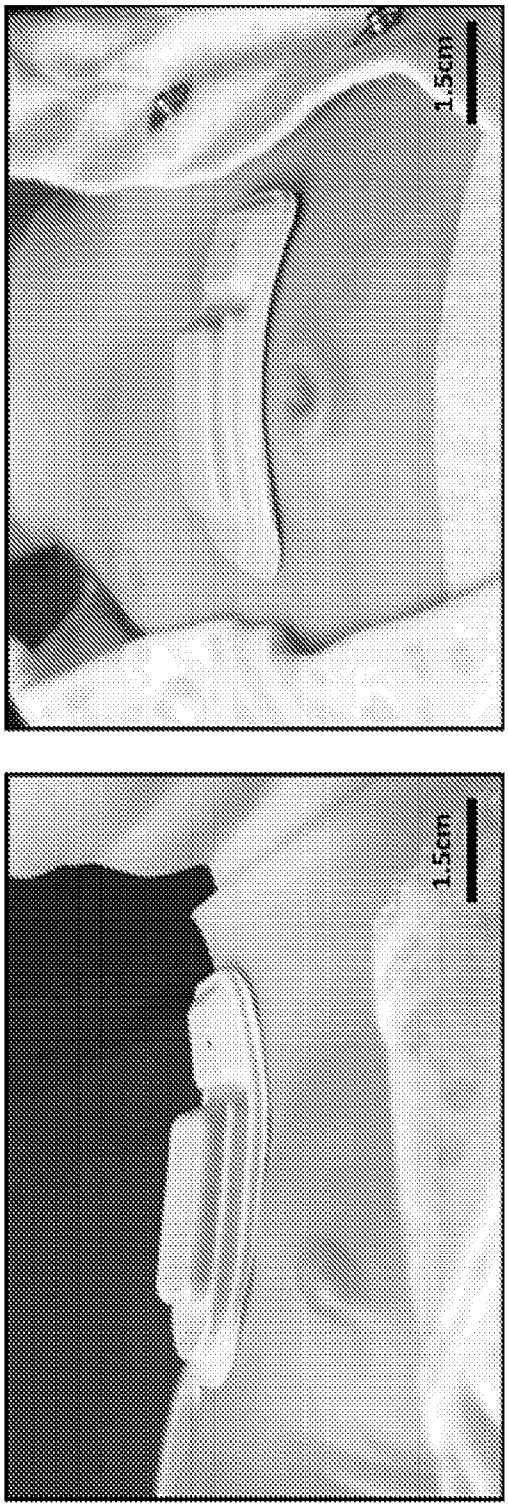

FIG. 49

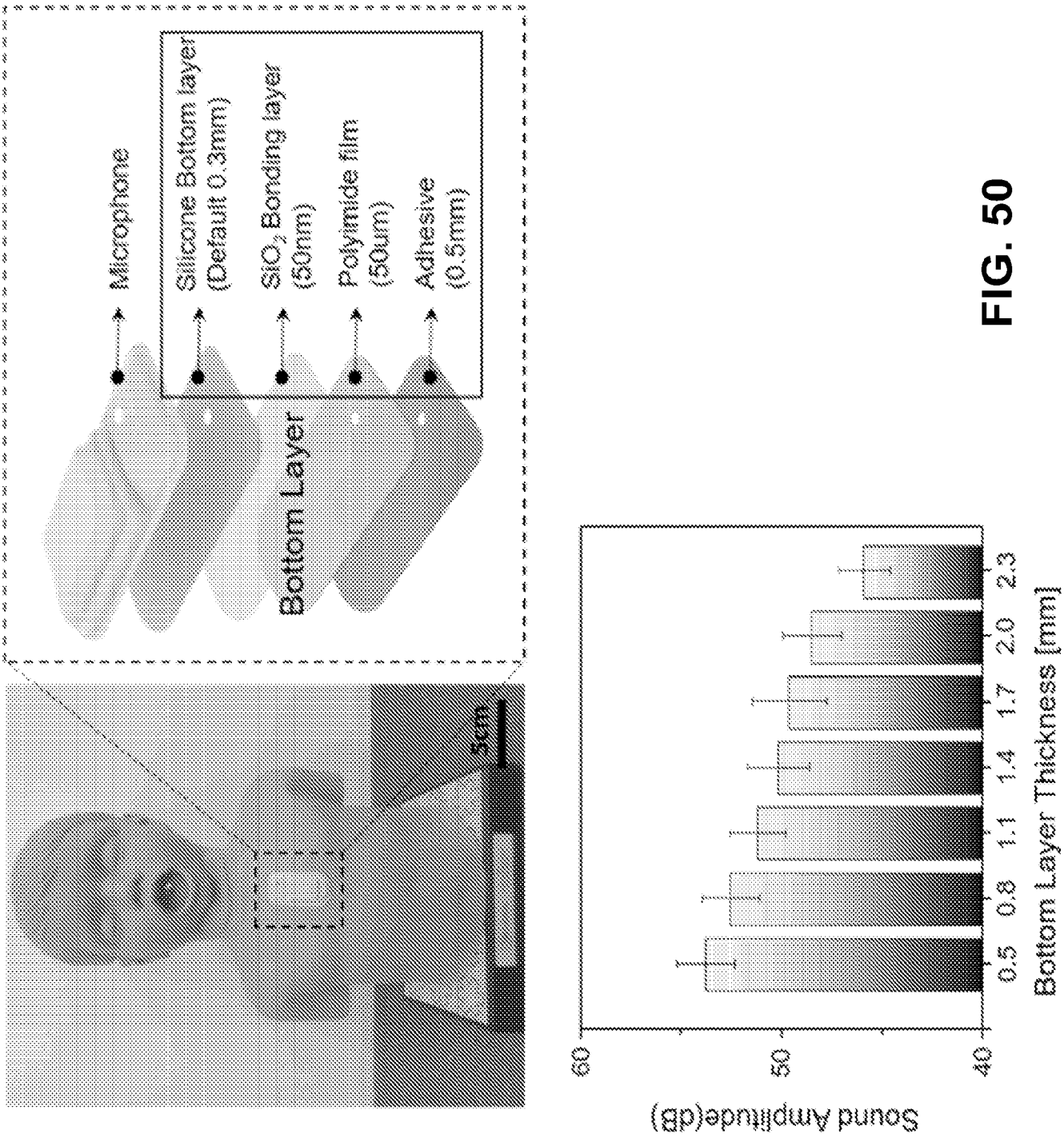
Microphone
Silicone Bottom layer (Default 0.3mm)
SiO_2 Bonding layer (50nm)
Polyimide film (50um)
Adhesive (0.5mm)
Bottom Layer
5cm
Sound Amplitude(dB)
60
50
40
0.5
0.8
1.1
1.4
1.7
2.0
2.3
Bottom Layer Thickness [mm]

FIG. 50

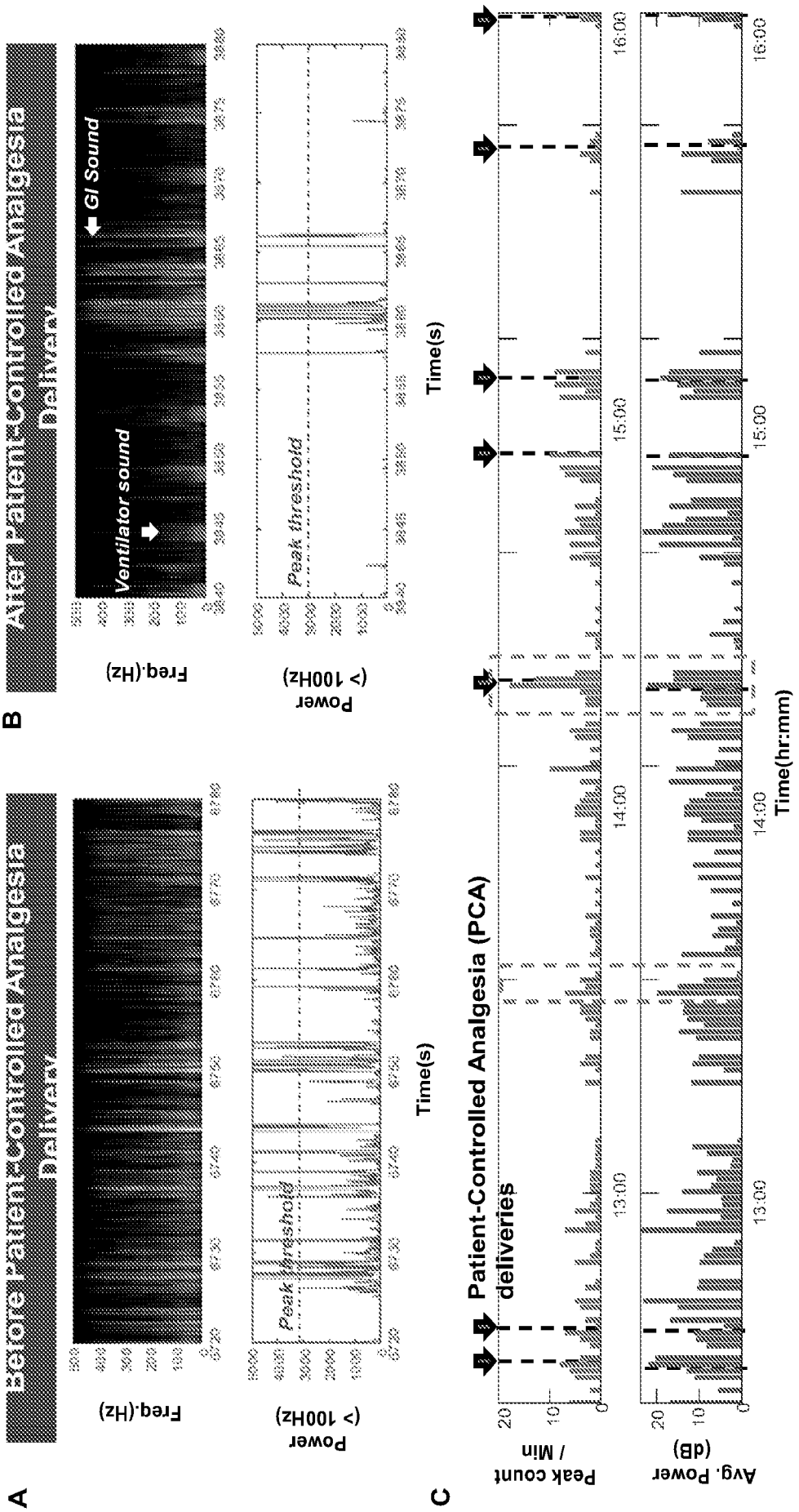
A
Before Patient-Controlled Analgesia Delivery
Freq.(Hz)
Power (> 100Hz)
Peak threshold
Time(s)
B
After Patient-Controlled Analgesia Delivery
GI Sound
Ventilator sound
Freq.(Hz)
Power (> 100Hz)
Peak threshold
Time(s)
C
Patient-Controlled Analgesia (PCA) deliveries
Peak count / Min
Avg. Power (dB)
13:00
14:00
15:00
16:00
Time(hr:mm)

FIG. 51

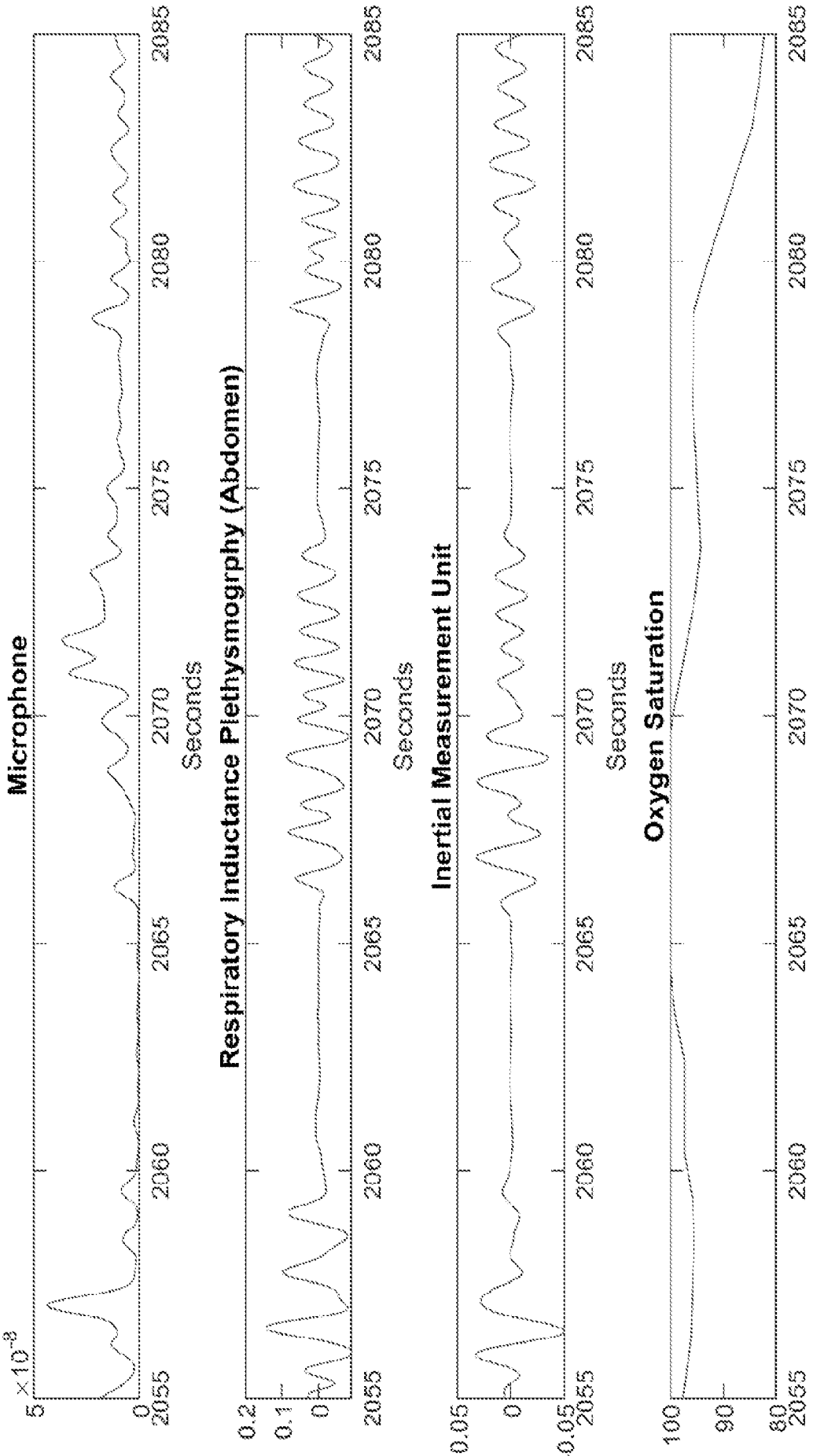
Microphone
×10^-3
5
0
2055
2060
2065
2070
2075
2080
2085
Seconds
Respiratory Inductance Plethysmography (Abdomen)
0.2
0.1
0
Inertial Measurement Unit
0.05
-0.05
Oxygen Saturation
100
90
80

FIG. 52

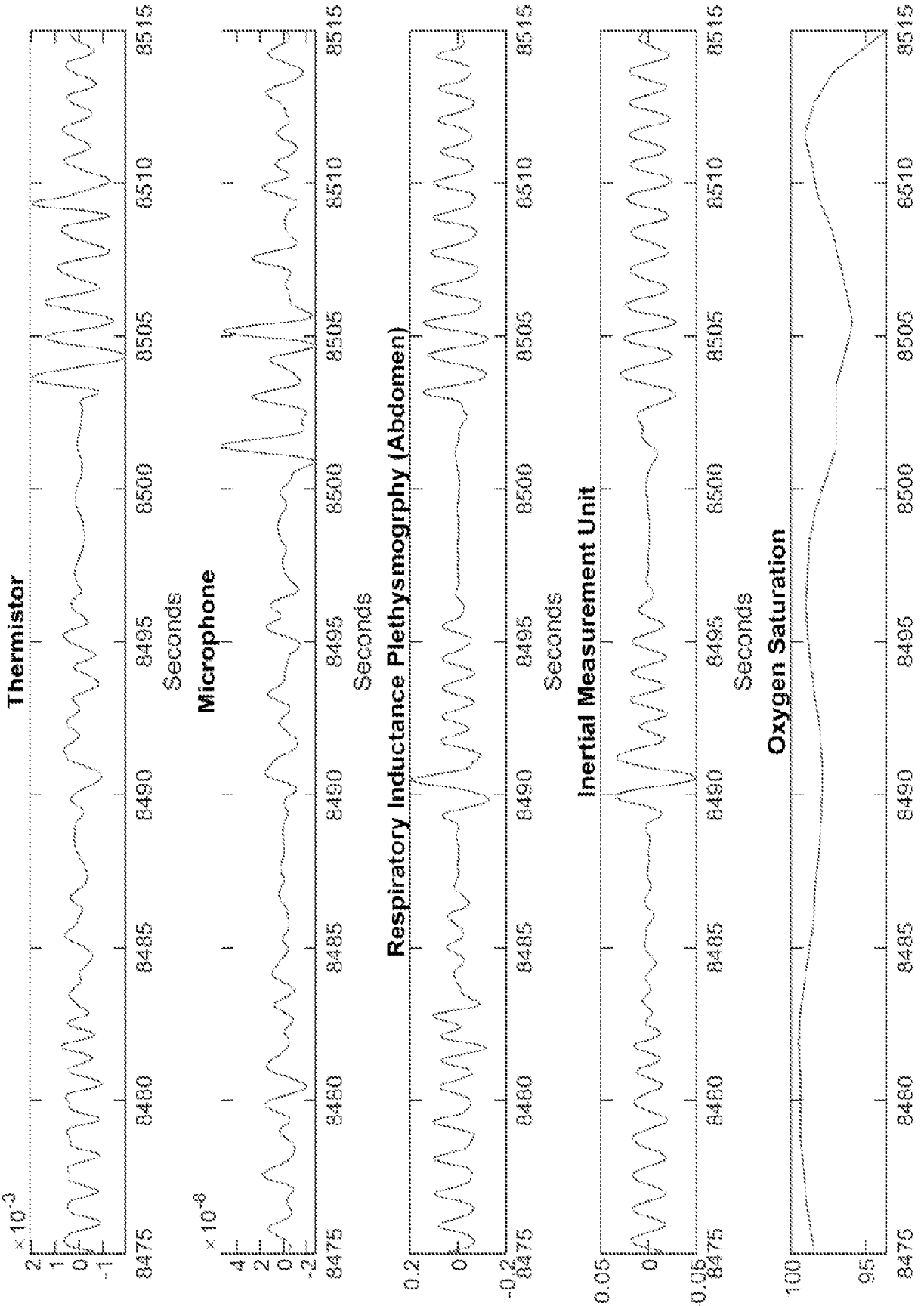
Thermistor
×10^-3
2
1
0
-1
8475
8480
8485
8490
8495
8500
8505
8510
8515
Seconds
Microphone
×10^-8
4
2
0
-2
Respiratory Inductance Plethysmography (Abdomen)
0.2
0
-0.2
Inertial Measurement Unit
0.05
0
-0.05
Oxygen Saturation
100
95

FIG. 53

INTERNATIONAL SEARCH REPORT

International application No.
PCT/US2024/054723

A. CLASSIFICATION OF SUBJECT MATTER

A61B 7/04(2006.01)i; **A61B 7/00**(2006.01)i; **A61B 5/00**(2006.01)i; **A61B 5/08**(2006.01)i; **A61B 5/11**(2006.01)i

According to International Patent Classification (IPC) or to both national classification and IPC

B. FIELDS SEARCHED

Minimum documentation searched (classification system followed by classification symbols)

A61B 7/04(2006.01); A61B 5/00(2006.01); A61B 5/0205(2006.01); A61B 5/091(2006.01); A61B 5/11(2006.01); A61B 7/00(2006.01)

Documentation searched other than minimum documentation to the extent that such documents are included in the fields searched

Korean utility models and applications for utility models
Japanese utility models and applications for utility models

Electronic data base consulted during the international search (name of data base and, where practicable, search terms used)

eKOMPASS(KIPO internal) & Keywords: broadband acousto-mechanical sensing (BAMS), acclerometer, acoutic, motion, sound, time-synchronized, wireless

C. DOCUMENTS CONSIDERED TO BE RELEVANT

Category*	Citation of document, with indication, where appropriate, of the relevant passages	Relevant to claim No.
X	US 2021-0386300 A1 (NORTHWESTERN UNIVERSITY) 16 December 2021 (2021-12-16) paragraphs [0039]-[0213]; claims 1-16; figure 2A	1-9,13-29
Y		10-12,30-37
Y	CN 112336320 A (CHEN RUJIAN) 09 February 2021 (2021-02-09) paragraph [0008]	10-12
Y	US 2023-0148954 A1 (RESMED SENSOR TECHNOLOGIES LIMITED) 18 May 2023 (2023-05-18) paragraph [0037]; claim 1	30-37
A	US 2020-0000371 A1 (RESPIRA LABS LLC) 02 January 2020 (2020-01-02) claim 1	1-37
A	WO 2023-043866 A1 (NORTHWESTERN UNIVERSITY) 23 March 2023 claims 1,15,49	1-37

☐ Further documents are listed in the continuation of Box C. ☑ See patent family annex.

* Special categories of cited documents:
"A" document defining the general state of the art which is not considered to be of particular relevance
"D" document cited by the applicant in the international application
"E" earlier application or patent but published on or after the international filing date
"L" document which may throw doubts on priority claim(s) or which is cited to establish the publication date of another citation or other special reason (as specified)
"O" document referring to an oral disclosure, use, exhibition or other means
"P" document published prior to the international filing date but later than the priority date claimed
"T" later document published after the international filing date or priority date and not in conflict with the application but cited to understand the principle or theory underlying the invention
"X" document of particular relevance; the claimed invention cannot be considered novel or cannot be considered to involve an inventive step when the document is taken alone
"Y" document of particular relevance; the claimed invention cannot be considered to involve an inventive step when the document is combined with one or more other such documents, such combination being obvious to a person skilled in the art
"&" document member of the same patent family

Date of the actual completion of the international search	Date of mailing of the international search report
17 February 2025	**17 February 2025**

Name and mailing address of the ISA/KR	Authorized officer
Korean Intellectual Property Office **189 Cheongsa-ro, Seo-gu, Daejeon** **35208, Republic of Korea**	**KIM, Yeon Kyung**
Facsimile No. **+82-42-481-8578**	Telephone No. **+82-42-481-3325**

INTERNATIONAL SEARCH REPORT
Information on patent family members

International application No.
PCT/US2024/054723

Patent document cited in search report			Publication date (day/month/year)	Patent family member(s)			Publication date (day/month/year)
US	2021-0386300	A1	16 December 2021	CN	113316414	A	27 August 2021
				EP	3863508	A1	18 August 2021
				EP	3863508	A4	03 August 2022
				JP	2022-509542	A	20 January 2022
				JP	7330281	B2	21 August 2023
				KR	10-2021-0072105	A	16 June 2021
				WO	2020-092786	A1	07 May 2020
CN	112336320	A	09 February 2021	None			
US	2023-0148954	A1	18 May 2023	CN	115697194	A	03 February 2023
				EP	4125572	A1	08 February 2023
				JP	2023-521656	A	25 May 2023
				WO	2021-198941	A1	07 October 2021
US	2020-0000371	A1	02 January 2020	CN	112040872	A	04 December 2020
				CN	112040872	B	24 March 2023
				CN	115844443	A	28 March 2023
				EP	3784137	A1	03 March 2021
				EP	3784137	A4	19 January 2022
				JP	2021-523760	A	09 September 2021
				JP	2024-057015	A	23 April 2024
				KR	10-2021-0005137	A	13 January 2021
				US	10709355	B2	14 July 2020
				US	11000210	B2	11 May 2021
				US	11147473	B2	19 October 2021
				US	11457836	B2	04 October 2022
				US	11647919	B2	16 May 2023
				US	2020-0367787	A1	26 November 2020
				US	2021-0196149	A1	01 July 2021
				US	2021-0345907	A1	11 November 2021
				US	2023-0044754	A1	09 February 2023
				US	2023-0346256	A1	02 November 2023
				WO	2019-210261	A1	31 October 2019
WO	2023-043866	A1	23 March 2023	US	2024-0382097	A1	21 November 2024